TECHNISCHE UNIVERSITÄT MÜNCHEN

1. Medizinische Klinik, Klinikum rechts der Isar

The effect of Sphingosine 1-phosphate (S1P) on thrombopoiesis

Lin Zhang

Vollständiger Abdruck der von der Fakultät für Medizin der Technischen Universität München zur Erlangung des akademischen Grades eines

Doctor of Philosophy (Ph.D.)

genehmigten Dissertation.

Vorsitzender: Univ.-Prof. Dr. Dirk Busch

Prüfer der Dissertation:

1. Univ.-Prof. Dr. Steffen Massberg
2. Univ.-Prof. Dr. Dr. Stefan Engelhardt

Die Dissertation wurde am 08.12.2011 bei der Fakultät für Medizin der Technischen Universität München eingereicht und durch die Fakultät für Medizin am 06.02.2012 angenommen.

ABSTRACT

Sphingosine 1-phosphate (S1P) is an evolutionarily conserved bioactive sphingosine metabolite with important roles in diverse cellular functions, including cell growth, survival, differentiation, migration, lymphocyte trafficking, vascular integrity, and angiogenesis. S1P is produced by one of two sphingosine kinases, sphingosine kinase 1 (Sphk1) and sphingosine kinase 2 (Sphk2). Extracellular S1P binds to five G protein-coupled receptors, called S1P1-5, and mediates a wide variety of biological effect. In addition to signal via S1P receptors located in the plasma membrane, S1P can also function intracellularly as a second messenger to influence the cellular responses. However, it is not clear whether S1P is also crucial for platelet biogenesis and thrombopoiesis.

Herein we investigated the effect of S1P-S1PRs signalling and sphingosine kinases on thrombopoiesis. First, we find S1P1 is essential for platelet production, since deficiency of S1P1 in the hematopoietic system or specific megakaryocytic lineages results in thrombocytopenia. We find that S1P gradient exists between tissue and blood, which by binding to the S1P1 receptor navigates megakaryocytes to form long cytoplasmic extensions (proplatelets) into sinusoids and triggered dissociation of proplatelets or platelet-like particles from megakaryocytes into blood. Mice lacking hematopoietic S1P1 expression show severe thrombocytopenia due to (1) formation of aberrant extravascular proplatelets and (2) defective intravascular proplatelet shedding. Second, hematopoietic deficiency of Sphk2 leads to the reduction in circulating platelets, suggesting that Sphk2 also plays an important role in thrombopoiesis. Our further investigations demonstrate that loss of Sphk2 retards the dissociation of proplatelets or platelet-like particles from megakaryocytes, which is responsive for the reduced platelet counts in Sphk2$^{-/-}$ mice. Taken together, we uncover a novel function of the S1P system in proplatelet formation and raise new options for the treatment of patients with thrombocytopenia.

TABLE of CONTENTS

Page number

LIST OF FIGURES

LIST OF TABLES

CHAPTER 1

A brief overview of this thesis work

1.1 Introduction

A normal count and function of platelets is very important for normal hemostasis. Platelets are generated from megakaryocytes (MKs) in the bone marrow and released into the circulation. Platelets are designed so that they avidly interact with the subendothelial matrix after vessel injury. Because MKs are located in the bone marrow interstitium in close contact with subendothelial matrix, it is unclear how platelets are released into the circulation without being activated. The hypothesis of “proplatelet” (PP) describes one of the most likely mechanisms explaining how newborn platelets get access to the blood: first, MKs stretch out long cytoplasmic extensions, termed as “proplatelet”, into the sinusoid and shed platelets from PP into blood [1]. It is still unclear whether and how proplatelets can be directed into the sinusoids without being activated in the subendothelial matrix. Next, platelets will be released from the end of proplatelets. However, it is also not clear how release of platelets or proplatelets from megakaryocytes is controlled. The biological mediators that guide the proplatelets and enhance their fragmentation in the blood remain still unknown.

S1P is an important bioactive lipid with pleiotropic cellular functions [2]. However, nothing is known about the effect of S1P on thrombopoiesis. The overall research goal of this thesis is to investigate the function of S1P in thrombopoiesis.

1.2. Objectives and specific aims

Objective 1: The function of S1P-S1PR signalling in thrombopoiesis

S1P can bind and signal through five G protein-coupled receptors, designated S1P1-5 [3].

These receptors are differentially expressed in different types of cells. Each S1P receptor couples to various G proteins and triggers different signalling pathways, leading to different cellular effects [4]. There is strong evidence that human platelets express S1P receptors [5-7]. As the precursors of platelets, megakaryocytes are predicted to also express S1P receptors. It is unclear whether S1P-S1PR signalling regulates thrombopoiesis.

The first aim of this thesis was to investigate if megakaryocytes express S1P receptors, and to determine the influence of distinctive S1PR on thrombopoiesis by measuring platelet counts in blood from S1PR knock out mice, and further to find out the mechanism how S1PRs regulate thrombopoiesis by *in vitro* and *in vivo* assays, in particular, using multi-photon intravital microscopy (MP-IVM) to observe the influences of S1PRs on thrombopoiesis in living mice.

In Chapter 3, we dissected the expression profile of different S1PR in both murine and human megakaryocytes. According to the S1PR expression profile, we analysed peripheral platelet counts in different S1PR knock out mice. We found severe thrombocytopenia in mice lacking hematopoietic S1P1 expression, but not in mice lacking S1P2 or S1P4. Further investigation shows that S1P1 plays an important role in thrombopoiesis by controlling proplatelet formation and proplatelet shedding in the bone marrow sinusoidal vasculature.

Objective 2: The function of sphingosine kinases in thrombopoiesis.

S1P levels are tightly regulated in a spatial-temporal manner by the balance between its synthesis and degradation [2]. The formation of S1P is catalyzed by sphingosine kinases (Sphk1 and Sphk2) [2]. Two enzymes mediate the degradation of S1P: first, S1P phosphatase reversibly degrades S1P into sphingosine; second, S1P lyase irreversibly degrades S1P into hexadecenal and phosphoethanolamine. High sphingosine kinase activity is found in platelets [2]. However, S1P lyase is absent in platelets [8]. Hence,

platelets produce a large amount of S1P and are considered as the source for plasma S1P [7]. Therefore, we hypothesized that megakaryocytes also expressed sphingosine kinases. However, it is unknown which isoenzyme of sphingosine kinases is expressed in megakaryocytes and the functions of sphingosine kinases in thrombopoiesis.

The second aim of this thesis was to identify which sphingosine kinase is expressed in megakaryocytes and to investigate the role of each sphingosine kinase for thrombopoiesis by measuring peripheral platelet counts from each sphingosine kinase knock out mice, and further to find out the mechanism how sphingosine kinases regulate thrombopoiesis and the potential involved signalling pathway.

In Chapter 4, we present the expression profile of sphingosine kinases in both murine and human megakaryocytes. We next measured the peripheral platelet counts in sphingosine kinase knock out mice. We found thrombocytopenia in Sphk2$^{-/-}$ mice, while Sphk1$^{-/-}$ mice display normal platelet counts. Further, we also found similar reduced platelet counts in bone marrow chimaeras, lacking hematopoietic Sphk2 expression; suggesting hematopoietic Sphk2 is crucial for thrombopoiesis. Finally our investigations show that loss of Sphk2 leads to a defect in proplatelet shedding in bone marrow vasculature, which contributes to the reduced platelet counts in Sphk2$^{-/-}$ mice.

1.3. References

1. Italiano, J.E., Jr., S. Patel-Hett, and J.H. Hartwig, *Mechanics of proplatelet elaboration.* J Thromb Haemost, 2007. **5 Suppl 1**: p. 18-23.
2. Spiegel, S. and S. Milstien, *Sphingosine-1-phosphate: an enigmatic signalling lipid.* Nat Rev Mol Cell Biol, 2003. **4**(5): p. 397-407.
3. Strub, G.M., et al., *Extracellular and intracellular actions of sphingosine-1-phosphate.* Adv Exp Med Biol. **688**: p. 141-55.
4. Rosen, H., et al., *Sphingosine 1-phosphate receptor signaling.* Annu Rev Biochem, 2009. **78**: p. 743-68.
5. Motohashi, K., et al., *Identification of lysophospholipid receptors in human platelets: the relation of two agonists, lysophosphatidic acid and sphingosine 1-phosphate.*

FEBS Lett, 2000. **468**(2-3): p. 189-93.

6. Randriamboavonjy, V., et al., *The S1P(2) receptor expressed in human platelets is linked to the RhoA-Rho kinase pathway and is down regulated in type 2 diabetes.* Basic Res Cardiol, 2009. **104**(3): p. 333-40.
7. Yatomi, Y., et al., *Sphingosine-1-phosphate: a platelet-activating sphingolipid released from agonist-stimulated human platelets.* Blood, 1995. **86**(1): p. 193-202.
8. Yatomi, Y., et al., *Sphingosine 1-phosphate: synthesis and release.* Prostaglandins, 2001. **64**(1-4): p. 107-122.

CHAPTER 2

Background

2.1 S1P

2.1.1 S1P metabolism:

Sphingosine-1-phosphate (S1P) is a bioactive sphingolipid metabolite [1]. Sphingolipids are structural components of the lipid bilayer of all eukaryotic cells. S1P was originally considered as merely the end product in the metabolite of sphingolipids [2]. Since the biological effects of S1P were reported in the early 1990s [3-5], numerous researches revealed important physiological and pathophysiological effects of S1P in higher organisms. S1P exerts pleiotropic effects on cellular processes, including cell growth, apoptosis, cytoskeletal rearrangements, angiogenesis, cell motility and migration, lymphocyte trafficking and immune surveillance [1]. S1P is also involved in many pathophysiological processes such as multiple sclerosis, allergy, cancer, and atherosclerosis [6].

De novo synthesis of sphingolipid occurs at the cytoplasmic aspect of the endoplasmic reticulum (ER). Serine palmitoyltransferase (SPT) catalyzes the condensation of serine (Ser) and palmitoyl CoA (Palm-CoA) to form 3-ketosphinganine (Keto) [7, 8]. 3-Ketosphinganine then is reduced to dihydrosphingosine, followed by acylation to form dihydroceramide (DH-Cer). DH-Cer is converted to ceramide after desaturation [9]. Ceramide is then translocated from the ER to the Golgi apparatus [10]. On the lumenal side of the Golgi, sphingomyelin synthase converts DH-Cer and ceramide to sphingomyelin (SM) and dihydrosphingomyelin (DH-SM), respectively [11]. Ceramide is generated from degradation of sphingolipids such as SM and subsequently deacylated by ceramidases to yield sphingosine. Sphingosine kinase catalyses the ATP-dependent phosphorylation of sphingosine to produce S1P [12]. S1P phosphatases degrade S1P by reversible dephosphorylation [13, 14]. S1P also can be irreversibly degraded into

hexadecenal and phosphoethanolamine by S1P lyase [15]. S1P levels are tightly controlled by the balance between synthesis and degradation [1] (Fig. 2.1).

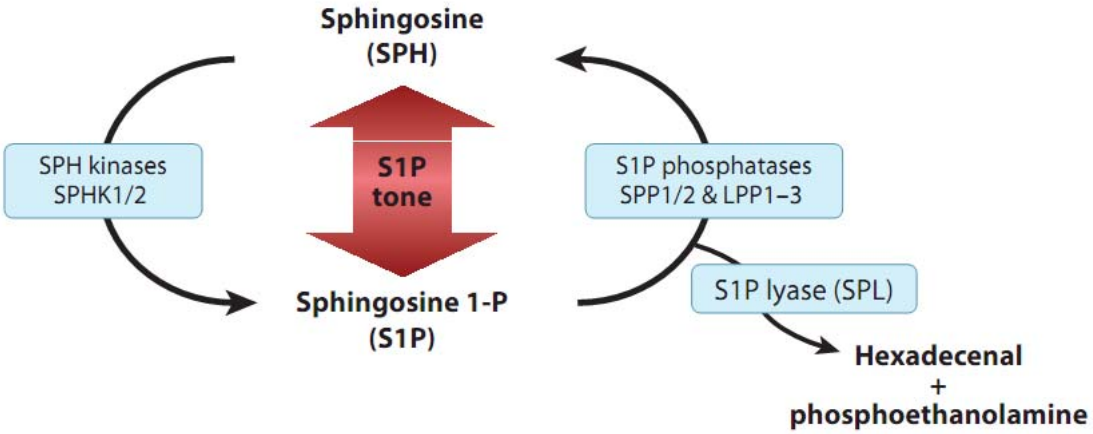

Fig. 2.1 S1P metabolism [16]

2.1.2 S1P receptors

Although S1P is a relatively simple lipid, extracellular S1P exerts pleiotropic functions via its five specific cell surface receptors (S1P1-5) [17]. Different cell types have distinct S1P receptors, which are coupled to various G proteins, triggering diverse downstream signalling pathways and resulting in regulation of different physiological processes [18].

S1P1 (known as EDG-1) was originally identified as an orphan GPCR in endothelial cells [19]. The S1P1 gene locus was reported on the human chromosome 1 (1p21) [20]. The S1P1 gene is composed of two exons and one intron, in which the 2^{nd} exon contains the whole coding region. S1P binds to S1P1 with high affinity (K_d = 8 nM) [21, 22]. S1P1 is reported to couple to the $G_{i/o}$ protein [16], which mediates versatile signalling pathways, including AC activation, ERK activation, PLC activation, PI3K activation, AKT activation, eNos activation, Rac activation, Ca^{2+} mobilization etc [23-25]. The activity of S1P1 can be regulated by phosphorylation. It is shown that phosphorylation of S1P1 mediated via Akt is necessary for Rac activation and S1P-induced chemotaxis [26]. The expression of S1P1

is ubiquitous and includes the brain, heart, spleen, liver, lungs, thymus, kidneys, lymphoid tissues, and bone marrow [27, 28]. Since the initial description of S1P1, multiple physiological functions of S1P1 have been identified. $S1P1^{-/-}$ embryos fail to survive because of serious haemorrhage during embryonic development [29]. The haemorrhage results from incomplete vascular maturation, since vascular smooth muscle cells and pericytes fail to migrate and cover endothelial tubes [29]. Rac1 is reported as effector of S1P1 action on vascular maturation [29]. Further studies in mice with conditional deficiency of S1P1 in endothelial cells show that these mice also have a defect in vascular maturation, suggesting S1P1 expression in endothelial cells is also required for normal vascular maturation [30]. S1P1 is also shown to regulate vascular integrity. Inhibition of S1P1 disrupts endothelial barriers and increases vascular permeability [31]. Besides the effect of S1P1 on vasculature, S1P1 is crucial for immune cell trafficking [32]. Matloubian et al reported S1P1 mutant chimeras, whose hematopoietic system was reconstituted with $S1P1^{-/-}$ hematopoietic cells, displayed almost absence of peripheral T cells and reduced B cell counts in the peripheral blood, because S1P1 has been shown to essentially control lymphocytes egress from the thymus and peripheral lymphoid organs [32].

S1P2 was first identified as an orphan GPCR gene from rat cardiovascular and nervous systems [33, 34]. The S1P2 gene locus was reported on the human chromosome 19 (19p13.2) [20]. The S1P2 gene contains two exons and one intron. The 2^{nd} exon contains the entire coding region. S1P2 is a high-affinity receptor for S1P (K_d=20-27 nM) [35]. It is reported that S1P2 can couple to $G_{i/o}$, G_q and $G_{12/13}$. S1P-S1P2 signalling triggers PLC activation, JNK activation, SRE activation, MAPK activation, Rho activation and Rac inhibition [23-25, 36]. S1P2 is widely expressed, especially in brain, heart and vascular smooth muscle cells [28, 37]. S1P2 null mutants can survive without apparent anatomical and histological abnormalities [38, 39]. It is reported that these mice have sporadic seizures, which are occasionally lethal between 3-7 weeks of age [38]. These mice also display deafness, suggesting S1P2 plays an important role in the development of the auditory and vestibular systems [40]. Experiments show that S1P2 is required for S1P-induced Rho activation and inhibition of cell migration, which is opposite to the effect

of S1P1 on cells [39, 41]. For example, osteoclast precursors migrate towards S1P in a positive chemotaxis manner via S1P1 [42], whereas S1P2 in these cells contributes to negative chemotaxis towards S1P (or chemorepulsion) [43].

S1P3 was first identified as an orphan GPCR from a human genomic DNA library [44]. The S1P3 gene locates in human chromosome 9 (9q22.1-2) and binds to S1P with high affinity (K_d=23-26 nM) [20, 45, 46]. The S1P3 gene contains only one exon. S1P3 couples with $G_{i/o}$, G_q, and $G_{12/13}$ and triggers different signalling in different cell types. Experiments show that S1P3 can activate ERK, PLC, Rho, Rac and MAPK signalling [1]. S1P3 is expressed in heart, lungs, skeletal muscle, kidneys, spleen, and cartilage [37]. $S1P3^{-/-}$ mice are fertile and healthy without apparent defects [28]. However, most of $S1P2^{-/-}$ $S1P3^{-/-}$ double knock out mice cannot survive beyond the perinatal period [39]. After the perinatal period, the $S1P2^{-/-}$ $S1P3^{-/-}$ survivors have no apparent abnormality [39]. S1P3 is reported to play a role in the regulation of heart rates [47]. S1P3 is also required for S1P-induced lung leakage by regulating epithelial barriers [48].

S1P4 was originally identified as an orphan GPCR gene from dendritic cells. The S1P4 gene locates in human chromosome 19 (19p13.3) [20]. S1P4 gene is composed of only a single exon. The affinity of S1P4 for S1P is also high (K_d=13-63 nM) [49], like S1P1, S1P2 and S1P3. S1P4 couples to $G_{i/o}$, $G_{12/13}$ and induces ERK activation, PLC activation, AC activation, Rho activation and Ca^{2+} mobilization [28, 50]. It is reported that S1P-S1P4 signalling induces cytoskeletal rearrangements and enhances pertussis toxin-sensitive cell motility [50]. The expression pattern of S1P4 is more restricted than S1P1, S1P2 and S1P3; it is present in lymphoid tissues, bone marrow, spleen, lungs and thymus [28]. $S1P4^{-/-}$ mice are viable and fertile without apparent abnormalities [51]. A recent study shows that $S1P4^{-/-}$ mice have a delay in platelet recovery after experimental depletion of platelets, although $S1P4^{-/-}$ mice display normal platelet counts under physiological conditions [51]. In immune system, S1P4 is suggested to regulate dendritic cell (DC) function and TH17 T-cell differentiation [52]. $S1P4^{-/-}$ mice showed decreased pathology in a model of dextran sulfate sodium-induced colitis [52].

S1P5 was first isolated as an orphan GPCR gene from rat pheochromcytoma 12 (P12) cells [53]. S1P5 gene locus is on the human chromosome 19 (19p13.2) [20]. Like other S1P receptors, S1P5 binds to S1P with high-affinity (K_d=2-10 nM) [54]. The S1P5 gene contains only one exon region. It is reported that S1P5 couples to $G_{i/o}$ and $G_{12/13}$. S1P-S1P5 signalling can activate MAPK, Ca^{2+} mobilization, etc [28, 54-56]. Like S1P4, S1P5 has a restricted expression pattern. It is primarily expressed in brain, spleen, and leukocytes [28, 54]. $S1P5^{-/-}$ mice were born at the expected mendelian frequencies, developed normally and were fertile [57]. It is reported that $S1P5^{-/-}$ mice have aberrant natural killer (NK) cell homing during steady-state condition [58].

2.1.3 S1P gradient

S1P is enriched to micromolar levels in the lymph and blood, where S1P is largely associated with plasma albumin and lipoprotein [59]. Recent investigations indicate that different cellular sources contribute to plasma S1P. Yatomi et al reported that platelets secreted S1P after stimulation and suggested that platelets were the major contributor to plasma S1P [60]. However, Pappu et al found normal S1P level in NF-E2 knock out mice, which lack platelets [61]. Moreover, Venkataraman et al found normal plasma S1P levels in mice, which were depleted of platelets *in vivo* by infusion of GPIb antibody [62]. These results suggest that platelets might not be the major source of plasma S1P. Further experiments support that erythrocytes are the major source of plasma S1P [63]. Besides hematopoietic cells, endothelial cells are also considered as another possible source of plasma S1P. Venkataraman et al reported that blood shear stress induces the release of S1P from endothelial cells [62]. In contrast to plasma S1P, tissue S1P concentrations are lower and in nM range [64, 65]. S1P is irreversibly degraded by S1P lyase, which is abundant in the tissue and absent in the blood, contributing to the establishment of the S1P gradient between plasma and tissue [65]. When hematopoietic cells migrate from the tissue into the blood, they will encounter a S1P gradient. It is clear that the S1P gradient plays a primary role in trafficking of lymphocytes and hematopoietic progenitor cells [65,

66]. Like hematopoietic cells, MKs possibly use the same paradigm to traverse into the blood [67]. Whether proplatelets, as cytoplasmic protrusions of MKs, could also be guided by S1P gradient s into the blood is not clear to date.

2.1.4 Sphingosine kinase

Sphingosine kinases are evolutionarily conserved lipid kinases [68]. They are widely expressed across different species from plants to humans. There are two isoenzymes in mammals (Sphk1 and Sphk2) [69]. Sphk1 and Sphk2 have distinct structural characteristics, catalytic properties, subcellular distribution, tissue distribution and cellular functions. Sphk1 and Sphk2 have five conserved domains (C1-C5) [70]. The C1-C3 domains form the unique catalytic domain. It is predicted that Sphk1 has no hydrophobic transmembrane region. In contrast, Sphk2 has four predicted transmembrane regions. Although both Sphk1 and Sphk2 synthesize S1P, Sphk1 prefers D-erythro-sphingosine and D-erythro-dihydrosphingosine, while Sphk2 catalyzes phytosphingosine and dihydrosphingosine [71]. SphK2 mainly contributes to phosphorylation of FTY720 [72], which is an immunosuppressive pro-drug. FTY720 can couple to S1P1, 3, 4 and 5 receptors after phosphorylation and results in lymphopenia *in vivo* [73, 74].

Both SphK1 and Sphk2 are cytosolic enzymes but have different subcellular distributions [75]. Translocation of Sphk1 to the plasma membrane is induced by many stimuli, including PMA, TNFα, LPS, C5a, NGF, and PDGF. Johnson et al reported that PMA induced the translocation of Sphk1 to the plasma membrane in HEK 293 cells and that the protein kinase C (PKC) was involved in translocation of Sphk1 [76]. TNFα is also reported to induce translocation of Sphk1 to the smooth muscle cell membrane [77]. Translocation and activation of Sphk1 is considered to be involved in C5a-induced macrophage activation [78, 79]. Toman et al reported that nerve growth factor (NGF)-induced neurite extension was dependent on translocation of Sphk1 to the plasma membrane and an S1P1-dependent activation of Rac GTPase [80]. PDGF is also shown to trigger the transport of Sphk1 to the leading edge of fibroblasts [81, 82]. Spatial distribution of

sphingosine kinases lead to local production of S1P, which is either flipped or secreted outside and trigger so-called “inside-out” signalling through its receptors through a paracrine and/or autocrine action [83]. On the other hand, many studies on Sphk2 have shown SphK2 was transported to cellular compartments other than the plasma membrane. For example, COS7 cells increase Sphk2 levels in the nucleus at higher cell confluence [84]. Accumulation of Sphk2 in the nucleus is supposed to inhibit DNA synthesis [84]. It is reported that SphK2 is transported to the ER under serum starvation, a process that enhances apoptosis [85]. Ding et al reported that protein kinase D activated a nuclear export signal sequence in Sphk2 by phosphorylation [86].

The expression of Sphk1 is ubiquitous with highest expression in lungs, kidneys, blood and spleen. Expression of Sphk2 is predominately found in liver, kidneys, brain and heart [71]. Overexperssion of Sphk1 is found in many solid tumors, e.g. of the kidneys, stomach, or breast [87, 88]. Highest expression of Sphk1 is found at embryonic day 7, whereas Sphk2 expression is greatest at embryonic day 17 [71, 89].

Many studies show that Sphk1 plays an important role in cell survival, cell growth, migration and calcium homeostasis. It is reported that overexpression of Sphk1 enhances cell growth and survival in various cell types, such as NIH3T3, MCF-7, U-87 MG, and U-1242 MG [90, 91]. In contrast to the effect of Sphk1 on survival, Sphk2 has been reported to induce proapoptosis effects. Liu et al reported overexpression of Sphk2 leaded to apoptosis, in a process involving Bcl-xL [92]. Recent investigations have shown that nuclear Sphk2 is associated with HDAC1 and HDAC2 in repressor complexes at the promoters of specific genes [93]. Different stimuli trigger phosphorylation and activation of Sphk2, leading to production of nuclear S1P. Nuclear S1P binds to HDAC1 and HDAC2 and inhibits their activity [93].

2.2 Thrombopoiesis

2.2.1 Megakaryocytic differentiation

Platelets are produced by megakaryocytes (MKs), which are derived from hematopoietic stem cells (HSC) [94]. HSCs have self-renewal capacities and enable long-term hematopoietic reconstitution. The immediate HSC progenies, the so-called multipotent progenitors (MPP), have a reduced the self-renewal capacity and can only reconstitute the hematopoietic system for short term. MPP give rise to the common lymphoid progenitor (CLP) and the common myeloid progenitor (CMP). The CLP can yield all lymphoid lineages. CMP is capable of generating all myeloid lineages (granulocyte, macrophage, erythrocytes and platelets). It is considered that CMP give rise to MK/Erythro progenitors (MEP) [95]. However, recent investigations suggest that the MEP may derive directly from HSC [96, 97]. The primitive MK progenitors are capable of proliferating and can form colonies *in vitro*. Based on *in vitro* colony assays, MK progenitors can be classified into highly proliferative potential-colony-forming unit-Megakaryocyte (HPP-CFU-MK), burst-forming unit-megakaryocyte (BFU-MK) and colony-forming unit-megakaryocyte (CFU-MK) [98-102]. CFU-MKs have a reduced proliferation capacity and differentiate into megakaryoblasts. Megakaryoblasts increase their ploidy and size. The process of increasing ploidy is termed endomitosis, which leads to polyploidy without cytokinesis [102]. During endomitosis, MKs form the demarcation membrane system (DMS) and synthesize platelet specific proteins, including granules and cytoskeletal proteins [102, 103]. After maturation, mature MKs form and release platelets into the blood.

MK progenitors express CD34 as do other hematopoietic progenitors. The pure CFU-MKs are enriched in $Lin^{-}c\text{-}Kit^{+}Scal\text{-}1^{-}FcgalmaR^{low}$ $IL7Ralpha^{-}Thy1.1^{-}CD34^{low}CD9^{+}CD41^{+}$ cells [104]. CD34 disappears during MK maturation. The expression of the main platelet glycoprotein, the integrin CD41, is upregulated during MK maturation and represents a relatively marker for MK [105-107]. CD41 expression is present on the surface of cells of the MKs earlier than another major platelet protein, the CD42 [108]. CD42 expression represents a late differentiation stage of MK [109]. Thus, $CD34^{+}CD41^{+}CD42^{-}$ cells represent MK progenitors or intermediately mature MKs, while $CD34^{-}CD41^{+}CD42^{+}$ correspond to more mature MKs.

Thrombopoietin (Tpo) is the principle cytokine to regulate megakaryopoiesis. The Tpo gene locates on the long arm of human chromosome 3 (3q26-27). Tpo, a 75 to 80 kD protein, binds to its receptor, c-Mpl, and enhances thrombopoiesis [110-113]. Tpo synthesis occurs primarily in the liver. Expression of Tpo is low in kidneys, bone marrow stromal cells and also in spleen. The expression of Tpo mRNA is considered to be constitutive. Platelet mass as well as MKs mass regulate Tpo levels by triggering internalisation and subsequent degradation of Tpo/c-Mpl complexes into platelets and MKs. Therefore, the plasma Tpo levels are usually inversely correlated to peripheral platelet counts. It seems that Tpo regulates all aspects of thrombopoiesis, including MK colony formation, MK differentiation and maturation [114]. Tpo was reported to induce cytoplasmic maturation, endomitosis and proplatelet formation [112, 115-117]. $Mpl^{-/-}$ mice were reported to have only about 10% MKs and platelets [118]. Interestingly, Tpo has no effect on cytoplasmic fragmentation and shedding of platelets [118]. Besides Tpo, other cytokines, such as interleukin-3 (IL- 3), granulocyte-macrophage colony-stimulating factor (GM-CSF) and granulocyte colony-stimulating factor (G-CSF), have effects on thrombopoiesis [119-121].

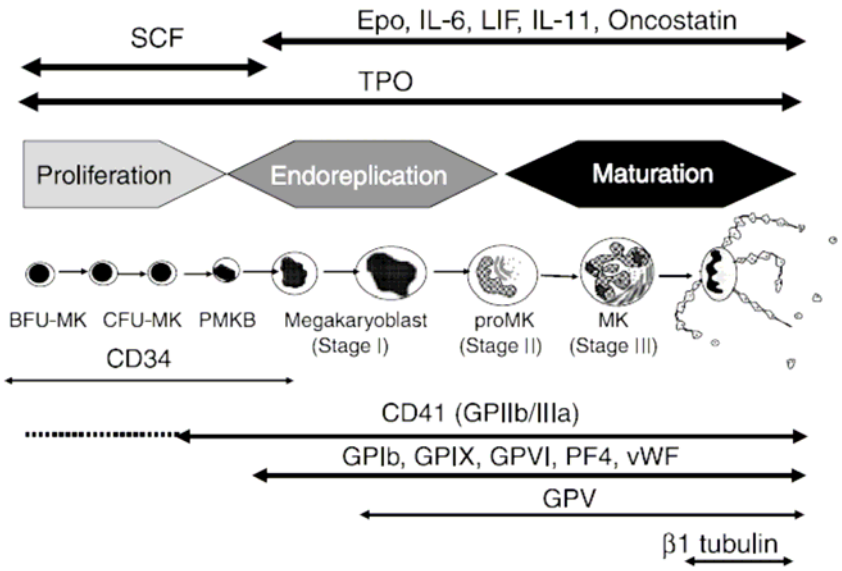

Fig. 2.2. Megakaryocytic differentiation [94]

2.2.2 Proplatelet formation

When MK cells differentiate into the final stage, they locate close to sinusoidal vessels in bone marrow and manage to release platelets [122]. Currently, the proplatelets formation model is supported by *in vitro* and *in vivo* data to explain the mechanism of platelet biogenesis [122, 123]. *In vitro* assays suggest that mature MK cells can extend long and complex cytoplasmic processes, termed proplatelets [123]. There are multiple platelet-size beads, which are connected by cytoplasmic bridges, along the proplatelet stems. It is considered that platelets are released from the tips of proplatelets. The platelets, which are released from MKs displaying proplatelets, show similar morphology and function as platelets in peripheral blood [123, 124]. The purpose of proplatelets is to transport platelet components such as granules, organelles and ribosomes from MK to the tips of the proplatelets. Microtubule dynamic movement is essential for the elaboration of proplatelets. The microtubules are organized into bundles, which are orientated in parallel to the plasma membrane of proplatelets. The sliding movement of microtubule bundles relative to each other contributes to the elongation of proplatelets. It is reported that dynein and kinesin are motor protein to move cargo along microtubules into the developing proplatelets [125]. Dynein contributes to the sliding movement of microtubules in proplatelets, and kinesin is involved in the transport of granules and organelles within the proplatelets [125, 126]. Besides the role of microtubules in proplatelet formation, actin organisation is also reported to affect proplatelets [123, 127]. Inhibition of actin polymerisation reduces branching of proplatelet shafts and decreases the number of proplatelet tips, where platelet shedding occurs [123, 127].

Although proplatelet formation is usually observed in *in vitro* culture, it was unclear until recently whether PP also form *in vivo* and contribute to platelet biogenesis. Recently, CD41-YFP$^{ki/wt}$ knock in mice were generated and enable to express YFP primarily in megakaryocyte and platelets [122, 128]. Junt et al used CD41-YFP$^{ki/wt}$ mice in combination with multiphoton intravital microscopy to directly visualize thrombopoiesis in the bone marrow in living mice [122]. They detected that proplatelet shed platelets into

sinusoids *in vivo* and further proved the proplatelet hypothesis. It is worth to notice that all the fragments, dissociated from MK into vessel, are much bigger than platelets. Hence, proplatelet fragmentation seems to continue in peripheral blood to generate final individual platelets. Blood shear stress is considered to contribute to proplatelet fragmentation [122].

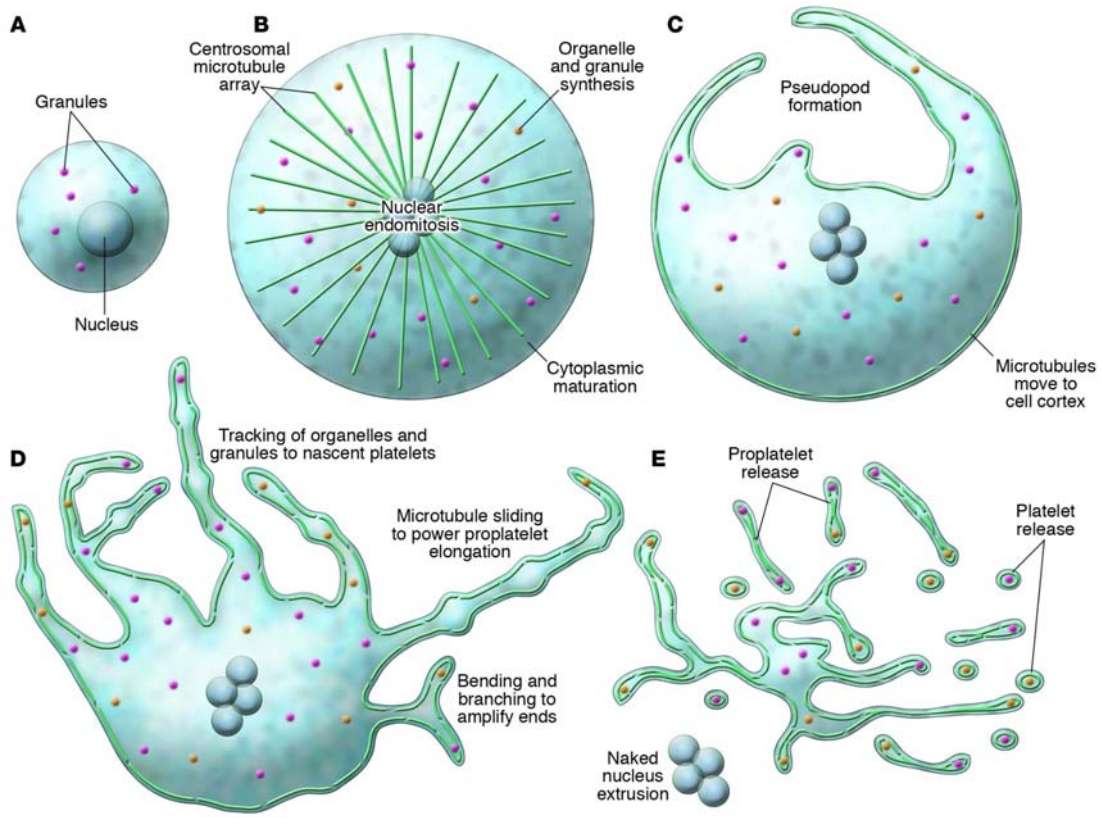

Fig. 2.3. Mechanics of proplatelet elaboration [129]

2.3 Conclusion

Despite the recent progress in understanding the mechanism of thrombopoiesis, many questions still remain to be addressed. How do the proplatelets find their way into the vessels? Which biological signals guide proplatelets into sinusoids? What triggers platelet shedding in the blood? What is the molecular mechanism behind platelet release? S1P is an important bioactive sphingolipid metabolite with pleiotropic cellular functions. Whether S1P also acts as an important biological signal to control thrombopoiesis remains unclear. In this thesis, we therefore investigated in details the role of S1P for thrombopoiesis.

2.4 References

1. Spiegel, S. and S. Milstien, *Sphingosine-1-phosphate: an enigmatic signalling lipid.* Nat Rev Mol Cell Biol, 2003. **4**(5): p. 397-407.
2. Tani, M., M. Ito, and Y. Igarashi, *Ceramide/sphingosine/sphingosine 1-phosphate metabolism on the cell surface and in the extracellular space.* Cell Signal, 2007. **19**(2): p. 229-37.
3. Zhang, H., et al., *Sphingosine-1-phosphate, a novel lipid, involved in cellular proliferation.* J Cell Biol, 1991. **114**(1): p. 155-67.
4. Olivera, A. and S. Spiegel, *Sphingosine-1-phosphate as second messenger in cell proliferation induced by PDGF and FCS mitogens.* Nature, 1993. **365**(6446): p. 557-60.
5. Cuvillier, O., et al., *Suppression of ceramide-mediated programmed cell death by sphingosine-1-phosphate.* Nature, 1996. **381**(6585): p. 800-3.
6. Takabe, K., et al., *"Inside-out" signaling of sphingosine-1-phosphate: therapeutic targets.* Pharmacol Rev, 2008. **60**(2): p. 181-95.
7. Futerman, A.H. and Y.A. Hannun, *The complex life of simple sphingolipids.* EMBO Rep, 2004. **5**(8): p. 777-82.
8. Merrill, A.H., Jr., *De novo sphingolipid biosynthesis: a necessary, but dangerous, pathway.* J Biol Chem, 2002. **277**(29): p. 25843-6.
9. Kolesnick, R. and Y.A. Hannun, *Ceramide and apoptosis.* Trends Biochem Sci, 1999. **24**(6): p. 224-5; author reply 227.
10. Hanada, K., et al., *Molecular machinery for non-vesicular trafficking of ceramide.* Nature, 2003. **426**(6968): p. 803-9.
11. van Meer, G. and J.C. Holthuis, *Sphingolipid transport in eukaryotic cells.* Biochim Biophys Acta, 2000. **1486**(1): p. 145-70.
12. Maceyka, M., S. Milstien, and S. Spiegel, *Sphingosine kinases, sphingosine-1-phosphate and sphingolipidomics.* Prostaglandins Other Lipid Mediat, 2005. **77**(1-4): p. 15-22.
13. Le Stunff, H., et al., *Sphingosine-1-phosphate phosphohydrolase in regulation of sphingolipid metabolism and apoptosis.* J Cell Biol, 2002. **158**(6): p. 1039-49.
14. Ogawa, C., et al., *Identification and characterization of a novel human sphingosine-1-phosphate phosphohydrolase, hSPP2.* J Biol Chem, 2003. **278**(2): p. 1268-72.
15. Maceyka, M., S. Milstien, and S. Spiegel, *Measurement of mammalian sphingosine-1-phosphate phosphohydrolase activity in vitro and in vivo.* Methods Enzymol, 2007. **434**: p. 243-56.
16. Rosen, H., et al., *Sphingosine 1-phosphate receptor signaling.* Annu Rev Biochem, 2009. **78**: p. 743-68.
17. Brinkmann, V., *Sphingosine 1-phosphate receptors in health and disease: mechanistic insights from gene deletion studies and reverse pharmacology.* Pharmacol Ther, 2007. **115**(1): p. 84-105.

18. Spiegel, S. and S. Milstien, *Sphingosine 1-phosphate, a key cell signaling molecule.* J Biol Chem, 2002. **277**(29): p. 25851-4.
19. Hla, T. and T. Maciag, *An abundant transcript induced in differentiating human endothelial cells encodes a polypeptide with structural similarities to G-protein-coupled receptors.* J Biol Chem, 1990. **265**(16): p. 9308-13.
20. Ishii, I., et al., *Lysophospholipid receptors: signaling and biology.* Annu Rev Biochem, 2004. **73**: p. 321-54.
21. Zondag, G.C., et al., *Sphingosine 1-phosphate signalling through the G-protein-coupled receptor Edg-1.* Biochem J, 1998. **330 (Pt 2)**: p. 605-9.
22. Lee, M.J., et al., *Lysophosphatidic acid stimulates the G-protein-coupled receptor EDG-1 as a low affinity agonist.* J Biol Chem, 1998. **273**(34): p. 22105-12.
23. Kluk, M.J. and T. Hla, *Signaling of sphingosine-1-phosphate via the S1P/EDG-family of G-protein-coupled receptors.* Biochim Biophys Acta, 2002. **1582**(1-3): p. 72-80.
24. Siehler, S. and D.R. Manning, *Pathways of transduction engaged by sphingosine 1-phosphate through G protein-coupled receptors.* Biochim Biophys Acta, 2002. **1582**(1-3): p. 94-9.
25. Takuwa, Y., *Subtype-specific differential regulation of Rho family G proteins and cell migration by the Edg family sphingosine-1-phosphate receptors.* Biochim Biophys Acta, 2002. **1582**(1-3): p. 112-20.
26. Lee, M.J., et al., *Akt-mediated phosphorylation of the G protein-coupled receptor EDG-1 is required for endothelial cell chemotaxis.* Mol Cell, 2001. **8**(3): p. 693-704.
27. Zhang, Q., et al., *Sphingosine 1-phosphate stimulates fibronectin matrix assembly through a Rho-dependent signal pathway.* Blood, 1999. **93**(9): p. 2984-90.
28. Ishii, I., et al., *Selective loss of sphingosine 1-phosphate signaling with no obvious phenotypic abnormality in mice lacking its G protein-coupled receptor, LP(B3)/EDG-3.* J Biol Chem, 2001. **276**(36): p. 33697-704.
29. Liu, Y., et al., *Edg-1, the G protein-coupled receptor for sphingosine-1-phosphate, is essential for vascular maturation.* J Clin Invest, 2000. **106**(8): p. 951-61.
30. Allende, M.L., T. Yamashita, and R.L. Proia, *G-protein-coupled receptor S1P1 acts within endothelial cells to regulate vascular maturation.* Blood, 2003. **102**(10): p. 3665-7.
31. McVerry, B.J. and J.G. Garcia, *Endothelial cell barrier regulation by sphingosine 1-phosphate.* J Cell Biochem, 2004. **92**(6): p. 1075-85.
32. Matloubian, M., et al., *Lymphocyte egress from thymus and peripheral lymphoid organs is dependent on S1P receptor 1.* Nature, 2004. **427**(6972): p. 355-60.
33. Okazaki, H., et al., *Molecular cloning of a novel putative G protein-coupled receptor expressed in the cardiovascular system.* Biochem Biophys Res Commun, 1993. **190**(3): p. 1104-9.
34. MacLennan, A.J., et al., *Cloning and characterization of a putative G-protein coupled receptor potentially involved in development.* Mol Cell Neurosci, 1994. **5**(3): p. 201-9.
35. Windh, R.T., et al., *Differential coupling of the sphingosine 1-phosphate receptors Edg-1, Edg-3, and H218/Edg-5 to the G(i), G(q), and G(12) families of heterotrimeric G proteins.* J Biol Chem, 1999. **274**(39): p. 27351-8.
36. Gonda, K., et al., *The novel sphingosine 1-phosphate receptor AGR16 is coupled via*

pertussis toxin-sensitive and -insensitive G-proteins to multiple signalling pathways. Biochem J, 1999. **337 (Pt 1)**: p. 67-75.

37. Zhang, G., et al., *Comparative analysis of three murine G-protein coupled receptors activated by sphingosine-1-phosphate.* Gene, 1999. **227**(1): p. 89-99.
38. MacLennan, A.J., et al., *An essential role for the H218/AGR16/Edg-5/LP(B2) sphingosine 1-phosphate receptor in neuronal excitability.* Eur J Neurosci, 2001. **14**(2): p. 203-9.
39. Ishii, I., et al., *Marked perinatal lethality and cellular signaling deficits in mice null for the two sphingosine 1-phosphate (S1P) receptors, S1P(2)/LP(B2)/EDG-5 and S1P(3)/LP(B3)/EDG-3.* J Biol Chem, 2002. **277**(28): p. 25152-9.
40. Kono, M., et al., *Deafness and stria vascularis defects in S1P2 receptor-null mice.* J Biol Chem, 2007. **282**(14): p. 10690-6.
41. Okamoto, H., et al., *Inhibitory regulation of Rac activation, membrane ruffling, and cell migration by the G protein-coupled sphingosine-1-phosphate receptor EDG5 but not EDG1 or EDG3.* Mol Cell Biol, 2000. **20**(24): p. 9247-61.
42. Ishii, M., et al., *Sphingosine-1-phosphate mobilizes osteoclast precursors and regulates bone homeostasis.* Nature, 2009. **458**(7237): p. 524-8.
43. Ishii, M., et al., *Chemorepulsion by blood S1P regulates osteoclast precursor mobilization and bone remodeling in vivo.* J Exp Med. **207**(13): p. 2793-8.
44. Yamaguchi, F., et al., *Molecular cloning of the novel human G protein-coupled receptor (GPCR) gene mapped on chromosome 9.* Biochem Biophys Res Commun, 1996. **227**(2): p. 608-14.
45. Kon, J., et al., *Comparison of intrinsic activities of the putative sphingosine 1-phosphate receptor subtypes to regulate several signaling pathways in their cDNA-transfected Chinese hamster ovary cells.* J Biol Chem, 1999. **274**(34): p. 23940-7.
46. Van Brocklyn, J.R., et al., *Sphingosine 1-phosphate-induced cell rounding and neurite retraction are mediated by the G protein-coupled receptor H218.* J Biol Chem, 1999. **274**(8): p. 4626-32.
47. Forrest, M., et al., *Immune cell regulation and cardiovascular effects of sphingosine 1-phosphate receptor agonists in rodents are mediated via distinct receptor subtypes.* J Pharmacol Exp Ther, 2004. **309**(2): p. 758-68.
48. Sanchez, T., et al., *Induction of vascular permeability by the sphingosine-1-phosphate receptor-2 (S1P2R) and its downstream effectors ROCK and PTEN.* Arterioscler Thromb Vasc Biol, 2007. **27**(6): p. 1312-8.
49. Yamazaki, Y., et al., *Edg-6 as a putative sphingosine 1-phosphate receptor coupling to Ca(2+) signaling pathway.* Biochem Biophys Res Commun, 2000. **268**(2): p. 583-9.
50. Graler, M.H., et al., *The sphingosine 1-phosphate receptor S1P4 regulates cell shape and motility via coupling to Gi and G12/13.* J Cell Biochem, 2003. **89**(3): p. 507-19.
51. Golfier, S., et al., *Shaping of terminal megakaryocyte differentiation and proplatelet development by sphingosine-1-phosphate receptor S1P4.* FASEB J. **24**(12): p. 4701-10.
52. Schulze, T., et al., *Sphingosine-1-phospate receptor 4 (S1P4) deficiency profoundly affects dendritic cell function and TH17-cell differentiation in a murine model.* FASEB

J.

53. Glickman, M., et al., *Molecular cloning, tissue-specific expression, and chromosomal localization of a novel nerve growth factor-regulated G-protein- coupled receptor, nrg-1.* Mol Cell Neurosci, 1999. **14**(2): p. 141-52.
54. Im, D.S., et al., *Characterization of the human and mouse sphingosine 1-phosphate receptor, S1P5 (Edg-8): structure-activity relationship of sphingosine1-phosphate receptors.* Biochemistry, 2001. **40**(46): p. 14053-60.
55. Malek, R.L., et al., *Nrg-1 belongs to the endothelial differentiation gene family of G protein-coupled sphingosine-1-phosphate receptors.* J Biol Chem, 2001. **276**(8): p. 5692-9.
56. Niedernberg, A., et al., *Comparative analysis of human and rat S1P(5) (edg8): differential expression profiles and sensitivities to antagonists.* Biochem Pharmacol, 2002. **64**(8): p. 1243-50.
57. Jaillard, C., et al., *Edg8/S1P5: an oligodendroglial receptor with dual function on process retraction and cell survival.* J Neurosci, 2005. **25**(6): p. 1459-69.
58. Walzer, T., et al., *Natural killer cell trafficking in vivo requires a dedicated sphingosine 1-phosphate receptor.* Nat Immunol, 2007. **8**(12): p. 1337-44.
59. Sato, K. and F. Okajima, *Role of sphingosine 1-phosphate in anti-atherogenic actions of high-density lipoprotein.* World J Biol Chem. **1**(11): p. 327-37.
60. Yatomi, Y., et al., *Sphingosine-1-phosphate: a platelet-activating sphingolipid released from agonist-stimulated human platelets.* Blood, 1995. **86**(1): p. 193-202.
61. Pappu, R., et al., *Promotion of lymphocyte egress into blood and lymph by distinct sources of sphingosine-1-phosphate.* Science, 2007. **316**(5822): p. 295-8.
62. Venkataraman, K., et al., *Vascular endothelium as a contributor of plasma sphingosine 1-phosphate.* Circ Res, 2008. **102**(6): p. 669-76.
63. Jessup, W., *Lipid metabolism: sources and stability of plasma sphingosine-1-phosphate.* Curr Opin Lipidol, 2008. **19**(5): p. 543-4.
64. Schwab, S.R. and J.G. Cyster, *Finding a way out: lymphocyte egress from lymphoid organs.* Nat Immunol, 2007. **8**(12): p. 1295-301.
65. Schwab, S.R., et al., *Lymphocyte sequestration through S1P lyase inhibition and disruption of S1P gradients.* Science, 2005. **309**(5741): p. 1735-9.
66. Massberg, S., et al., *Immunosurveillance by hematopoietic progenitor cells trafficking through blood, lymph, and peripheral tissues.* Cell, 2007. **131**(5): p. 994-1008.
67. Hla, T., K. Venkataraman, and J. Michaud, *The vascular S1P gradient-cellular sources and biological significance.* Biochim Biophys Acta, 2008. **1781**(9): p. 477-82.
68. Maceyka, M., et al., *Sphingosine kinase, sphingosine-1-phosphate, and apoptosis.* Biochim Biophys Acta, 2002. **1585**(2-3): p. 193-201.
69. Liu, H., et al., *Sphingosine kinases: a novel family of lipid kinases.* Prog Nucleic Acid Res Mol Biol, 2002. **71**: p. 493-511.
70. Kohama, T., et al., *Molecular cloning and functional characterization of murine sphingosine kinase.* J Biol Chem, 1998. **273**(37): p. 23722-8.
71. Liu, H., et al., *Molecular cloning and functional characterization of a novel mammalian sphingosine kinase type 2 isoform.* J Biol Chem, 2000. **275**(26): p. 19513-20.
72. Billich, A., et al., *Phosphorylation of the immunomodulatory drug FTY720 by*

sphingosine kinases. J Biol Chem, 2003. **278**(48): p. 47408-15.

73. Brinkmann, V., et al., *The immune modulator FTY720 targets sphingosine 1-phosphate receptors.* J Biol Chem, 2002. **277**(24): p. 21453-7.
74. Mandala, S., et al., *Alteration of lymphocyte trafficking by sphingosine-1-phosphate receptor agonists.* Science, 2002. **296**(5566): p. 346-9.
75. Strub, G.M., et al., *Extracellular and intracellular actions of sphingosine-1-phosphate.* Adv Exp Med Biol. **688**: p. 141-55.
76. Johnson, K.R., et al., *PKC-dependent activation of sphingosine kinase 1 and translocation to the plasma membrane. Extracellular release of sphingosine-1-phosphate induced by phorbol 12-myristate 13-acetate (PMA).* J Biol Chem, 2002. **277**(38): p. 35257-62.
77. Scherer, E.Q., et al., *Tumor necrosis factor-alpha enhances microvascular tone and reduces blood flow in the cochlea via enhanced sphingosine-1-phosphate signaling.* Stroke. **41**(11): p. 2618-24.
78. Melendez, A.J. and F.B. Ibrahim, *Antisense knockdown of sphingosine kinase 1 in human macrophages inhibits C5a receptor-dependent signal transduction, Ca2+ signals, enzyme release, cytokine production, and chemotaxis.* J Immunol, 2004. **173**(3): p. 1596-603.
79. Ibrahim, F.B., S.J. Pang, and A.J. Melendez, *Anaphylatoxin signaling in human neutrophils. A key role for sphingosine kinase.* J Biol Chem, 2004. **279**(43): p. 44802-11.
80. Toman, R.E., et al., *Differential transactivation of sphingosine-1-phosphate receptors modulates NGF-induced neurite extension.* J Cell Biol, 2004. **166**(3): p. 381-92.
81. Rosenfeldt, H.M., et al., *EDG-1 links the PDGF receptor to Src and focal adhesion kinase activation leading to lamellipodia formation and cell migration.* FASEB J, 2001. **15**(14): p. 2649-59.
82. Hobson, J.P., et al., *Role of the sphingosine-1-phosphate receptor EDG-1 in PDGF-induced cell motility.* Science, 2001. **291**(5509): p. 1800-3.
83. Alvarez, S.E., S. Milstien, and S. Spiegel, *Autocrine and paracrine roles of sphingosine-1-phosphate.* Trends Endocrinol Metab, 2007. **18**(8): p. 300-7.
84. Igarashi, N., et al., *Sphingosine kinase 2 is a nuclear protein and inhibits DNA synthesis.* J Biol Chem, 2003. **278**(47): p. 46832-9.
85. Maceyka, M., et al., *SphK1 and SphK2, sphingosine kinase isoenzymes with opposing functions in sphingolipid metabolism.* J Biol Chem, 2005. **280**(44): p. 37118-29.
86. Ding, G., et al., *Protein kinase D-mediated phosphorylation and nuclear export of sphingosine kinase 2.* J Biol Chem, 2007. **282**(37): p. 27493-502.
87. Van Brocklyn, J.R., et al., *Sphingosine kinase-1 expression correlates with poor survival of patients with glioblastoma multiforme: roles of sphingosine kinase isoforms in growth of glioblastoma cell lines.* J Neuropathol Exp Neurol, 2005. **64**(8): p. 695-705.
88. French, K.J., et al., *Discovery and evaluation of inhibitors of human sphingosine kinase.* Cancer Res, 2003. **63**(18): p. 5962-9.
89. Kihara, A., Y. Anada, and Y. Igarashi, *Mouse sphingosine kinase isoforms SPHK1a and SPHK1b differ in enzymatic traits including stability, localization, modification, and*

oligomerization. J Biol Chem, 2006. **281**(7): p. 4532-9.

90. Shu, X., et al., *Sphingosine kinase mediates vascular endothelial growth factor-induced activation of ras and mitogen-activated protein kinases.* Mol Cell Biol, 2002. **22**(22): p. 7758-68.
91. Sukocheva, O., et al., *Estrogen transactivates EGFR via the sphingosine 1-phosphate receptor Edg-3: the role of sphingosine kinase-1.* J Cell Biol, 2006. **173**(2): p. 301-10.
92. Liu, H., et al., *Sphingosine kinase type 2 is a putative BH3-only protein that induces apoptosis.* J Biol Chem, 2003. **278**(41): p. 40330-6.
93. Hait, N.C., et al., *Regulation of histone acetylation in the nucleus by sphingosine-1-phosphate.* Science, 2009. **325**(5945): p. 1254-7.
94. Chang, Y., et al., *From hematopoietic stem cells to platelets.* J Thromb Haemost, 2007. **5 Suppl 1**: p. 318-27.
95. Debili, N., et al., *Characterization of a bipotent erythro-megakaryocytic progenitor in human bone marrow.* Blood, 1996. **88**(4): p. 1284-96.
96. Adolfsson, J., et al., *Identification of Flt3+ lympho-myeloid stem cells lacking erythro-megakaryocytic potential a revised road map for adult blood lineage commitment.* Cell, 2005. **121**(2): p. 295-306.
97. Forsberg, E.C., et al., *New evidence supporting megakaryocyte-erythrocyte potential of flk2/flt3+ multipotent hematopoietic progenitors.* Cell, 2006. **126**(2): p. 415-26.
98. Long, M.W., et al., *Phorbol diesters stimulate the development of an early murine progenitor cell. The burst-forming unit-megakaryocyte.* J Clin Invest, 1985. **76**(2): p. 431-8.
99. Briddell, R.A., et al., *Characterization of the human burst-forming unit-megakaryocyte.* Blood, 1989. **74**(1): p. 145-51.
100. McLeod, D.L., M.M. Shreve, and A.A. Axelrad, *Induction of megakaryocyte colonies with platelet formation in vitro.* Nature, 1976. **261**(5560): p. 492-4.
101. Vainchenker, W., et al., *Megakaryocyte colony formation from human bone marrow precursors.* Blood, 1979. **54**(4): p. 940-5.
102. Schulze, H. and R.A. Shivdasani, *Molecular mechanisms of megakaryocyte differentiation.* Semin Thromb Hemost, 2004. **30**(4): p. 389-98.
103. Radley, J.M. and C.J. Haller, *The demarcation membrane system of the megakaryocyte: a misnomer?* Blood, 1982. **60**(1): p. 213-9.
104. Nakorn, T.N., T. Miyamoto, and I.L. Weissman, *Characterization of mouse clonogenic megakaryocyte progenitors.* Proc Natl Acad Sci U S A, 2003. **100**(1): p. 205-10.
105. Mathur, A., et al., *Assays of megakaryocyte development: surface antigen expression, ploidy, and size.* Methods Mol Biol, 2004. **272**: p. 309-22.
106. Debili, N., et al., *Different expression of CD41 on human lymphoid and myeloid progenitors from adults and neonates.* Blood, 2001. **97**(7): p. 2023-30.
107. Vainchenker, W. and N. Kieffer, *Human megakaryocytopoiesis: in vitro regulation and characterization of megakaryocytic precursor cells by differentiation markers.* Blood Rev, 1988. **2**(2): p. 102-7.
108. Debili, N., et al., *Expression of CD34 and platelet glycoproteins during human megakaryocytic differentiation.* Blood, 1992. **80**(12): p. 3022-35.
109. Debili, N., F. Louache, and W. Vainchenker, *Isolation and culture of megakaryocyte*

precursors. Methods Mol Biol, 2004. **272**: p. 293-308.

110. Bartley, T.D., et al., *Identification and cloning of a megakaryocyte growth and development factor that is a ligand for the cytokine receptor Mpl.* Cell, 1994. **77**(7): p. 1117-24.
111. de Sauvage, F.J., et al., *Stimulation of megakaryocytopoiesis and thrombopoiesis by the c-Mpl ligand.* Nature, 1994. **369**(6481): p. 533-8.
112. Kaushansky, K., et al., *Promotion of megakaryocyte progenitor expansion and differentiation by the c-Mpl ligand thrombopoietin.* Nature, 1994. **369**(6481): p. 568-71.
113. Lok, S., et al., *Cloning and expression of murine thrombopoietin cDNA and stimulation of platelet production in vivo.* Nature, 1994. **369**(6481): p. 565-8.
114. Kaushansky, K., *The enigmatic megakaryocyte gradually reveals its secrets.* Bioessays, 1999. **21**(4): p. 353-60.
115. Debili, N., et al., *The Mpl receptor is expressed in the megakaryocytic lineage from late progenitors to platelets.* Blood, 1995. **85**(2): p. 391-401.
116. Cramer, E.M., et al., *Ultrastructure of platelet formation by human megakaryocytes cultured with the Mpl ligand.* Blood, 1997. **89**(7): p. 2336-46.
117. Choi, E.S., et al., *Platelets generated in vitro from proplatelet-displaying human megakaryocytes are functional.* Blood, 1995. **85**(2): p. 402-13.
118. de Sauvage, F.J., et al., *Physiological regulation of early and late stages of megakaryocytopoiesis by thrombopoietin.* J Exp Med, 1996. **183**(2): p. 651-6.
119. Schattner, M., et al., *Thrombopoietin-stimulated ex vivo expansion of human bone marrow megakaryocytes.* Stem Cells, 1996. **14**(2): p. 207-14.
120. Robinson, B.E., H.E. McGrath, and P.J. Quesenberry, *Recombinant murine granulocyte macrophage colony-stimulating factor has megakaryocyte colony-stimulating activity and augments megakaryocyte colony stimulation by interleukin 3.* J Clin Invest, 1987. **79**(6): p. 1648-52.
121. Ku, H., et al., *Thrombopoietin, the ligand for the Mpl receptor, synergizes with steel factor and other early acting cytokines in supporting proliferation of primitive hematopoietic progenitors of mice.* Blood, 1996. **87**(11): p. 4544-51.
122. Junt, T., et al., *Dynamic visualization of thrombopoiesis within bone marrow.* Science, 2007. **317**(5845): p. 1767-70.
123. Italiano, J.E., Jr., et al., *Blood platelets are assembled principally at the ends of proplatelet processes produced by differentiated megakaryocytes.* J Cell Biol, 1999. **147**(6): p. 1299-312.
124. Choi, E.S., et al., *Functional human platelet generation in vitro and regulation of cytoplasmic process formation.* C R Acad Sci III, 1995. **318**(3): p. 387-93.
125. Patel, S.R., et al., *Differential roles of microtubule assembly and sliding in proplatelet formation by megakaryocytes.* Blood, 2005. **106**(13): p. 4076-85.
126. Richardson, J.L., et al., *Mechanisms of organelle transport and capture along proplatelets during platelet production.* Blood, 2005. **106**(13): p. 4066-75.
127. Tablin, F., M. Castro, and R.M. Leven, *Blood platelet formation in vitro. The role of the cytoskeleton in megakaryocyte fragmentation.* J Cell Sci, 1990. **97 (Pt 1)**: p. 59-70.
128. Zhang, J., et al., *CD41-YFP mice allow in vivo labeling of megakaryocytic cells and reveal a subset of platelets hyperreactive to thrombin stimulation.* Exp Hematol, 2007.

35(3): p. 490-499.

129. Patel, S.R., J.H. Hartwig, and J.E. Italiano, Jr., *The biogenesis of platelets from megakaryocyte proplatelets.* J Clin Invest, 2005. **115**(12): p. 3348-54.

Chapter 3: The function of S1P receptors in thrombopoiesis

3.1 Introduction:

Here we investigated the role of S1P for platelets biogenesis. Using two-photon intravital microscopy to visualize MKs in BM, we provided strong evidences to support the existence of proplatelets *in vivo* and demonstrated that the direction of proplatelet formation is controlled by a transendothelial S1P gradient through the S1P1 receptor. Our dynamic visualization of MKs enables us to visualize proplatelet fragmentation events *in vivo* and revealed that S1P enhances the shedding of platelets from proplatelets by binding to the S1P1 receptor.

3.2 Materials and methods:

3.2.1 Material

VPC23019 and W146 were purchased from Avanti Polar Lipids (Al, USA) and prepared according to the manuals. D-erythro-Sphingosine-1-phospate (S1P), SEW2871 was purchased from CALBIOCHEM (San Diego, CA, USA)

3.2.2 Mice

C57BL/6J (CD45.2+), B6.SJL-PtprcPep3/BoyCrl (CD45.1 +) and CD1 mice were purchased from Charles River Laboratories (Sulzfeld, Germany). Transgenic β-actin EGFP mice (C57BL/6J) ubiquitously expressing enhanced GFP driven by the chicken β-actin promoter and CMV enhancer were obtained from von Andrian UH (Immune Disease Institute and Department of Pathology, Harvard Medical School, USA). $S1P1^{+/-}$ mice were generated and kindly provided from von Andrian UH (Immune Disease Institute and Department of Pathology, Harvard Medical School, USA). $S1P2^{-/-}$ mice were kindly provided from Steffen-Sebastian Bolz (Department of Physiology and Heart &

Stroke/Richard Lewar Centre of Excellence in Cardiovascular Research, University of Toronto, Canada) and described previously [1]. Sphk1$^{-/-}$, Sphk2$^{-/-}$ and S1P4$^{-/-}$ mice were produced and kindly provided from Danilo Guerini (Novartis Institute for BioMedical Research, Basel, Switzerland). CD41-YFP$^{ki/+}$ mice were described previously [2] and kindly provided from Thomas Graf (Center of Genomic Regulation and ICREA, Spain). To generate S1P1$^{+/-}$ x CD41-YFP$^{ki/+}$, S1P2$^{-/-}$ x CD41-YFP$^{ki/+}$, S1P4$^{-/-}$ x CD41-YFP$^{ki/+}$ and Sphk2$^{-/-}$ x CD41-YFP$^{ki/+}$ mice, the CD41-YFP$^{ki/+}$ mouse strain was crossed with S1P1$^{+/-}$ mice, S1P2$^{-/-}$, S1P4$^{-/-}$, and Sphk2$^{-/-}$ respectively. PF4-cre and ROSA26-flox-stop-flox-EYFP mice were obtained from The Jackson Laboratory. S1P1$^{fl/fl}$ mice were obtained from Richard Proia (Genetics of Development and Disease Branch, National Institutes of Health, Bethesda, Maryland, USA). PF4-cre mice were crossed with ROSA26-flox-stop-flox-EYFP mice to get PF4-cre-EYFP mice. S1P1$^{fl/fl}$ mice were mated to Mx1-cre or Pf4-cre mice. Mx1-cre expression was induced by intraperitoneally injecting 500 µg of polyinosinic-polycytidylic acid (pIpC) (Sigma Aldrich), on seven alternative days, into S1P1$^{fl/fl}$ or S1P1$^{+/+}$ chimaeras. All animals were bred and maintained at the animal facility of the German Heart Centre Munich. Age- and gender-matched mice were used in these studies. All experimental procedures performed on animals met the requirements of the German legislation on protection of animals and were approved by the Government of Bavaria/Germany.

3.2.3 Chimeras

To create S1P1-deficient fetal liver chimaeras, approximately 1 x 10^6 fetal liver mononuclear cells (CD45.2 +) isolated from E12.5 embryos of parenteral mice S1P1$^{+/-}$ were injected into lethally irradiated (two doses of 6.5 Gy) CD45.1 mice (B6.SJL-PtprcPep3/BoyCrl) via tail vein. The genotypes of the embryos were confirmed by polymerase chain reaction (PCR). S1P1 deficient mice were amplified by further transplanting S1P1 deficient bone marrow mononuclear cells in a secondary transplantation step after confirming that more than 90% of the blood cells were donor derived.

3.2.4 Lentiviral and retroviral infection

We constructed GPIbα-EGFP (coding EGFP under the transcriptional control of 238-bp GpIb alpha prmoter), GpIIb-cre (coding Cre recombinase under the GpIIb promoter), GPIbα -S1P1 (coding S1P1 under the GpIb alpha promoter) lentiviral vectors. Bone marrow or fetal liver cells were incubated with lentiviral particles and 8 μg/ml polybrene (Sigma Aldrich) at 37 °C for 12 hours in serum-free medium supplemented with 1% BSA, 100 ng/ml Flt3-ligand, 100 ng/ml stem cell factor (SCF) (Sigma Aldrich), 20 ng/ml Tpo (ImmunoTools, Friesoythe, Germany). After transduction with lentiviral vectors, BM and FL cells were injected into irradiated mice (two doses of 6.5 Gy). For reexpression of S1P1 in $S1P1^{-/-}$ megakaryocytes, $S1P1^{-/-}$ FL cells were transduced with Lenti-GPIbα-S1P1 viral vectors to express S1P1 under the control of megakaryocyte promoter GPIbα. 1×10^5 $S1P1^{-/-}$ FL cells transduced with lenti-GPIbα-S1P1 or empty lentiviral particles and 2×10^6 bone morrow cells from β-actin EGFP mice were coinjected into irradiated CD45.1 mice. The percentage of $EGFP^+$ positive platelets was determined by flow cytometry. Since all the chimerism of all chimaeras were more than 99% and 100% of platelets from β-actin EGFP mice were $EGFP^+$, almost all the $EGFP^-$ platelets were from $S1P1^{-/-}$ FL donor cells. For conditional deletion of S1P1 in megakaryocytes, $S1P1^{fl/fl}$ BM cells were transduced with lenti-GPIIb-cre viral vectors to express Cre recombinase under the control of the megakaryocytic promoter GPIIb and transferred into irradiated mice. S1P1 floxed allele was excised in megakaryocytes in $S1P1^{fl/fl}$ BM chimaeras.

3.2.5 Quantitative RT-PCR

RNA was isolated with the RNeasy micro kit (Qiagen, Hilden, Germany) and quantified with RiboGreen reagent (Invitrogen, Kalsruhe, Germany). 0.5 μg RNA was used for cDNA synthesis with SuperScript II reverse transcriptase (Invitrogen, Kalsruhe, Germany). Quantitative real-time PCR was performed on ABI PRISM 7700 Sequence Detection System (Applied Biosystems, Weiterstadt, Germany). All reactions were performed in

triplicate in a total reaction volume of 20 µl using MaximaTM SYBR Green PCR Master mix (Fermentas, St. Leon-Rot, Germany) containing 300nM of each primer with the following parameters: 50°C for 2min followed by 95 °C for 10min, followed by 40 two steps cycles at 95°C for 15s and at 60°C for 1 min. Ct value was calculated by the Sequence Detection System software (Applied Biosystems, Weiterstadt, Germany). The absolute number of mRNA copies was determined according to the standard curve on the basis of constructed plasmids and normalized to Glyceraldehyde 3-phosphate dehydrogenase (GAPDH) mRNA levels. Primers sequences are in Appendix.

3.2.6 Platelet measurement

We anaesthetized mice with 5.0 Vol. % Isofluran (Forene®, Abbott GmbH, Wiesbaden) and 0.35 l/l oxygen. Using the facial vein technique we collected 90 µl 1:10-heparinized (Ratiopharm, Ulm, Germany) whole blood and diluted it 1:3 in PBS. We measured platelet counts by Sysmex (Norderstedt, Germany).

3.2.7 Serum Tpo measurement

200µl anticoagulated blood were collected from the facial vein, and kept at 4°C overnight, and then centrifuged at 2000 x g for 20min at 4°C to collect blood serum in the supernatant. Qunantikine Murine Tpo Immunoassay Kit (R&D Systems, Minneapolis, USA) was used to measure serum Tpo levels according to the manufacturer's protocol.

3.2.8 Immunostaining

Megakaryocytes were seeded on slides coated with poly-L-lysine and fixed in 4% paraformaldehyde (Pierce, Bonn, Germany) for 15min at room temperature. For staining of bone marrow tissue, we used serial frozen sections of 8 µm in thickness. All the slides were permeabilized with 0.1% Triton X-100 (Sigma, Deisenhofen, Germany) for 10min, except for the surface staining, and incubated with different primary antibodies overnight

at 4 °C and secondary antibody at room temperature for 1 hour and then mounted with mounting medium (DAKO, Harmberg, Germany). Antibodies included rabbit anti-mouse S1P1 (Zytomed, Berlin, Germany), Goat anti-S1P2 (Santa Cruz), Goat anti-S1P4 (Santa Cruz, Califomia, USA), rabbit anti-tubulin (Cell Signalling Technology, Danvers, MA, USA), Rabbit Anti-GFP, goat anti rabbit Alexa-488, rabbit anti goat Alexa-594 and DAPI nucleic acid stain (Invitrogen, Karlsruhe, Germany). For actin staining, we used rhodamine-phalloidin (Invitrogen, Karlsruhe, Germany) or Alexa-488-phalloidin (Invitrogen, Karlsruhe, Germany). The samples were examined using Leica Microscopy equipped with 40× objective lens (N=0.7) or 20× objective lens (N=0.5) and commercial CCD camera (Axiocam, CarlZeiss, Göttingen, Germany). Images were acquired by Axiovision software (CarlZeiss, Göttingen, Germany). For quantification of MKs number and size in BM, we counted the total number of MKs in five randomly selected 20× microscopic fields and the area of MK cell body was analyzed by imageJ software (open source NIH software, http://rsb.info.nih.gov/ij/).

3.2.9 Megakaryocyte culture

Mouse fetal livers were isolated from E12.5-14.5 embryos and kept in Dulbecco's Modified Eagle Medium (DMEM; Invitrogen, Karlsruhe, Germany) supplemented with 10% charcoal treated fetal bovine serum (FBS) (PAN, Aidenbach, Germany) in the presence of hTpo (ImmunoTools, Friesoythe, Germany) for 12 hours or 6 days to obtain immature or mature megakaryocytes in humidified 5% CO2/95% air incubator at 37°C. Mature megakaryocytes were enriched by bovine serum albumin (BSA) gradient centrifugation. Briefly, The BSA step gradient was prepared by placing PBS containing 1.5% BSA on top of PBS with 3% BSA (PAA, Austria). Cells were loaded on top of the gradient and spun at 1g for 30 minutes at room temperature. Mature megakaryocytes formed a pellet at the bottom of the tube. The mature megakaryocytes were enriched by BSA gradient, as described previously [2, 3]. For analysis of proplatelets, we distinguished and scored proplatelets in fetal liver culture according to the criteria mentioned in a previous report [4] under phase-contrast microscopy. The mature MKs were recorded on the basis of their

unique morphology of the megakaryocyte— that is, a large size, and high refringence (producing a clearly defined cell border). To compare the PPF formation in $S1P1^{-/-}$ and WT fetal liver cells culture, we incubated the cells in the presence of hTpo (100ng/ml) for 3 days and then recorded the number of mature MKs by hemocytometer and the number of MKs displaying proplatelets in the whole well of 24-well plates (Sarstedt, Newton, NC) by phase-contrast microscopy. For analysis of the short term effect of S1P on proplatelets, we firstly cultured fetal liver cells with 100ng/ml hTpo in DMEM for 4 days to get enough proplatelets in 24-well plates, and then MKs culture were treated with 10 μM S1P or vehicle. After 2 hours, the number of PPF was counted by phase-contrast microscopy.

3.2.10 Megakaryocyte colony-forming unit (CFU-MK) assay

We seeded 10, 000 bone marrow mononuclear cells into Megacult-C medium (Stem Cell Technologies) and scored CFU-MKs on day 5 according to the manufacturer's instructions.

3.2.11 Flow cytometry

For analysis of platelet size, heparinized blood was diluted 25 times with PBS and then stained with fluorescein isothiocyanate (FITC)-Conjugated rat anti mouse CD41 mAb (clone MwReg30, BD Pharmingen, Heidelberg, Germany) for 20 min at room temperature. Platelets were identified by forward and side scatter plotting and CD41 positivity. Mean platelet size was recorded as forward scatter (FSC) of platelets by flow cytometric analysis. For platelet life span experiment, the mice were injected with N-hydroxysuccinimide-biotin (30mg/kg) (Pierce, Bonn, Germany) via the lateral tail vein. After in vivo biotinylation, 20μl blood was collected from facial vein using heparin-tubes at different time point and diluted it 1:25 with PBS. Biotinylated platelets were detected by binding of phycoerythrin(PE)/cy7-conjugated streptavidin (eBioscience, CA, USA) and FITC- conjugated antibody to CD41. The percentage of biotinylated platelets on the first day was determined and used to normalize the percentage of biotinylated platelets on the

subsequent days to calculate the percentage of platelets remaining. The platelet half-lives and life spans of platelets were determined by linear regression of the data. For analysis of PPF fragmentation, fetal liver-derived MK culture were treated with various concentration of S1P or vehicle for 4 hours at 37°C and then stained with FITC-conjugated rat anti mouse CD41 mAb (clone MwReg30, BD Pharmingen, Heidelberg, Germany) and PE/cy5-conjugated anti–mouse CD61 (BD Pharmingen, Heidelberg, Germany) for 20 min at room temperature. The proplatelet population was identified by CD41+CD61+ and FSC character.

3.2.12 Fluorescence-activated cell sorting (FACS)

For isolation of immature megakaryocytes, E12.5-14.5 fetal liver cells were first cultured in hTpo-containing (100ng/ml) medium for 12 hours and incubated with the following antibodies for 30 min at room temperature: FITC–conjugated rat monoclonal anti–mouse CD41 (Becton Dickinson, Heidelberg, Germany), PE/cy5 anti-mouse CD34 (Biolegend, San Diego, California, USA). The immature megakaryocytes were identified as CD41+ /CD34+ and enriched by FACSAria cell sorter (BD, Heidelberg, Germany). For proplatelets isolation, the E12.5-E14.5 fetal liver cells were cultured in the presence of hTpo (100ng/ml) for 6 days and then stained with FITC-conjugated CD41 (BD, Heidelberg, Germany) and PE/cy5-CD61 antibody (BD Pharmingen, Heidelberg, Germany) at RT for 20min. To isolate BM-derived megakaryocytes, we sorted YFP postive BM cells from CD41-YFP$^{ki/+}$ mice using a FACSAria cell sorter.

3.2.13 Subclonning and transfection

hS1P1 and hS1P2 sequences were cloned into pCI-neo (Promega, Madison, WI, USA). The hS1P4 sequence lacking the stop codon was cloned into pEGFP-N1 vector (Clontech, Palo Alto, CA, USA) to generate a N-terminal GFP fusion protein. The Meg01 cell line was transfected with the above mentioned plasmids using Nucleofector Kit C and the Nucleofector technology (Amaxa, Cologne, Germany).

3.2.14 PPF direction assay

E12.5-14.5 fetal liver cells were cultured in hTpo-containing medium for 6 days and then MKs were isolated by a BSA gradient as mentioned above. MKs were resuspended in serum free DMEM (Gibco, Karlsruhe, Germany) adjusted to 1×10^5 cells/ml. MKs were loaded into chemotaxis µ-slides (ibidi, GmbH, Munich, Germany) coated with poly-L-lysine in a total volume of 10 µl per chamber and incubated at 37°C for 1 hour to allow cell attachment. 10 µM S1P or vehicle was applied into one reservoir. 1µM VPC23019 or vehicle was incubated with MKs 1 hour before treatment of S1P. MKs were cultured for 10 hours at 37°C and then imaged using a Axiovert microscope (Nikon Instruments, New York, USA). Images were analyzed using Photoshop CS (Adobe, USA).

3.2.15 Western Blot analysis

Fetal liver-derived MKs were starved for 2 hours prior to stimulation with 100 ng/ml hTpo (ImmunoTools) combined with 10 µM S1P or vehicle for 5 min. We detected the activity of p-MLC2 in MKs lysate as described previously [5]. L8057 cells were cultured in IMDM medium supplemented with 10% FCS and 25 ng/ml Tpo for 1 day and then starved overnight on 100 mm plates coated with 0.5% fatty acid-free BSA (Sigma Aldrich). The starved L8057 cells were simulated with 10 µM S1P or vehicle for 2 min. Rac1 activity were measured using Rac1 assay kit (Cell Biolab).

3.2.16 Two-photon intravital imaging of the bone marrow

We prepared the mouse calvarial bone marrow according to the protocol described previously [6]. Briefly, mice were anaesthetized with 5.0 Vol. % Isofluran (Forene®, Abbott GmbH, Wiesbaden) and 0.35 l/l oxygen. Narcosis was initialized by intraperitoneal injection of a solution of midazolam (5mg/kg body weight, Ratiopharm, Ulm, Germany), medetomidine (0.5mg/kg body weight, Pfizer, Berlin, Germany). The hair in the neck and on the skullcap was removed with hair removal lotion (MAXIM, Koeln, Germany). A PE-10

catheter was placed into the tail vein for injection of liquid. After skin incision the front parietal skull was exposed and a plastic ring was inserted in incision. The mouse head was immobilized on a custom-made stereotactic holder. We used a BioTech TriM Scope system based on a Ti: Sa laser (MaiTai, Spectra Physics, Darmstadt, Germany) and with TriM Scope Scanhead (LaVision BioTec, Bielefeld, Germany) to capture images through a 20× water immersion objective lens with NA =0.95 (Olympus, Hamburg, Germany). YFP were detected using a laser at a wavelength of 920nm through a 525/50nm filter. Vasculature was visualized by immediate administration of 2 MDa Tetramethylrhodamineisothiocyanato-dextran (TRITC-dextran, Invitrogen, Karlsruhe, Germany). We used a laser at a wavelength 800nm or 920nm to excite TRITC-dextran and detect emission signal through 560-615nm filter. Images were acquired with Inspector software (LaVisionBioTec, Bielefeld, Germany). For three-dimensional acquisition, the stacks were first acquired at 920 nm wavelengths at vertical spacing of 2 μm to cover a axial depth of 30-100 μm (for YFP), and then the same stacks were immediately acquired at 800nm wavelength (for TRITC). For analysis of PPF fragmentation efficiency, all the four-dimensional acquisitions were performed at 920nm wavelength by capturing 3D image stacks at axial (z) distance of 3-5 μm to form a volume of 315 × 315 × 12-20 μm at 60 seconds intervals for 60 min. For other four-dimensional acquisition, 3D stacks were collected at a distance of 3-5 μm in z at 30 seconds interval for 60 min. To generate 4D movies, 3D image stacks were flattened along the z axis as maximum intensity projections representing a ‘‘top’’ (x–y) view of the volume and then constructed movies with different time point frames using Volocity (Improvision, Lexington, MA, USA). To measure the growth speed of proplatelets, we used Volocity to track the tips of proplatelets in a overlay of consecutive images as mentioned above to get the lateral proplatelet growth speed. Volocity was used to reconstruct 3D structures from the stacks in green channel detected at wavelength 920 nm and the stacks in red detected at wavelength 800 nm. The measurement of distances between MKs and vasculature were performed in reconstructed 3D structure using Volocity. To analyze the volume of MKs or MKs fragments, YFP-positive areas from 3D stack images were manually selected by Photoshop CS, and then reconstituted and measured in Volocity. The Wadell sphericity is

a parameter to determine how spherical an object is. For the ideal sphere, Waddell sphericity index is 1. The sphericity, Ψ, of a particle is the ratio of the surface area of a sphere with the same volume as the given particle (Vp) to the surface area (Ap) of the particle: $\psi = \frac{\sqrt[3]{\pi(6Vp)^2}}{Ap}$. All the mice were treated with murine mTpo (ImmunoTools, Friesoythe, Germany) 8 µg/kg/d for 3 days before imaging. W146 or vehicle was injected i.p 3 mg/kg body weight every 8 hours for 24 hours before imaging. For fragmentation study, mice were injected (i.p) with W146 (3 mg/kg body weight) or vehicle and immediately visualized by two-photon microscopy. For FTY720 experiments, the same megakaryocytes were visualized in mice before and 8 hours after a single injection of FTY720 (3 mg/kg i.p.) or DMSO using MP-IVM.

3.2.17 Shear stress

MKs from β-actin EGFP mice were seeded in Ibidi µ-slide VI (ibidi Integrated BioDiagnostics, Munich, Germany) coated with 100ng/ml mouse fibrinogen (BD, Heidelberg, Germany) for 4 hours at 37°C. The slides were then connected to ibidi pump system (Ibidi Integrated BioDiagnostics, Munich, Germany). 4 dynes/cm^2 of laminar shear stress was applied to cells in serum-free PBS with 5 µM S1P or vehicle. MKs were kept on a heated stage to keep the temperature at 37°C and immediately monitored using a two-photon microscope system as mentioned above, equipped with a 60× water-immersion objective lens with NA =1.10 (Olympus, Hamburg, Germany). We used laser at 800nm wavelength to excite EGFP and collected signal through 525/50 nm filter. Images stacks were acquired at 2 µm in z to cover a 20 µm vertical distance at 30 seconds intervals for 20min. We processed raw imaging data using Imspector (LaVisionBioTec, Bielefeld, Germany) and reconstructed the image sequences into the movies using Volocity. The length of proplatelets at 0 min and their length at 20 min were measured using Volocity. The fragmentation index was determined by the length at 20 min time point divided by the length at 0 min time point.

3.2.18 Live cell imaging

Mature MKs were isolated as mentioned above and cultured in serum-free DMEM medium in custom-made Petri dishes coated with mouse fibrinogen (100 μg/ml) overnight. We treated MKs with 10 μM S1P together with 25 μM NSC23766 (TOCRIS) to inhibit Rac1. We incubated MKs with 500ng/ml pertussis toxin [7-9] (PTX, Sigma Aldrich) to inhibit Gi signal or PP2 to inhibit SFKs activity 1 hour prior to the addition of 10 μM S1P. MKs were imaged with Axiovert 200M microscope equipped with a 40× objective lens and a coolSNAP HQ CCD. The raw data were processed with MetaMorph software.

3.2.19 Statistical analysis

All data are presented as the means ±s.e.m. Statistical methods used in this study are Student's unpaired t-test and chi-square tests. We considered P values of less than 0.05 as statistically significant

3.3 Results

3.3.1 S1P receptor expression profile in megakaryocytes

Using real-time PCR and immunostaining methods, we investigated the expression profile of S1P receptors during megakaryocytic differentiation. We modified the published protocol to collect immature and mature megakaryocytes [3]. The immature megakaryocytes were identified as $CD41^{+}CD34^{+}$ population from the E12.5-14.5 fetal liver cells treated with thrombopoietin (Tpo) for 12 hours and were isolated by FACS sorting [3, 12, 13]. The mature megakaryocytes were isolated by a BSA gradient after 6 days of culture with Tpo [2]. Our results show that S1P1 and S1P2 mRNA are detected in immature megakaryocytes, whereas significant S1P1, S1P2 and S1P4 mRNA expression are found in mature megakaryocytes. S1P2 and S1P4 mRNA were upregulated during

megakaryocyte development (Fig. 3.1). We further found here that the human megakaryocytic cell lines Meg01 and CMK each express the S1P receptor subtypes S1P1 and S1P4 (Fig. 3.2). Immunostaining revealed S1P1 protein expression in immature megakaryocytes, and S1P1, S1P2, S1P4 in mature megakaryocytes (Fig. 3.3 and 3.4). Notably, S1P1 was present in megakaryocytes predominantly in a surface location with asymmetric distribution, suggesting S1P1 might contribute to the polarity of MKs (Fig. 3.3). *In situ* staining also shows that both murine and human megakaryocytes express S1P1 in the bone marrow (Fig. 3.5-6). This S1PRs expression profile in megakaryocytes is similar to Golfier's report [10].

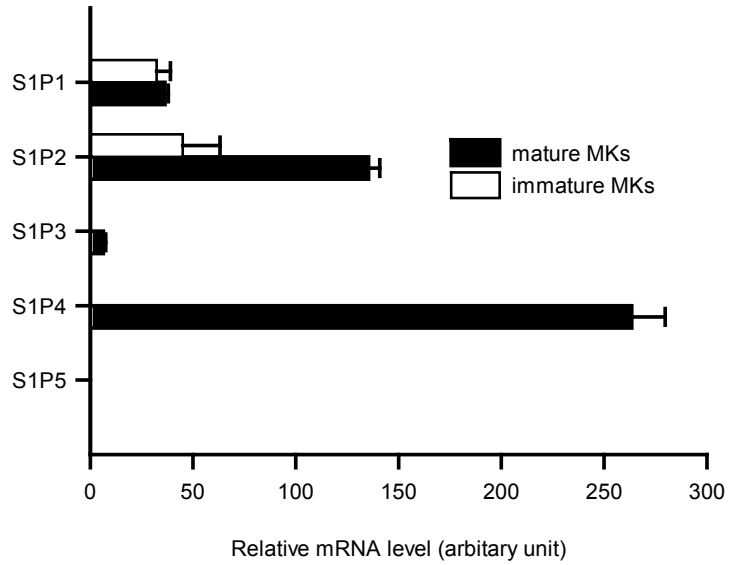

Fig. 3.1. Expression of S1P receptors by megakaryocytes. Relative expression of S1P receptor mRNA by FL-derived mature (black) and immature megakaryocytes (white)

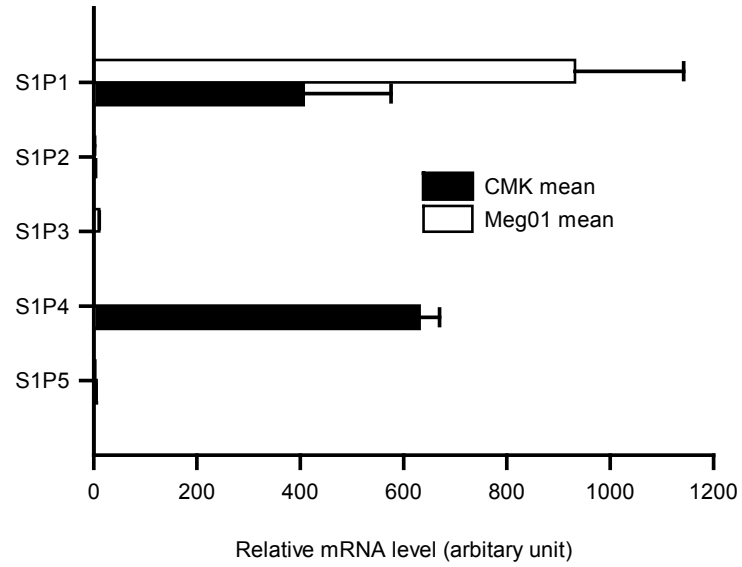

Fig. 3.2. Relative expression of S1P receptor mRNA in human megakaryocytic cell lines. Black bars, CMK; White bars, Meg01.

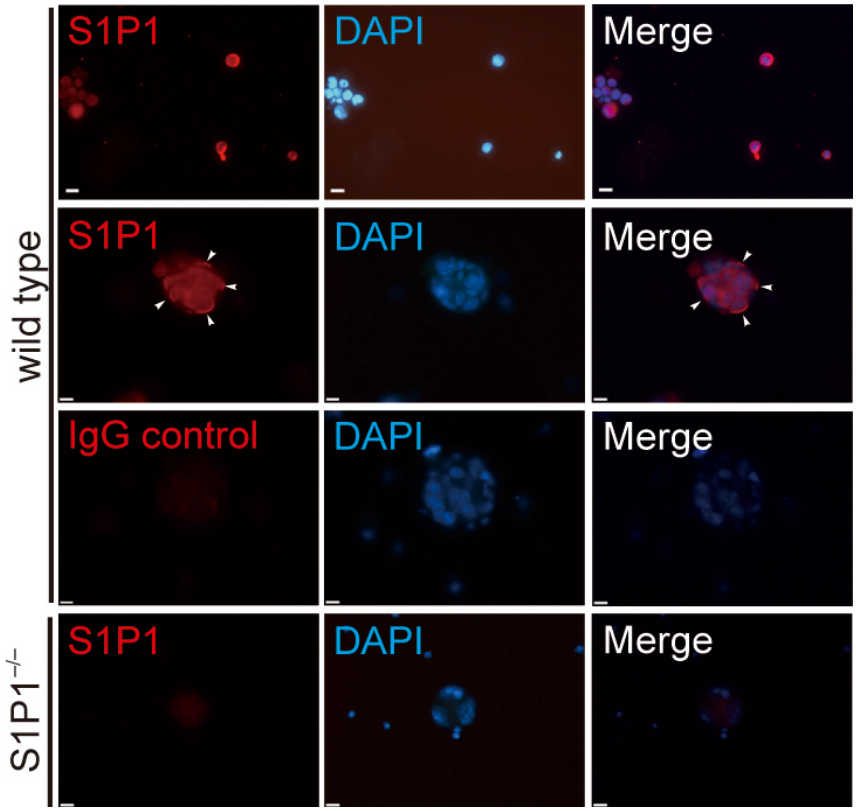

Fig. 3.3. Immunostaining of S1P1 protein in immature (upper) and mature (upper middle) FL-derived MKs. Wild type (WT) MKs stained with irrelevant control IgG (lower middle), or

anti-S1P1-stained S1P1 null MKs (lower) served as controls. Arrowhead indicates asymmetric membrane localization of S1P1.

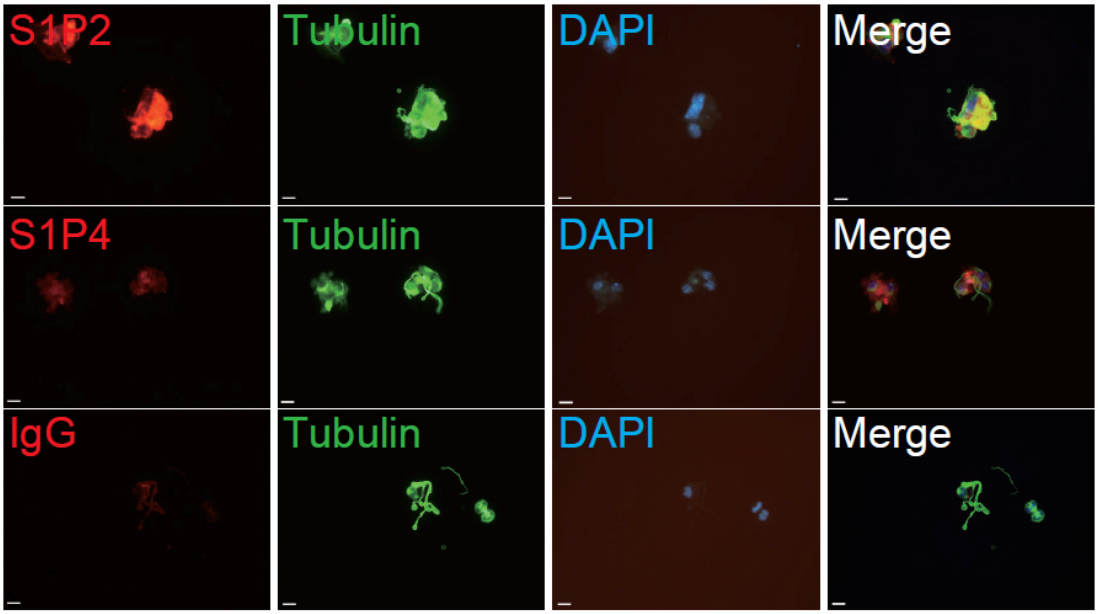

Fig. 3.4. Immunofluorescence analysis of S1P2 (upper) and S1P4 (middle) in murine FL-derived mature megakaryocytes. S1P receptors or IgG control, red; DAPI, blue; Tubulin, green. Scale bars for all images are 10 μm.

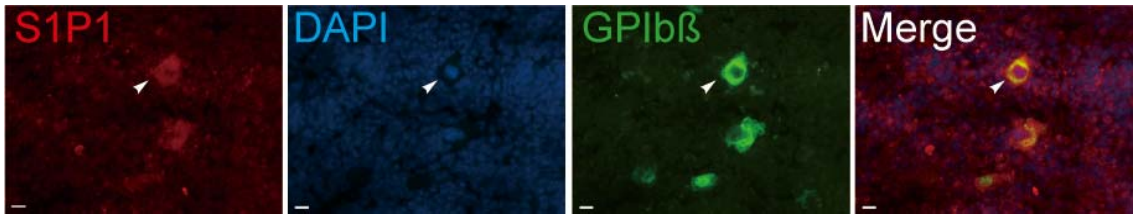

Fig. 3.5. Expression of S1P1 in murine BM sections. Arrowhead, MKs; Red, S1P1; Green, GPIbß (as marker of MKs); Blue, DAPI; Scale bar, 10 μm.

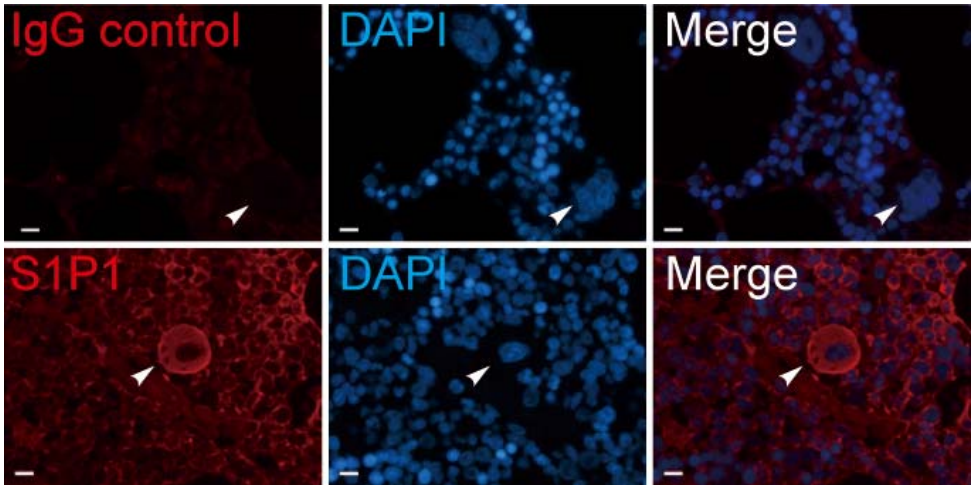

Fig. 3.6. Expression of S1P1 in human BM sections. Arrowhead, MKs; Red, S1P1; Green, GPIbß (the marker for MKs); Blue, DAPI; Scale bar, 10 μm.

3.3.2 Platelet counts in peripheral blood

To directly test whether S1P receptors play a role for megakaryo- or thrombopoiesis, we determined platelet counts in peripheral blood of wild type (WT) mice and mice lacking distinct S1P receptors that we found to be expressed by MKs. We first compared the platelet counts in peripheral blood between heterozygous $S1P1^{+/-}$ and wild type control (WT). We found that $S1P1^{+/-}$ mice have a moderate reduction in platelet counts in comparison with WT (Fig. 3.7, Table 3.1). Loss of both alleles ($S1P1^{-/-}$ mice) was embryonic lethal [11]; hence, to circumvent embryonic lethality, we generated fetal liver (FL) chimaeras lacking S1P1 only in the hematopoietic compartment by transferring FL cells from $S1P1^{-/-}$ or $S1P1^{+/-}$ or $S1P1^{+/+}$ into irradiated wild-type mice. Then we transferred bone marrow (BM) cells from these $S1P1^{-/-}$ or $S1P1^{+/-}$ or $S1P1^{+/+}$ FL chimaeras into 2nd recipient mice to generate BM cell chimaeras. Platelet counts in $S1P1^{+/-}$ and $S1P1^{-/-}$ BM cell chimaeras were reduced by more than 50%, 80% compared to $S1P1^{+/+}$ BM cell chimaeras, respectively (Fig. 3.7, Table 3.2). We further investigated platelet counts in S1P2 and S1P4 knout out mice. $S1P4^{-/-}$ and $S1P2^{-/-}$ mice also showed a slight reduction in platelet counts (Fig. 3.8, Table 3.1). However, complete loss of S1P2 or S1P4 in only the hematopoietic system in chimeras did not affect peripheral platelet counts (Fig. 3.8, Table 3.2), which demonstrates that S1P2 and S1P4 do not play an

essential and intrinsic role in thrombopoiesis. In contrast, S1P1 is essential for thrombopoiesis.

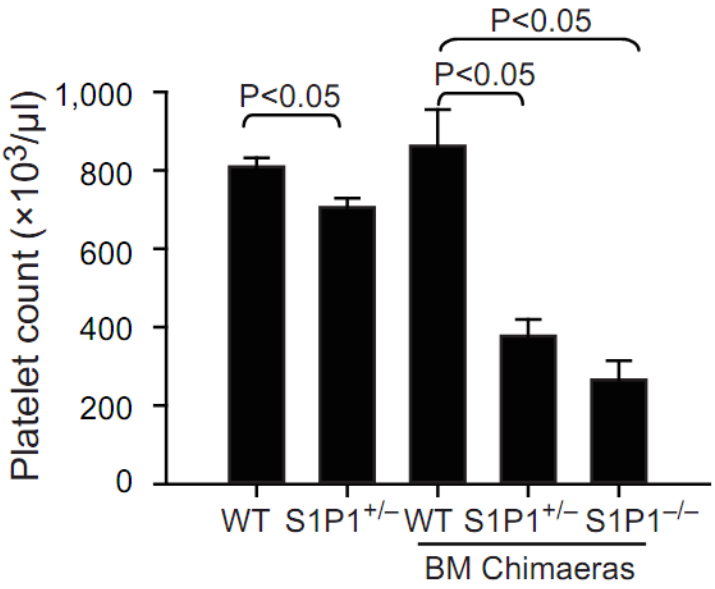

Fig. 3.7. Platelet counts in peripheral blood from WT or S1P1 mutant mice.

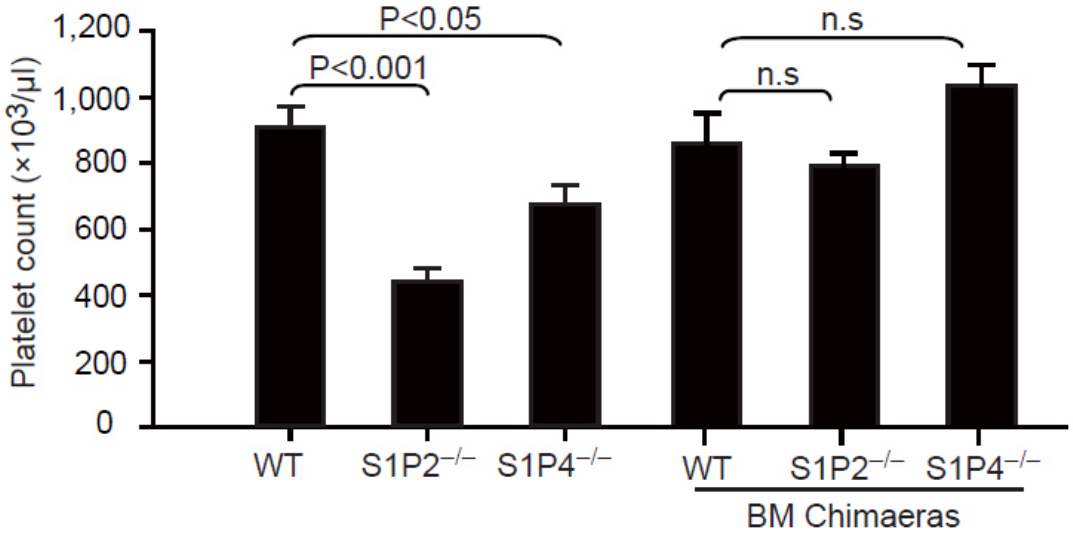

Fig. 3.8. Platelet counts in peripheral blood from WT mice or S1P2 or S1P4 mutants.

	WT	$S1P1^{+/-}$	$S1P2^{-/-}$	$S1P4^{-/-}$
WBC (× 10^3/μl)	7.99±3.08	5.33±2.15	9.87±4.00	6.54±2.73
RBC (× 10^6/μl)	11.17±1.29	9.82±0.58	9.09±0.57*	9.58±0.52
HGB (g/dl)	17.98±2.86	16.15±1.17	15.28±1.00	15.17±0.76
HCT (%)	56.50±6.54	48.45±1.83	48.96±2.69	49.58±2.68
MCV (fl)	50.55±0.68	49.35±1.05	53.88±1.35*	51.80±1.10
MCH (pg)	16.03±0.64	16.40±0.52	16.79±0.34***	15.83±0.19
MCHC (g/dl)	31.73±1.35	33.32±1.42	31.19±0.37	30.61±0.61
Platelet (× 10^3/μl)	809.19±55.96	705.96±47.17*	441.39±97.38**	678.33±163.88*
Lym (× 10^3/μl)	6.87±2.62	4.04±1.65	7.84±2.99	3.39±0.85**
MPV (fl)	5.5±0.24	5.65±0.30	5.88±0.23*	5.55±0.17

Table 3.1. Complete blood cell counts in non-transplanted WT and S1P receptor mutant mice. *, P<0.05; **, P<0.01; ***, P<0.001.

	WT chimaeras	$S1P1^{+/-}$ chimaeras	$S1P1^{-/-}$ chimaeras	$S1P2^{-/-}$ chimaeras	$S1P4^{-/-}$ chimaeras
WBC (× 10^3/μl)	20.31±4.23	13.12±3.85**	6.77±3.55***	17.52±2.32	15.76±7.81
RBC (× 10^6/μl)	9.95±1.73	10.60±0.99	9.15±1.03	9.79±0.87	10.42±0.54
HGB (g/dl)	14.96±3.52	15.27±2.11	13.68±1.14	15.58±1.06	16.32±1.15
HCT (%)	50.06±7.69	50.31±5.46	44.48±4.52	51.15±3.87	51.50±1.95
MCV (fl)	50.50±1.92	47.41±1.35***	48.66±1.21*	52.30±1.33	49.47±0.70
MCH (pg)	14.92±1.16	14.37±0.92	15.04±1.23	15.96±0.95**	15.67±0.78
MCHC (g/dl)	29.64±2.65	30.30±1.53	30.89±2.24	30.52±1.62*	31.67±1.70**
Platelet (× 10^3/μl)	926±418	406±150**	171±108***	795±87	1036±111
Lym (× 10^3/μl)	16.41±3.11	10.68±3.66**	5.74±2.36***	14.23±2.68	14.06±7.00
MPV (fl)	6.14±0.72	6.65±0.17	6.88±0.18*	6.08±0.16	5.70±0.10

Table 3. 2. Complete blood cell counts in BM cell chimaeras. *, P<0.05; **, P<0.01; ***, P<0.001.

3.3.3 Conditional deletion of S1P1 in megakaryocytes

To further test whether S1P1 plays an intrinsic role in megakaryopoiesis, we expressed Cre recombinase under the control of the megakaryocytic specific promoter GPIIb in $S1P1^{fl/fl}$ BM cells *in vivo* to delete the floxed S1P1 allele in megakaryocytic lineage [12]. We found that S1P1 levels are reduced in platelets from $S1P1^{fl/fl}$ BM chimaeras infected with GPIIb-Cre lentivirus (Fig. 3.10). Platelet counts were significantly reduced in $S1P1^{fl/fl}$ BM chimaeras infected with GPIIb-Cre lentivirus as compared to empty lentivirus, supporting the intrinsic role of S1P1 in thrombopoiesis (Fig. 3.9-10).

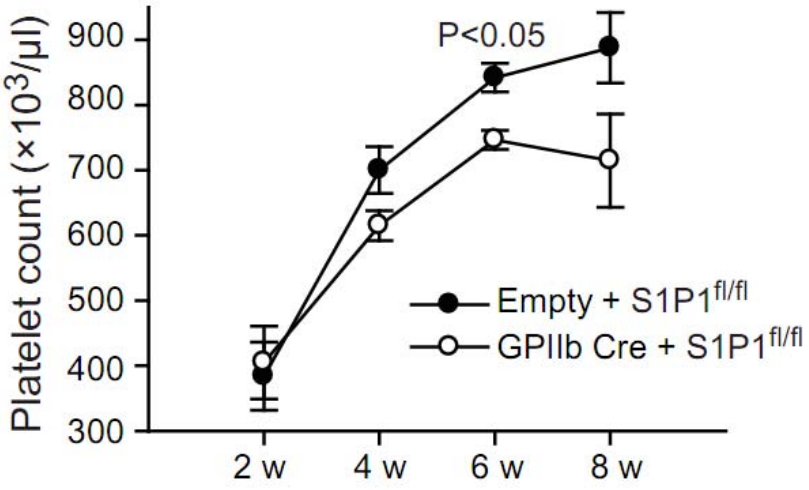

Fig. 3.9. Platelet counts in chimaeras after transferring $S1P1^{fl/fl}$ FL cells transduced with Lenti-GPIIb-cre or empty control vectors into irradiated recipient mice. All error bars indicate s.e.m.

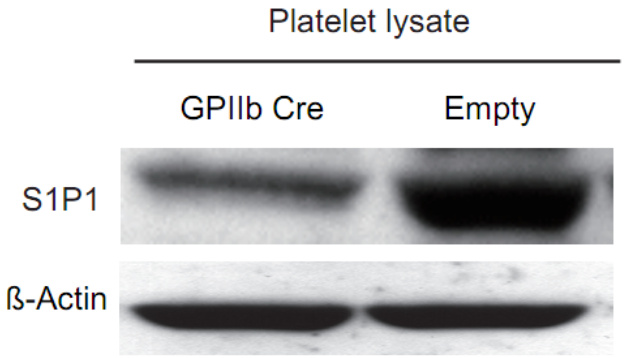

Fig. 3.10. Expression of S1P1 in platelet lysate obtained from chimaeras in **Fig. 3.9**. β-actin, loading controls.

3.3.4 Gain of function of S1P1 in $S1P1^{-/-}$ megakaryocytes

To avoid any compensatory effect on thrombopoiesis caused by S1P1 loss, we reexpressed S1P1 in $S1P1^{-/-}$ FL cells under the megakaryocytic promoter GPIbα by infection with GPIbα-S1P1 lentivirus and transferred the FL cells into lethally irradiated recipient mice. $S1P1^{-/-}$ megakaryocytes generated more platelets in peripheral blood after GPIbα-S1P1 lentiviral infection compared to FL transfected with empty lentivirus, demonstrating that S1P1 is essential and plays an intrinsic role for thrombopoiesis (Fig.

3.11).

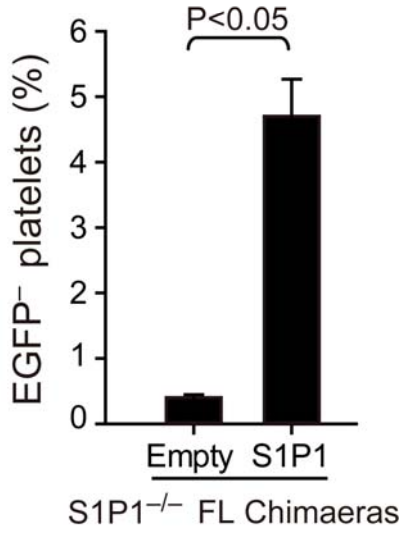

Fig. 3.11. Percentage of EGFP- platelets in chimaeras after hematopoietic reconstitution by transferring EGFP+ S1P1$^{+/+}$ BM cells and EGFP- S1P1$^{-/-}$ FL cells at a ratio of 20:1 into irradiated mice. The EGFP- S1P1$^{-/-}$ FL cells were transduced with Lenti-GPIbα-S1P1 or empty control vectors before transplantation.

3.3.5 The reduced platelet counts caused by a loss of S1P1 is independent of mouse background

Repetitive treatment of C57Bl/6J mice with the S1P1 specific antagonist, W146, to inhibit S1P1 *in vivo* for 24 hours resulted in a significant reduction in circulating young reticulated platelets with an elevated RNA content (Fig. 3.12), consistent with a central role of the S1P/S1P1 pathway for platelet biogenesis. Moreover, W146 also reduced platelet counts in CD1 mice (Fig. 3.13), suggesting that the function of S1P1 in thrombopoiesis is also essential in mice across different genetic backgrounds.

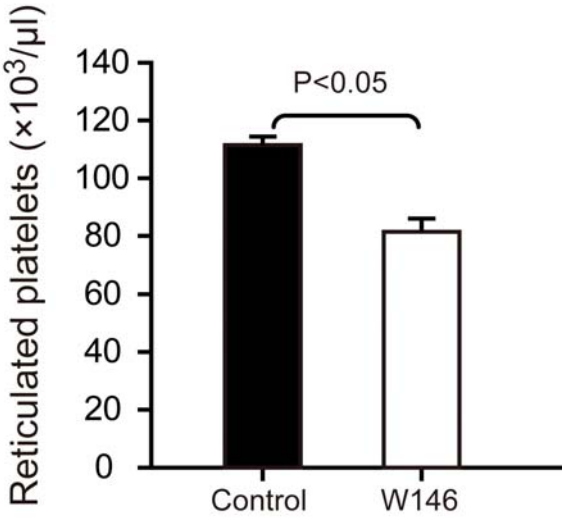

Fig. 3.12. Circulating reticulated (young) platelets in mice treated with W146 or vehicle as assessed by flow cytometry.

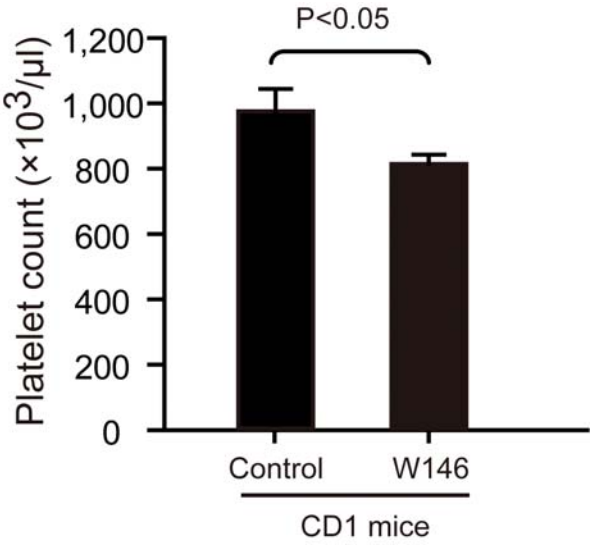

Fig. 3.13. Circulating platelet counts in CD1 mice treated with W146 or vehicle.

3.3.6 MK maturation

To find out the reasons for thrombocytopenia in S1P1$^{-/-}$ mice, we next investigated megakaryocytic maturation using *in vitro* assays and histological analysis. *In vitro* assays showed that S1P$^{-/-}$ FL-derived hematopoietic stem cells generate similar numbers of MK progenitors and MKs as WT (Fig. 3.14). CFU-MKs assays revealed that S1P1$^{-/-}$ BM chimeras have a similar percentage of megakaryocytic progenitors in total unfractionated

bone marrow cells as WT (Fig. 3.15). Histological analysis of bone marrow sections revealed no significant differences in the number of megakaryocytes in S1PR mutants in comparison to WT controls (Fig. 3.16-17). Together this indicates that loss of S1P1 does not result in a gross defect of MK development and that WT and $S1P1^{-/-}$ mice contain comparable numbers of MK progenitors.

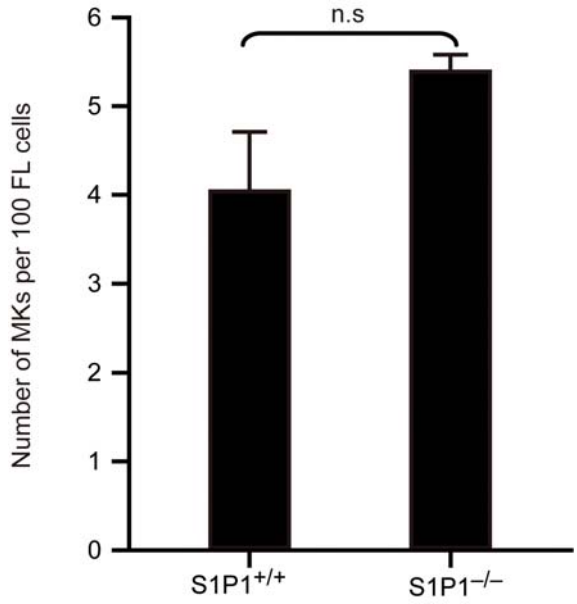

Fig. 3.14. Percentage of mature MKs in cultured FL cells. All error bars represent s.e.m.

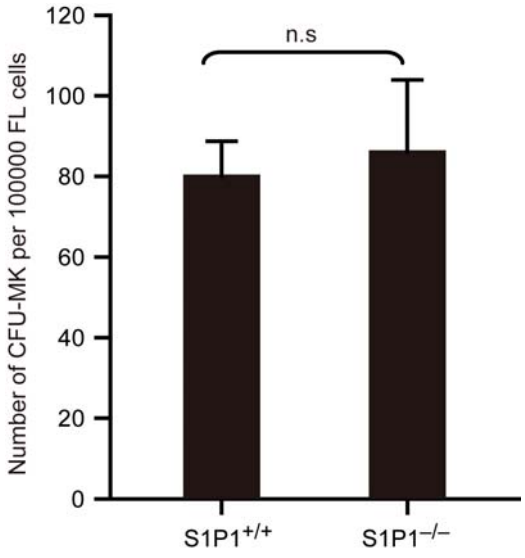

Fig. 3.15. Quantification of CFU-MKs numbers in fetal liver cells. All error bars represent s.e.m.

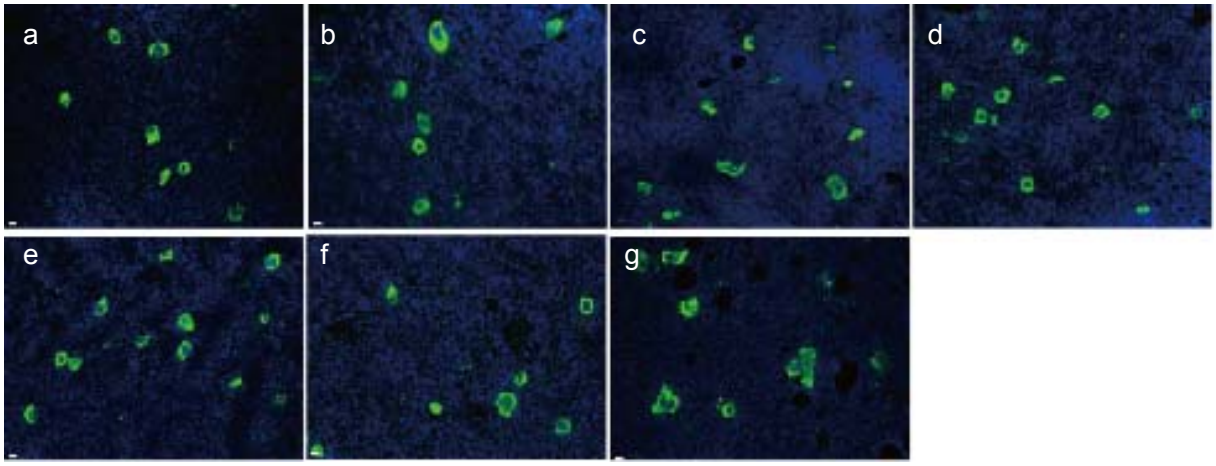

Fig. 3.16. Representative immunostaining of megakaryocytes in mouse femoral BM sections. Megakaryocytes were detected by the megakaryocyte-specific marker CD41 (green). DAPI (blue); Images **a-g** represent S1P1$^{+/+}$, S1P1$^{+/-}$, S1P2$^{-/-}$, S1P4$^{-/-}$, S1P1$^{+/+}$ chimera, S1P1$^{+/-}$ chimeras and S1P1$^{-/-}$ chimeras, respectively. Scale bar, 10 μm.

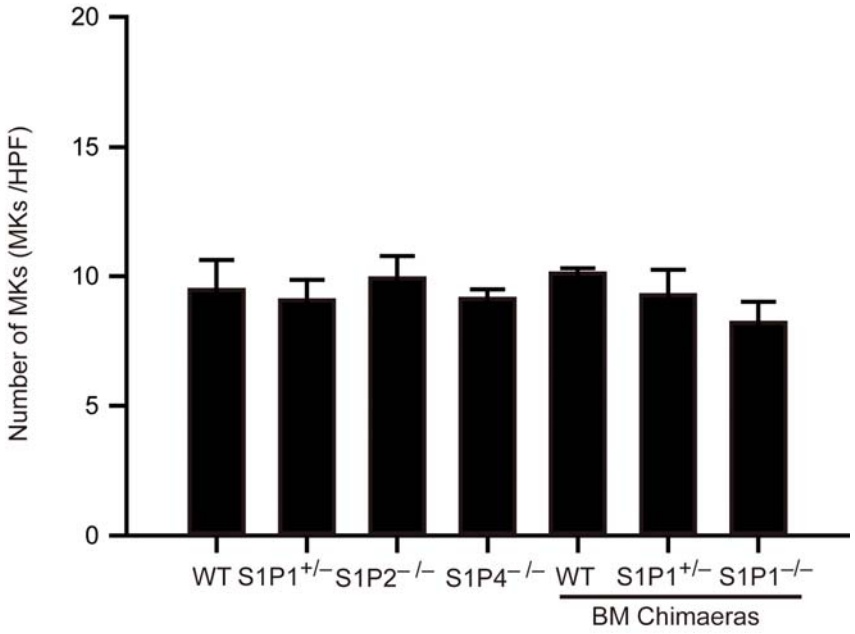

Fig. 3.17. Quantification of megakaryocyte numbers per 20× high-power fields in femoral BM sections.

3.3.7 Motibility of MKs and distribution of MKs *in vivo*

We next examined whether S1P1 controls platelet biogenesis by modulating MK motility

or positioning within the BM compartment. To this end we performed multiphoton intravital microscopy (MP-IVM) of calvaria BM [13] of two different sets of $S1P1^{+/+}$ or $S1P1^{-/-}$ chimaeras, in which MKs and their progeny were genetically marked: (i) $S1P1^{+/+}$ or $S1P1^{-/-}$ CD41-$YFP^{ki/+}$ FL cell chimaeras, in which MKs and platelets express the yellow fluorescent protein (YFP) driven by the endogenous CD41 gene locus[14], and (ii) $S1P1^{+/+}$ or $S1P1^{-/-}$ lenti-GPIbα-EGFP BM cell chimaeras, in which MKs and platelets express the enhanced green fluorescent protein (EGFP) under the transcriptional control of the murine GpIbalpha promoter [15]. The experiments revealed no obvious differences in MK size, positioning or motility when we compared between $S1P1^{+/+}$ CD41-$YFP^{ki/+}$ or lenti-GPIbα-EGFP chimaeras and naïve (non-transplanted) $S1P1^{+/+}$ CD41-$YFP^{ki/+}$ or Pf4-Cre-Rosa-YFP transgenic mice, in which Cre is driven by the MK-specific platelet factor 4 (PF4) promoter. The Cre expression results in an event that unleashes the ability of express the reporter gene YFP by removing a floxed transcriptional block. This excludes a major influence of irradiation and BM transplantation (Fig. 3.18). As reported previously [13], $S1P1^{+/+}$ MKs were large, mostly sessile cells, always located in close proximity to BM sinusoids (Fig. 3.18). In $S1P1^{-/-}$ chimaeras and $S1P1^{+/-}$ mice, MKs were significantly larger compared to $S1P1^{+/+}$ chimaeras and WT, respectively, while the positioning and motility of MKs were not different between the distinct genotypes (Fig 3.19-21). The above results suggest that in contrast to other cells in the BM [16], neither positioning nor migration of MKs or their committed progenitors in marrow spaces is controlled by S1P1.

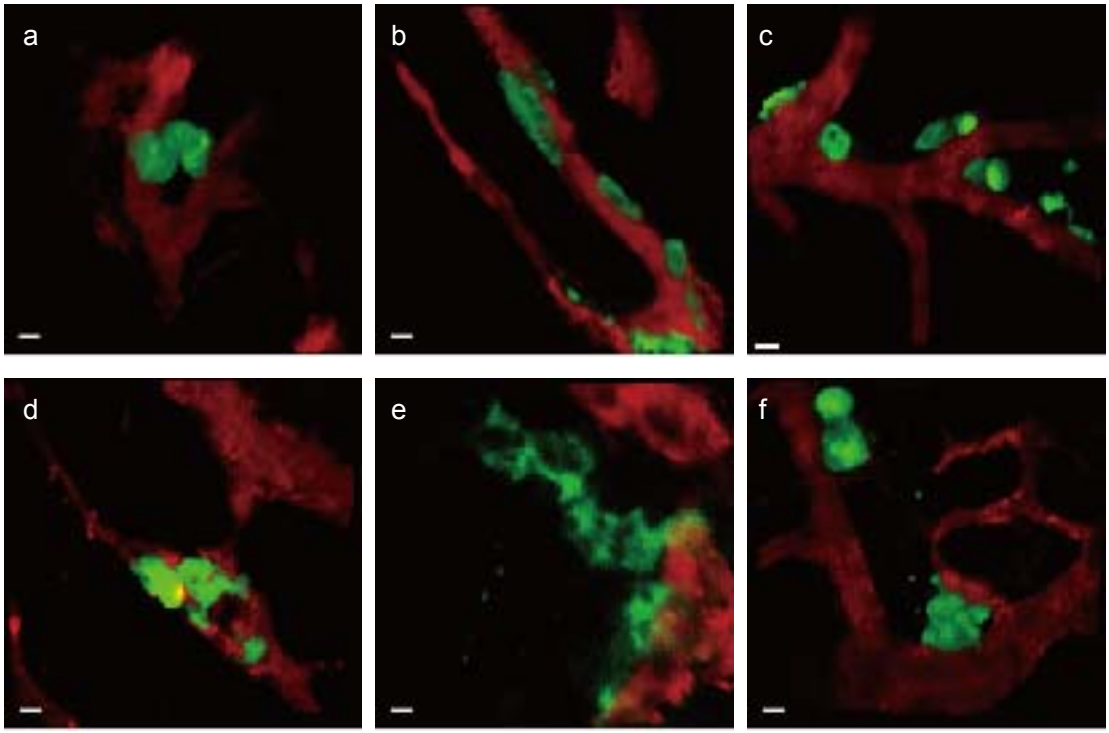

Fig. 3.18. Representative *in vivo* images of YFP+ or EGFP+ MKs (green) and vasculature (red) in mouse BM. Upper row, lenti-GPIbα-EGFP;S1P1$^{+/+}$ BM chimaeras (a) or CD41-YFP$^{ki/+}$S1P1$^{+/+}$ FL chimaeras (b) or CD41-YFP$^{ki/+}$S1P1$^{+/+}$ naïve (non-transplanted) mice (c); lower row, S1P1$^{-/-}$ BM chimaeras (d) or S1P1$^{-/-}$ FL chimaeras (e) or S1P1$^{+/-}$CD41-YFP$^{ki/+}$ naïve (non-transplanted) mice (f). Scale bar, 20 μm.

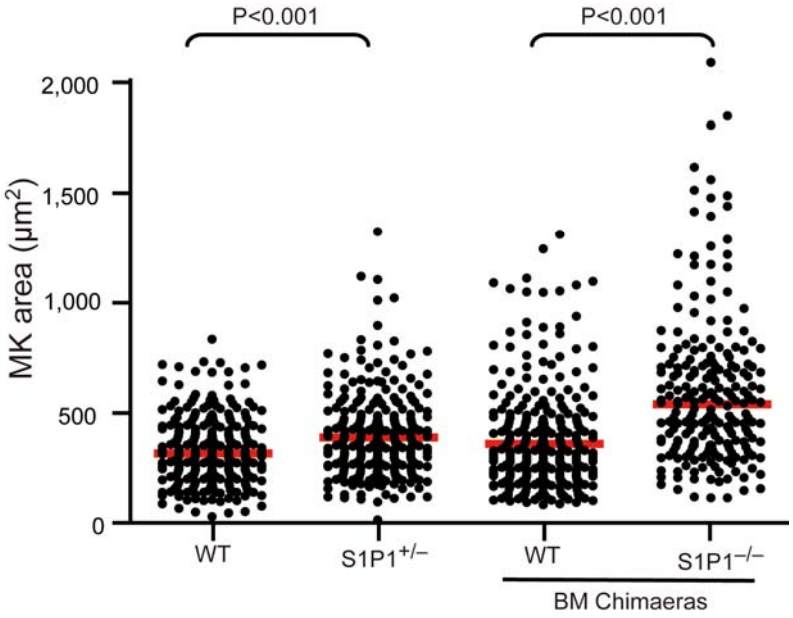

Fig. 3.19. Surface area of MKs in BM. Red lines, medians.

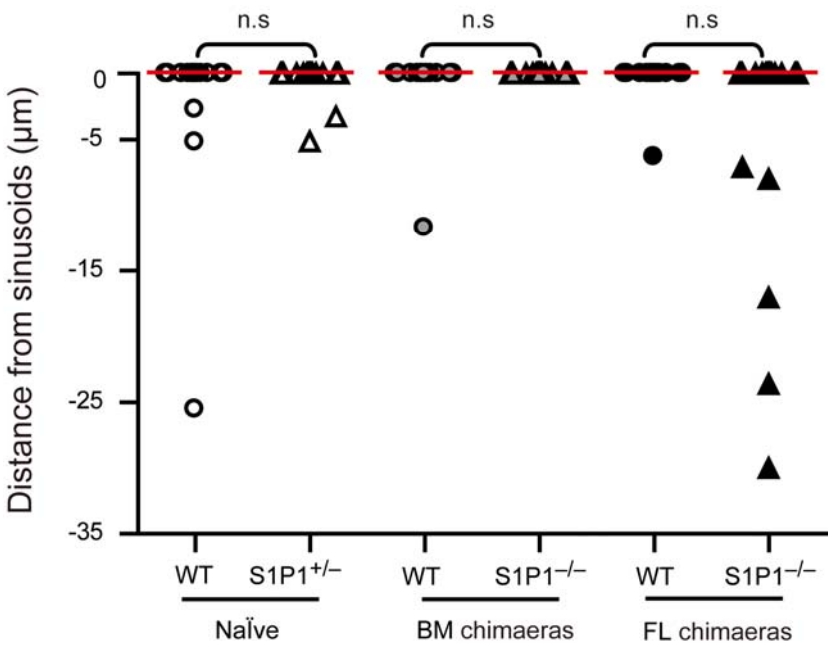

Fig. 3.20. Distance of MKs from BM sinusoids. Red lines, medians.

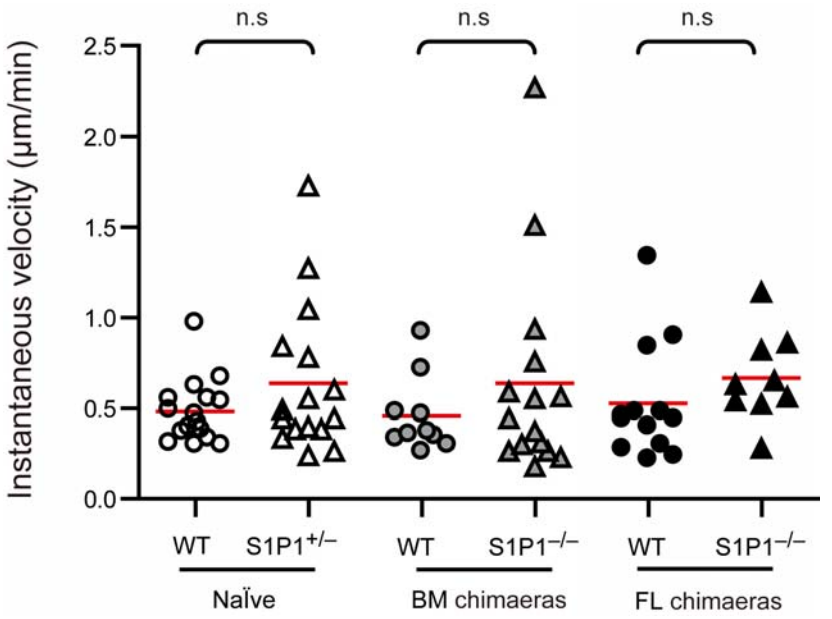

Fig. 3.21. Instantaneous lateral (x-y) velocity of MKs. Red lines, means.

3.3.8 Platelet life span

Besides the influences of thrombopoiesis on platelet counts in peripheral blood, the clearance of platelets also affects peripheral platelet numbers. To investigate the platelet life span in WT and S1P receptor mutants, the platelets were biotinylated by intravenous

administration of N-hydroxysuccinimide-biotin, and the percentage of biotinylated platelets in peripheral blood was identified by staining with PE/cy7-conjugated streptavidin and monitored for 6 days by flow cytometric analysis. Platelet life span and half-life were also unaffected in all examined mice (Fig. 3.22), which suggested that the clearance rate of aged platelets does not explain thrombocytopenia in S1P1 deficient mice.

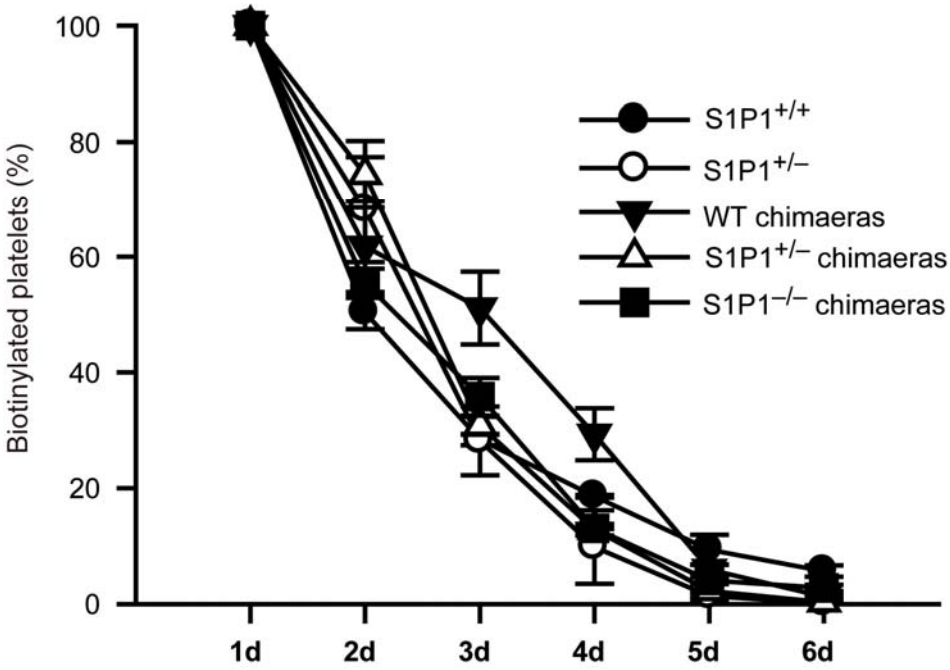

Fig. 3.22. Analysis of platelet life span in mice of the indicated genotype. Error bars represent s.e.m (n=3-5 per group). t-test.

3.3.9 Tpo level and Tpo receptor expression expression

Because thrombopoietin (Tpo) is the principle physiological regulator of thrombopoiesis [17], we next analyzed serum Tpo levels and Tpo receptor expression in WT and S1P1 receptor mutants. Our data showed that the Tpo levels of $S1P1^{+/-}$ chimera and $S1P1^{-/-}$ mice are not significantly different from WT controls (Fig. 3.23). Moreover, Tpo receptor expression is higher but not reduced in $S1P1^{+/-}$ and $S1P1^{-/-}$ MKs than in WT MKs (Fig. 3.24). Therefore Tpo-Tpo receptor signalling does not account for thrombocytopenia in S1P1 null mutants.

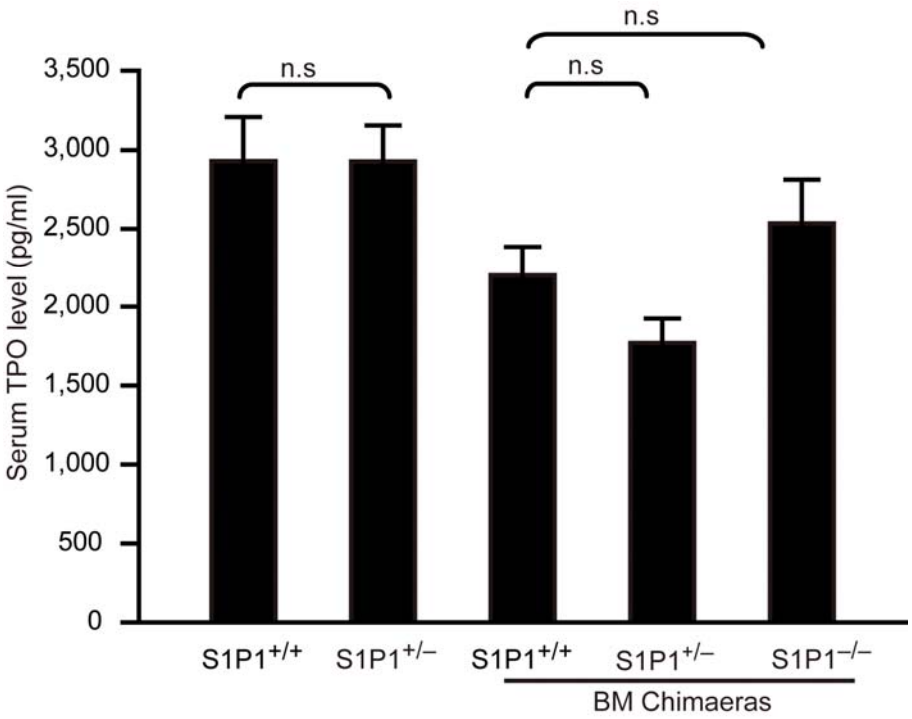

Fig. 3.23. Serum Tpo levels. Error bar, s.e,m; n=3-5 per group. t-test.

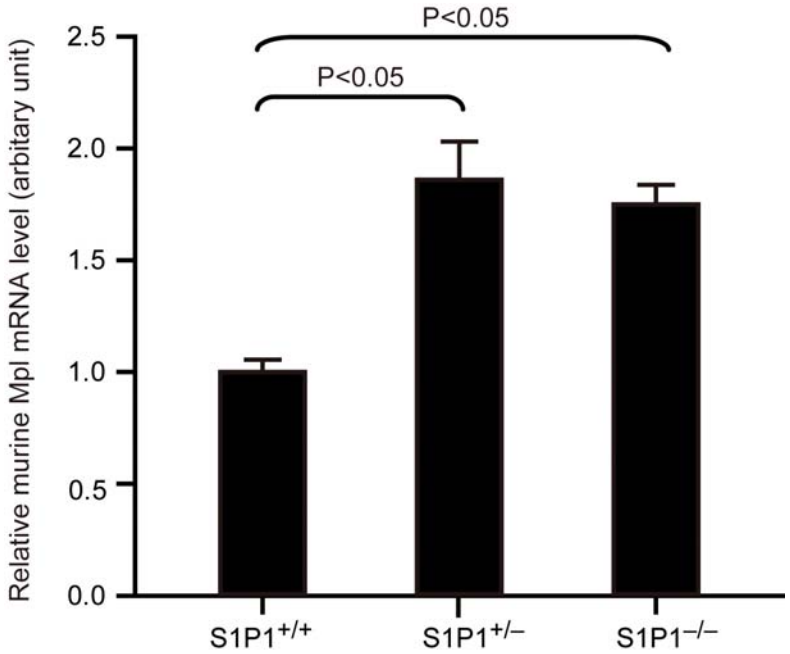

Fig. 3.24. Relative expression of murine Tpo receptor, Mpl, mRNA levels in murine FL-derived WT, S1P1$^{+/-}$ and S1P1$^{-/-}$ megakaryocytes. The data were normalized to the mRNA level of CD41. Error bars represent s.e.m. (n=3 per group). t-test.

3.3.10 Proplatelet formation *in vitro*

During thrombopoiesis mature MKs extend transendothelial protrusions, termed proplatelets (PP), into BM microvessels [13]. We therefore considered next whether S1P/S1P receptor signalling might play a role during PP formation. When we examined PP formation by cultured MKs *in vitro* [2], in average nine out of 100 WT MKs spontaneously formed PP as assessed by phase-contrast microscopy (Fig. 3.25A). S1P2$^{-/-}$ and S1P4$^{-/-}$ MKs generated similar PP *in vitro* when compared to WT MKs (Fig. 3.26A-B). In sharp contrast, PP formation was reduced by more than 70% in S1P1$^{-/-}$ MKs, as less than 2 out of 100 S1P1$^{-/-}$ MKs formed PP (Fig. 3.25A). When we specifically reexpressed S1P1 in S1P1$^{-/-}$ MKs by infection with a GPIb-S1P1 lentivirus, encoding S1P1 under the control of the megakaryocytic promoter GP-Ibalpha, gain of S1P1 function caused more PP formation in S1P1$^{-/-}$ MKs *in vitro* (Fig. 3.25B). These results clearly indicate that S1P1 plays a critical and intrinsic role for PP extension and elongation by MKs.

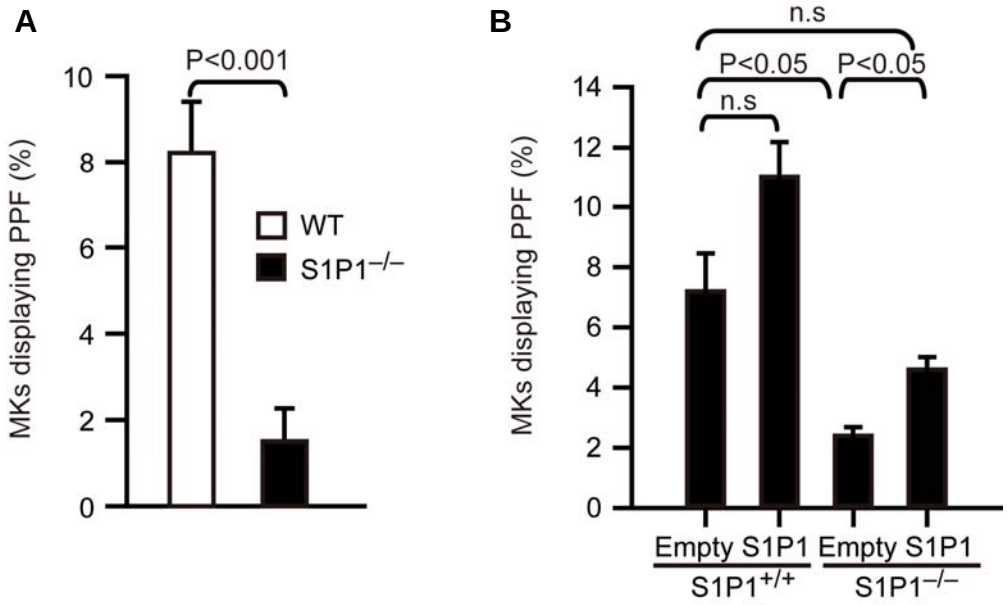

Fig. 3.25. Loss of S1P1 reduces proplatelet formation. A, Number of MKs displaying PP formation (PPF). PP formation is expressed as percentage of MKs carrying PPs. B, The percentage of MKs displaying PP formation (PPF) in S1P1$^{+/+}$ or S1P1$^{-/-}$ MKs transduced with Lenti-GPIbα-S1P1 or empty control vectors.

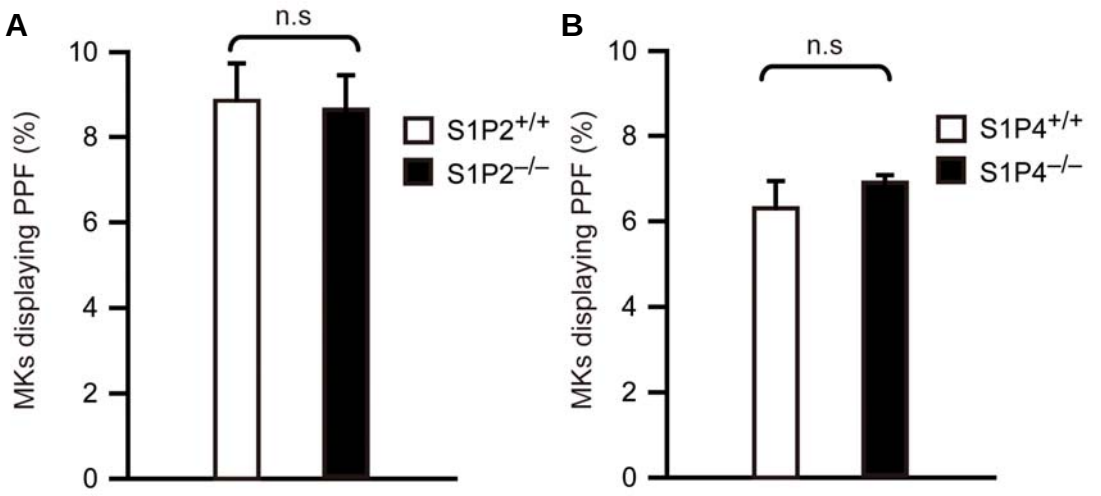

Fig. 3.26. Normal unaffected proplatelet formation in S1P2$^{-/-}$ and S1P4$^{-/-}$ MKs. Number of MKs displaying PP formation (PPF) in S1P2$^{-/-}$ (A) and S1P4$^{-/-}$ (B). PP formation is expressed as percentage of MKs carrying PPs

3.3.11 Demarcation membrane system (DMS)

In S1P1$^{-/-}$ MKs, electron microscopic analysis of S1P1$^{-/-}$ BM MKs did not reveal abnormalities of the DMS when compared to S1P1$^{+/+}$ BM MKs (Fig. 3.27), excluding a primary lack of the invaginated demarcation membrane system (DMS), the predominant reservoir for PP membranes [18, 19],

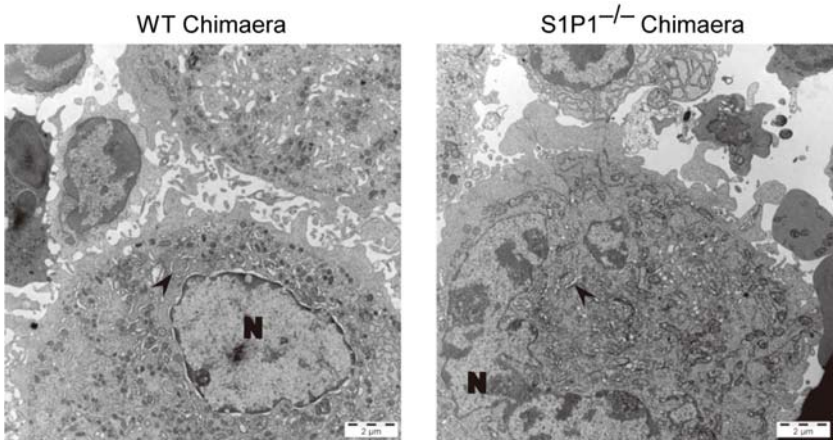

Fig. 3.27. Representative electron micrographs of WT (left) and S1P1$^{-/-}$ (right) MKs in BM. Arrowhead, DMS. N, nucleus. Scale bar, 2 μm.

3.3.12 Polarization of proplatelet formation

Next we tested whether S1P serves as a chemoattractant for polarizing MKs and for inducing the formation of PP protrusions. The local S1P concentrations are exceedingly low within the normal BM compartment (Fig. 3.28), reflecting similar concentrations reported for other tissues such as lymph nodes [20, 21]. In contrast, high S1P concentrations exist in the blood stream [22, 23]. Due to their positioning at the vascular interface, MKs are exposed to a steep transendothelial S1P gradient. To mimic the situation in the BM, we exposed cultured MKs to a gradient of S1P in a chemotactic Ibidi slides *in vitro*. Notably, PP extensions developed preferentially towards increasing concentrations of S1P, but not of vehicle (Fig. 3.29-30). This phenomenon was also observed in $S1P2^{-/-}$ and $S1P4^{-/-}$ MKs (Fig. 3.29). Inhibition of the megakaryocytic S1P1 with the antagonist VPC23019 abolished this directionality of PP formation; MKs projected PP extensions into random directions (Fig. 3.29-30). These findings suggest that S1P-S1P1 signalling is essential for PP formation and provides a chemoattractant stimulus controlling the polarization of PP processes generated by MKs in culture.

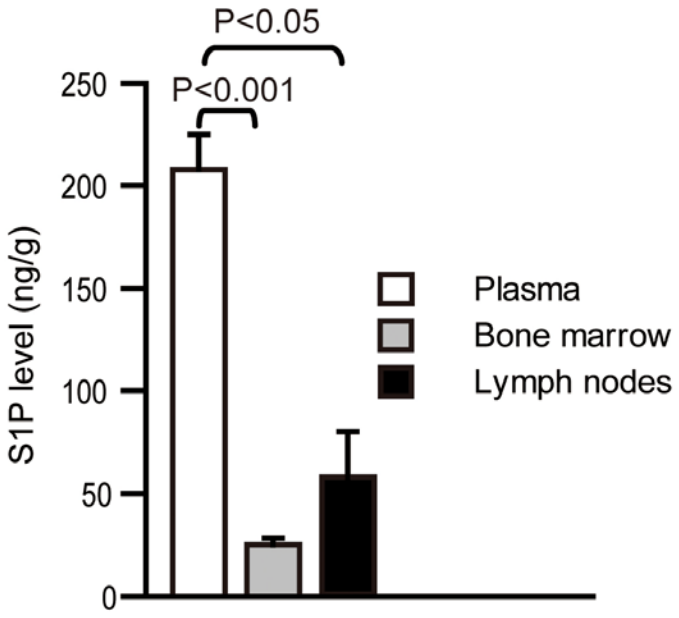

Fig. 3.28. S1P levels in plasma, BM and lymph nodes.

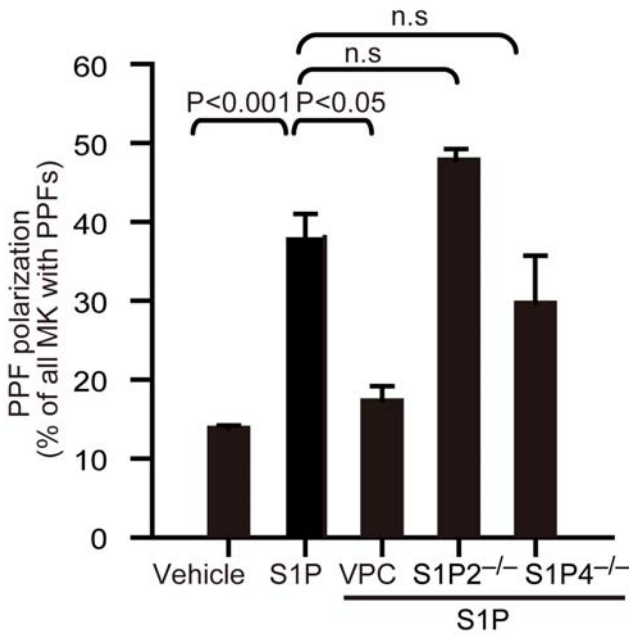

Fig. 3.29 The percentage of MKs with polarized PP formation (PPF) in the presence or absence of S1P and the S1P1-specific inhibitor VPC23019.

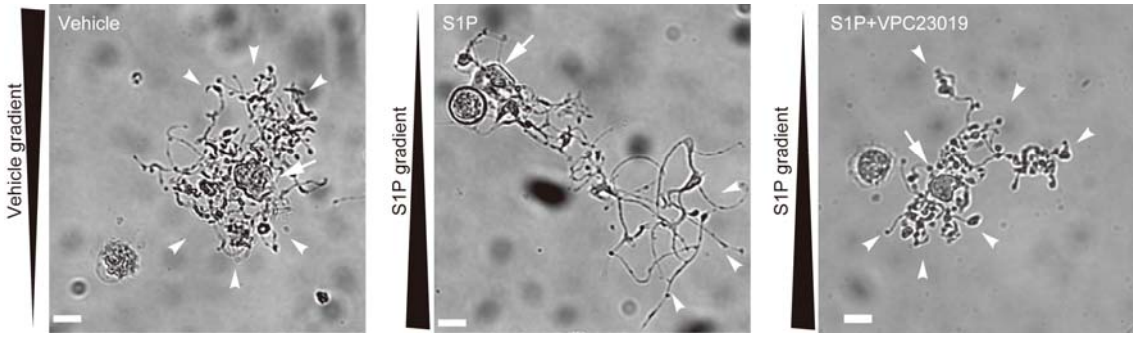

Fig. 3.30. Polarized PPF under the S1P gradient. Middle image, polarized PPF; Left and right images, non-polarized PPF. (Arrowhead, proplatelets; Arrow, MK body centres)

3.3.13 Formation of sinusoidal proplatelet *in vivo*

To evaluate the *in vivo* relevance of S1P and S1P1 for PP formation, we examined CD41-YFP$^{ki/+}$ mice by MP-IVM. In S1P1$^{+/+}$CD41-YFP$^{ki/+}$ mice 59% of all MKs extended plump or long PP protrusions into BM sinusoids (Fig. 3.31-32), indicating active participation in platelet biogenesis. PP protrusions extended almost exclusively into marrow sinusoids of S1P1$^{+/+}$ WT mice, while we rarely detected extravascular PP processes (Fig. 3.31-32). To determine whether S1P induced S1P receptors signalling provides the guidance information necessary to direct PP processes into BM sinusoids,

we examined S1P2$^{-/-}$CD41-YFP$^{ki/+}$, S1P4$^{-/-}$ CD41-YFP$^{ki/+}$, S1P1$^{+/-}$CD41-YFP$^{ki/+}$ mice as well as S1P1$^{-/-}$ CD41-YFP$^{ki/+}$ FL and lenti-GPIbα-EGFP BM chimaeras, respectively. Most of the PP processes were inside vasculatures in S1P2$^{-/-}$CD41-YFP$^{ki/+}$ and S1P4$^{-/-}$ CD41-YFP$^{ki/+}$ mutants (Fig. 3.31-32). In contrast to S1P1$^{+/+}$ MKs, S1P1$^{+/-}$ or S1P1$^{-/-}$ MKs projected PP extensions in random directions (Fig. 3.31-32). As a consequence, we found aberrant PP processes in the marrow interstitial space, while intrasinusoidal PPs were rarely detected in S1P1-deficient chimaeras (Fig. 3.31-32). Likewise, when we treated S1P1$^{+/+}$ CD41-YFP$^{ki/+}$ mice with the S1P1-specific antagonist W146 for 24 hours, the physiologic directionality of PP formation was entirely disrupted. We frequently observed long cytoplasmic extensions outside sinusoids in mice treated with W146, but not in vehicle-treated animals (Fig. 3.31-32).

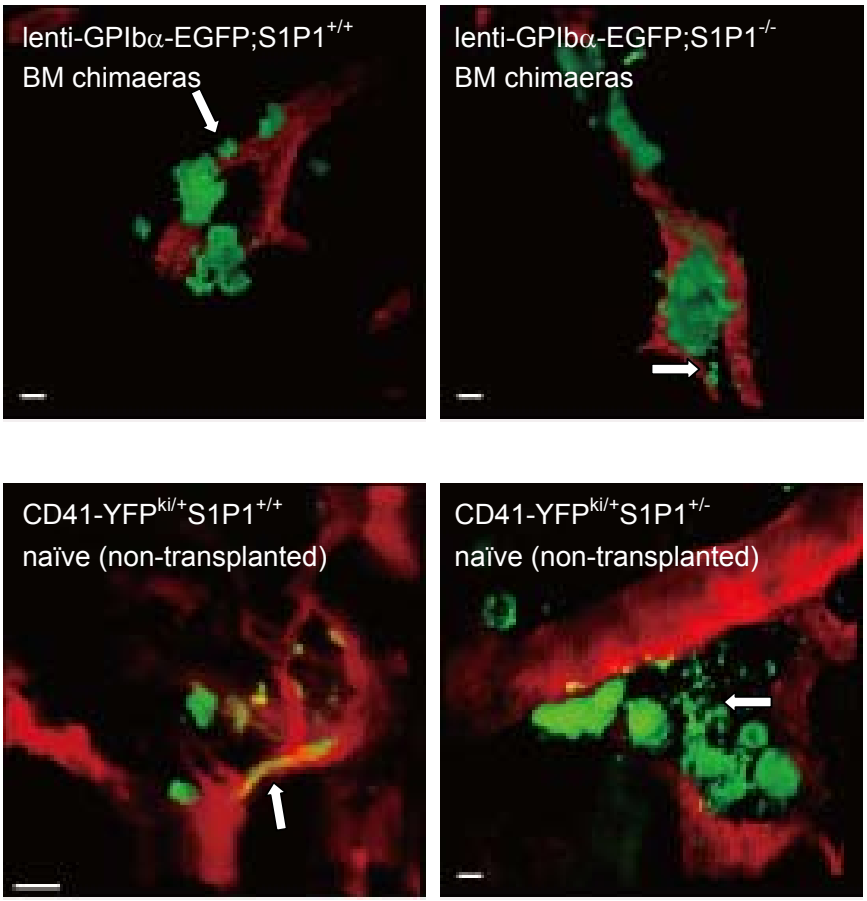

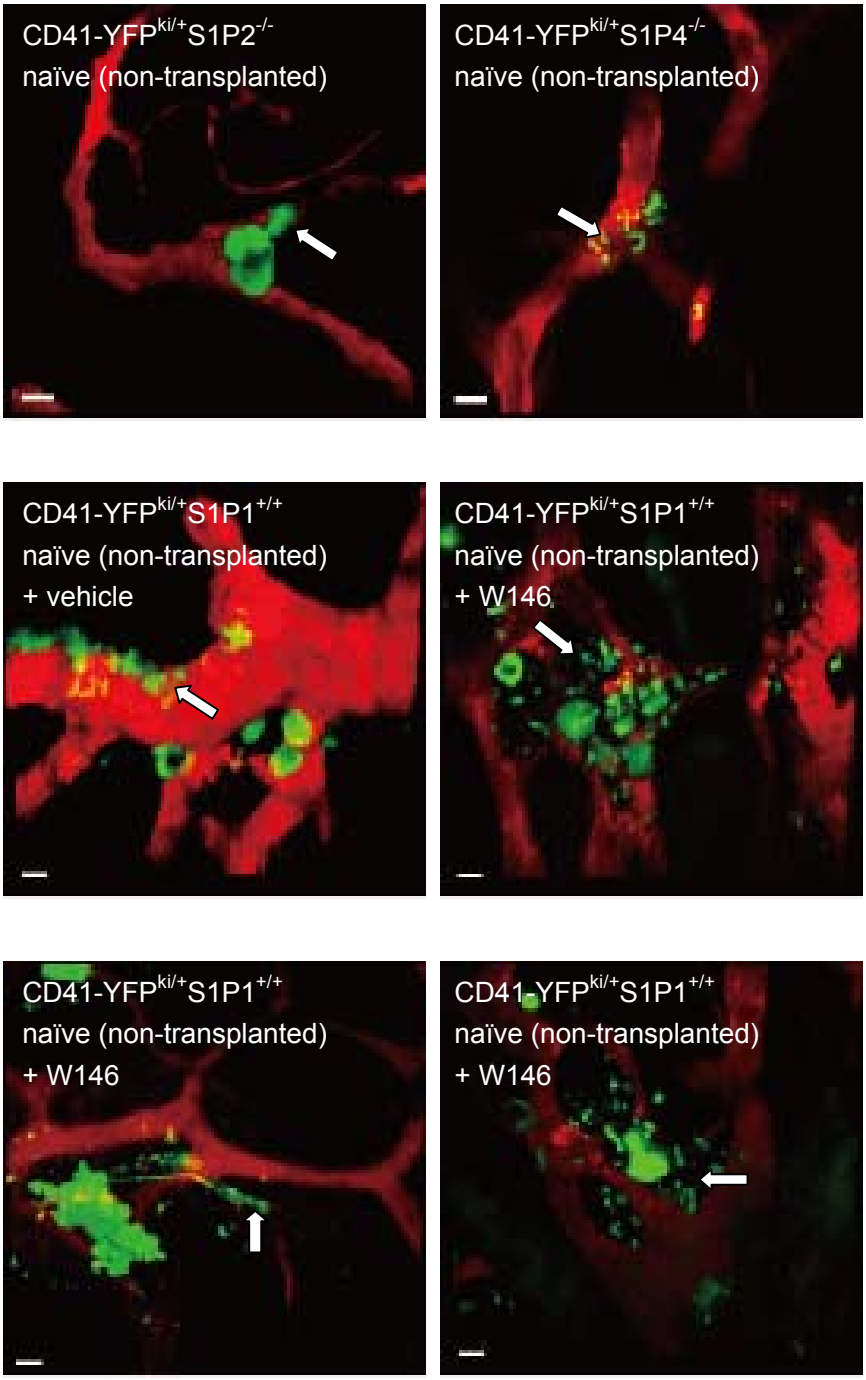

Fig. 3.31. Representative MP-IVM images of MKs with YFP+ or EGFP+ PPs. Green, MKs and PP; Red, sinusoids; Arrows, YFP+ or EGFP+ PPs.

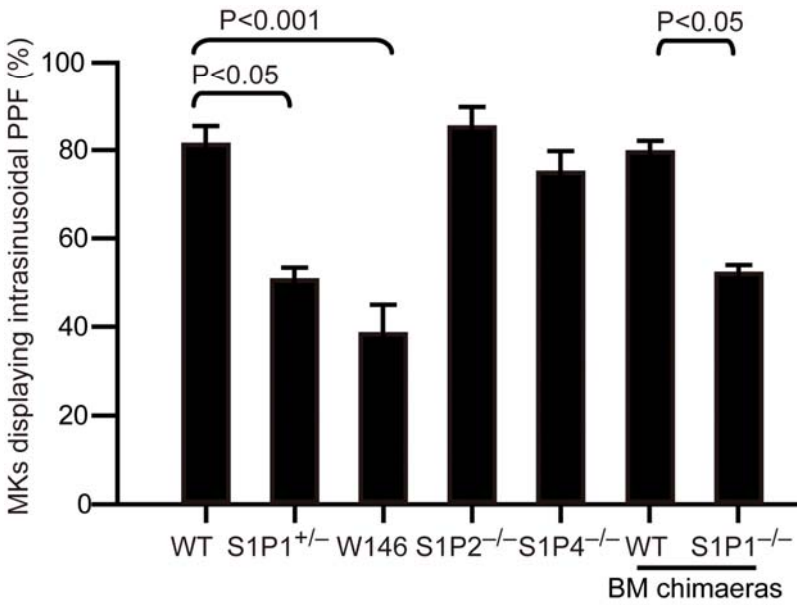

Fig. 3.32. MKs displaying intrasinusoidal PP formation (PPF) *in vivo*. The data are presented as percentage (means ± s.e.m) of all MKs carrying PPs.

3.3.14 Proplatelet fragmentation *in vitro*

To our surprise, when we incubated cultured MKs to allow PP formation and then added micromolar concentrations of S1P, we found a significant reduction in the number of MKs displaying PP extensions (Fig. 3.33). Using DIC microscopy of cultured MKs, we observed that exposure to micromolar S1P concentrations resulted in almost immediate shedding of PPs from their parental MKs (Fig. 3.34). Platelets were shed from 25.6% of PPs treated with S1P, while platelets were spontaneously released from only 2.9% of PPs treated with vehicle within 1 hour (Fig. 3.35). To further quantify the effect of S1P on PP shedding, we determined the number of fragmentation events by flow cytometry (Fig. 3.36). S1P increased PP fragmentation at concentrations that exist in the plasma, but not at low concentration present in the BM interstitium (Fig. 3.36). *In vivo*, blood flow-induced shear stress might facilitate the separation of intravascular cell fragments from MKs [13]. We, therefore, evaluated whether S1P also plays a role for PP fragmentation under flow conditions. Cultured MKs exposed to the physiological shear stress of BM sinusoids (4 dynes/cm^2) [13] in the absence of S1P (serum-free buffer) rarely shed PPs from their MK stems. In contrast, in the presence of S1P (5 μM) PPs were rapidly released (Fig. 3.37-38),

indicating that S1P is required for PP shedding under static as well as flow conditions. We did not find a significant difference when we examined S1P2$^{-/-}$, S1P4$^{-/-}$ and WT MKs (Fig. 3.34-35). However, lack of the megakaryocytic S1P1 completely abolished S1P-induced release of PPs (Fig. 3.34-35), indicating that this receptor subtype plays a predominant role for S1P-directed PP shedding, whereas S1P2 and S1P4 are dispensable.

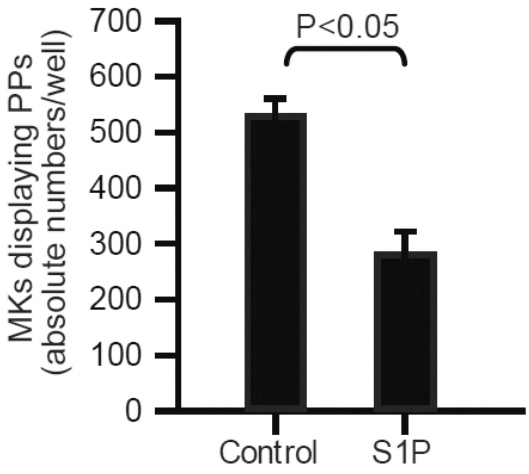

Fig. 3.33. Micromolar S1P concentrations reduce the number of MKs displaying PP formation. The number of MKs displaying PP formation in the absence or presence of 5 μM S1P.

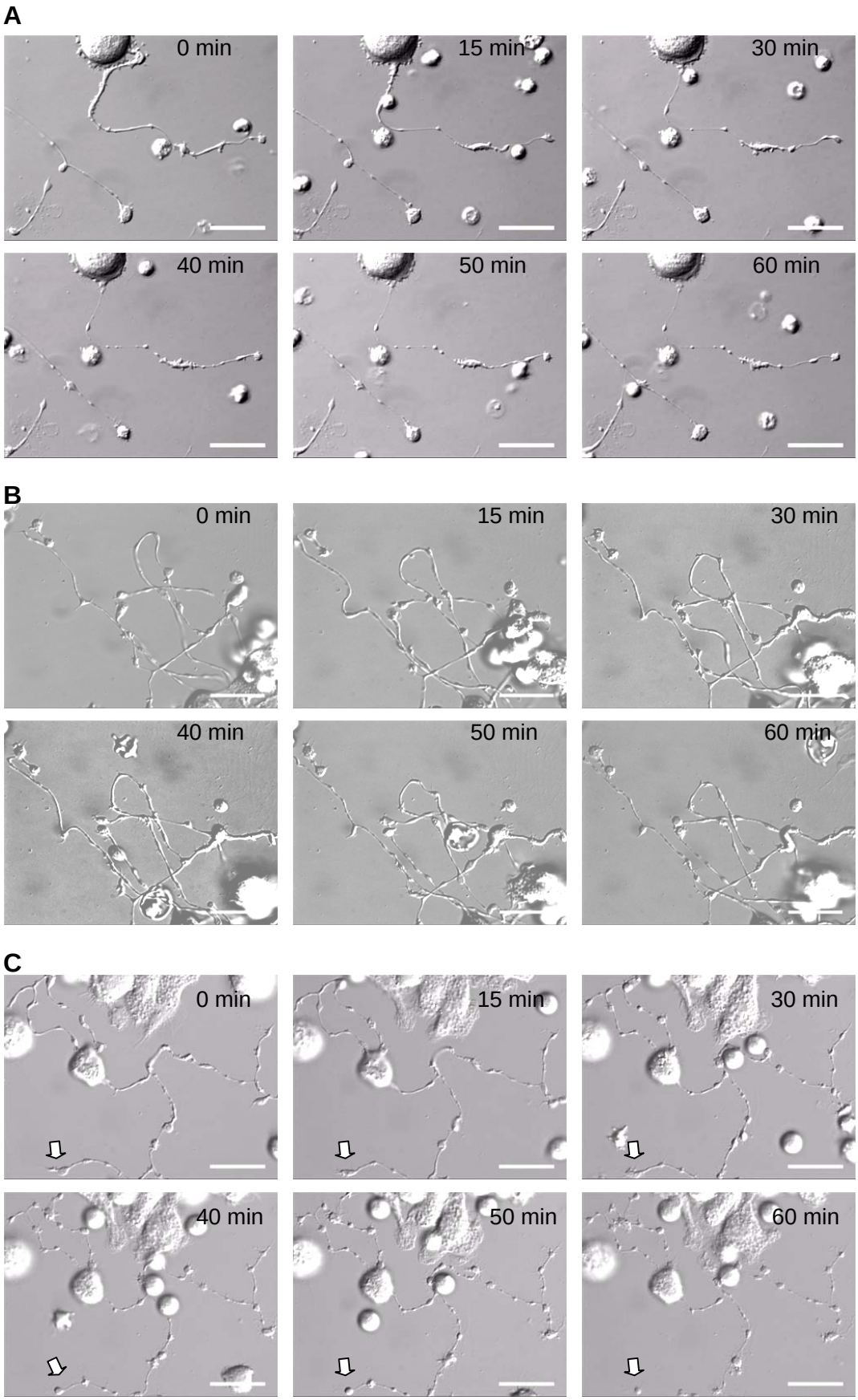
A
0 min
15 min
30 min
40 min
50 min
60 min
B
0 min
15 min
30 min
40 min
50 min
60 min
C
0 min
15 min
30 min
40 min
50 min
60 min

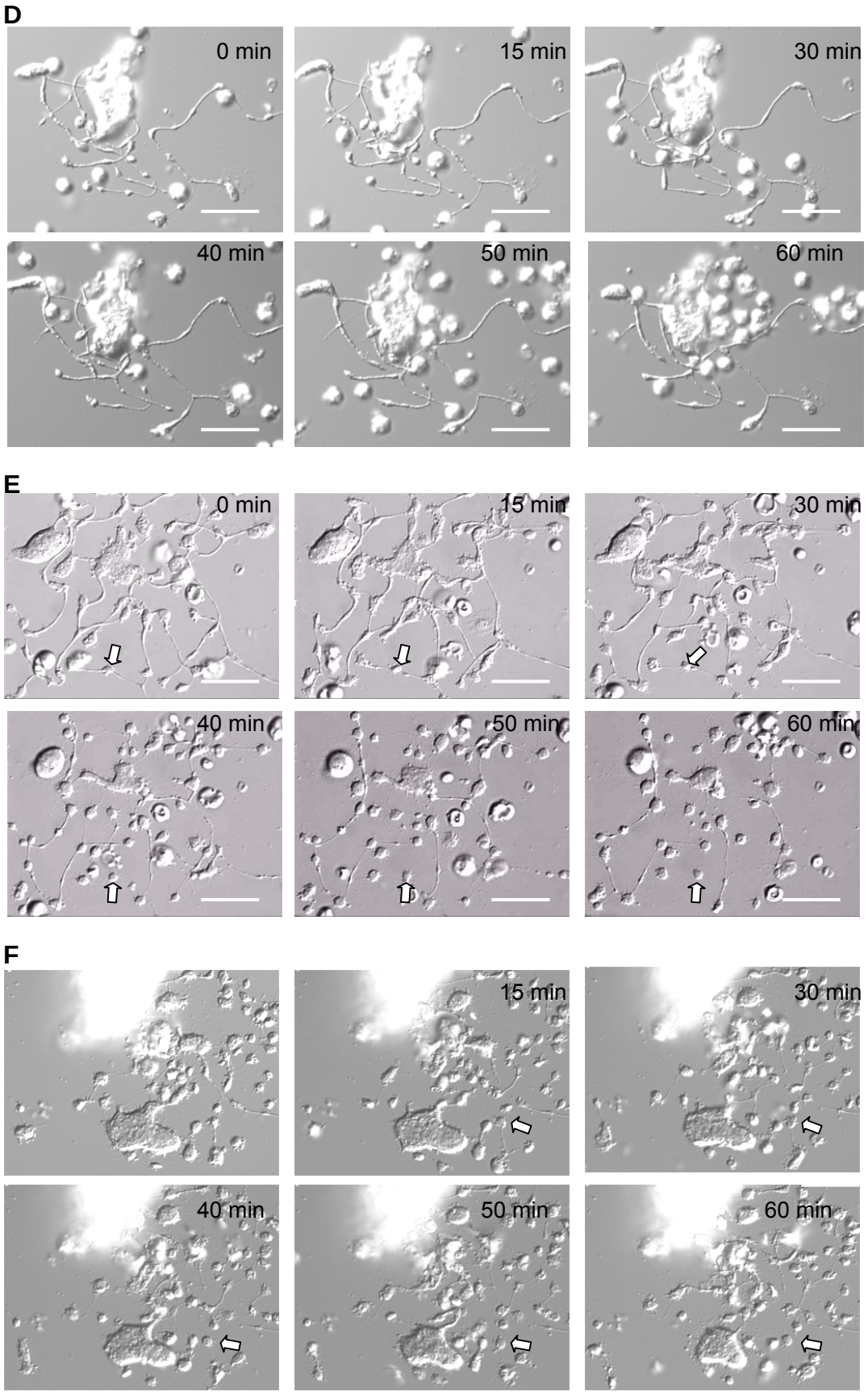

Fig. 3.34. DIC microscopic analysis of proplatelet fragmentation. DIC microscopy image sequences of PPs *in vitro*. **A**, WT MKs without treatment; **B**, WT MKs treated with

vehicle; **C**, WT MKs treated with S1P; **D**, S1P1$^{-/-}$ MKs treated with S1P; **E**, S1P2$^{-/-}$ MKs treated with S1P; **F**, S1P4$^{-/-}$ MKs treated with S1P. Arrows, Platelet-like particles released from PP stems; Scale bars, 20 μm; Time in minutes.

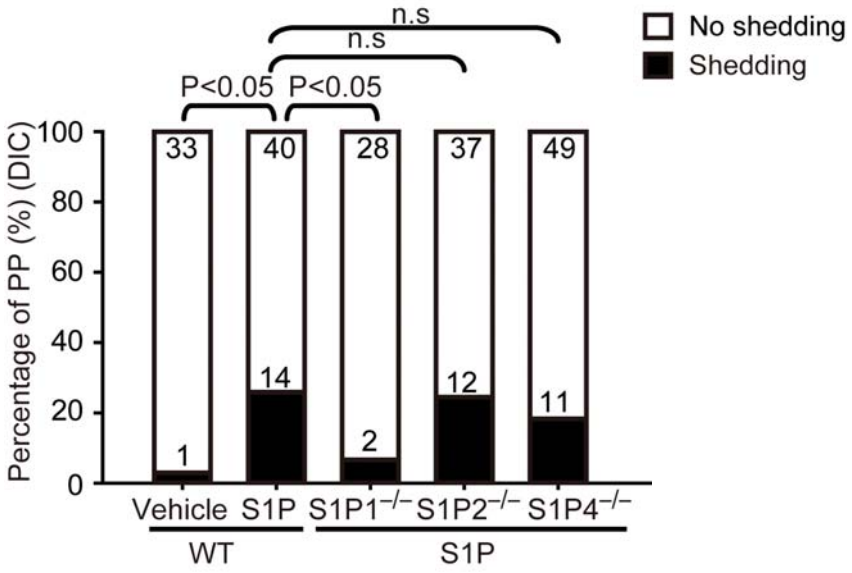

Fig. 3.35. S1P-induced PP fragmentation is dependent on S1P1. The number of PPs with or without fragmentation observed by DIC microscopy *in vitro* over 1 hour in the indicated groups.

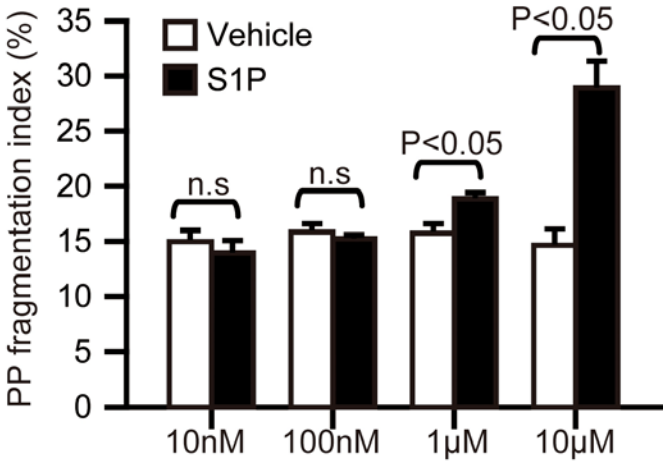

Fig. 3.36. S1P-induced PP fragmentation is dose dependent on S1P levels. Flow cytometric analysis of the PP fragmentation index in the presence or absence of various concentrations of S1P.

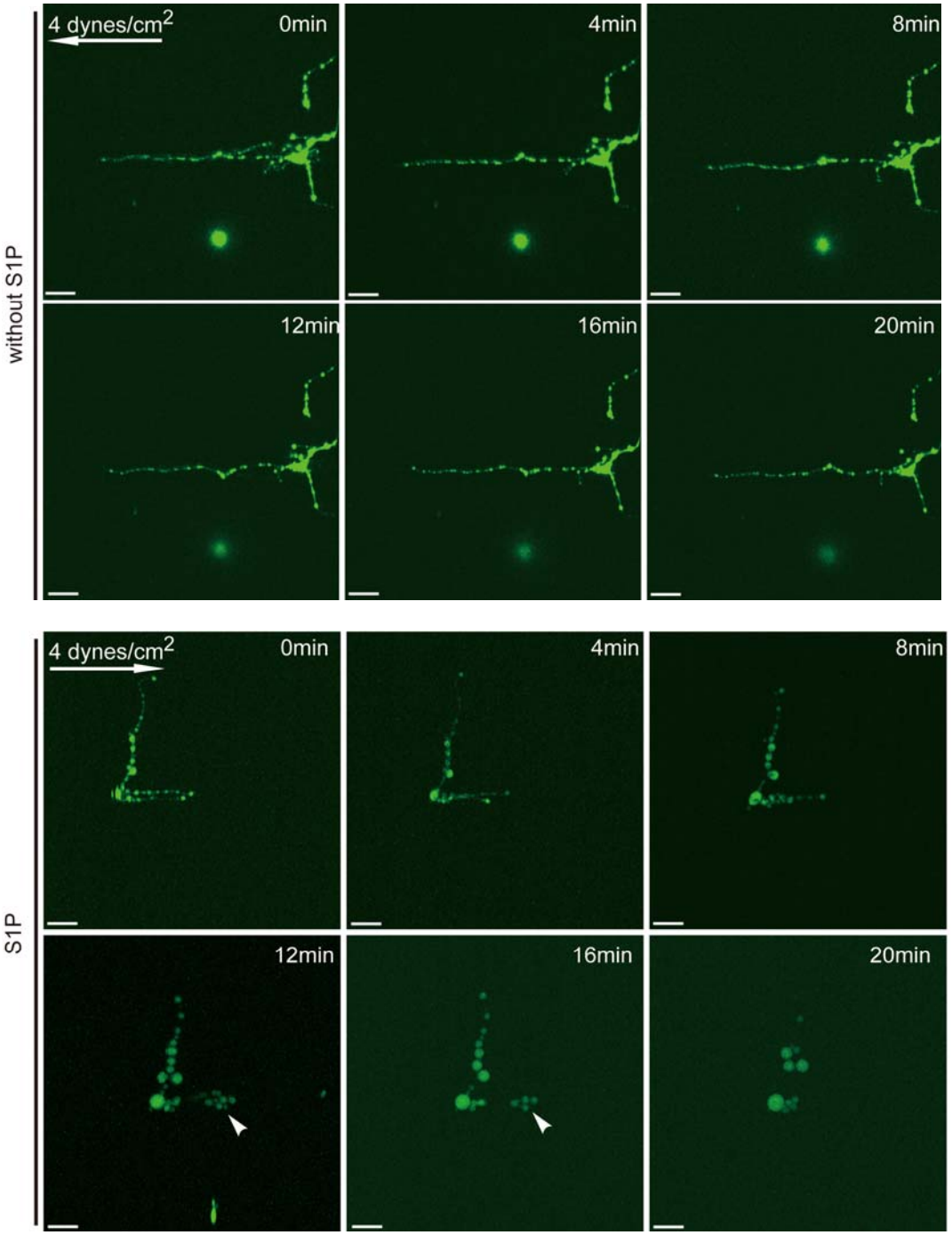

Fig. 3.37. S1P-induced PP fragmentation under shear stress. Time-lapse sequences of PPs in the presence or absence of 5 μM S1P under shear stress (4 dynes/cm^2). Arrow, direction of flow; arrowhead, PP shedding events.

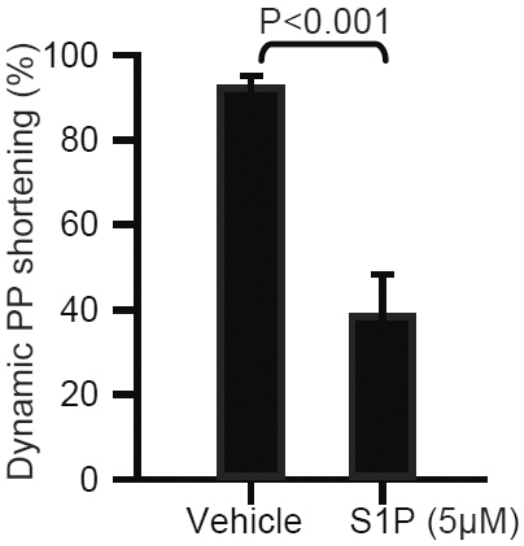

Fig. 3.38. PP fragmentation by MKs exposed to shear. The percentage of dynamic PP shortening was calculated as described in the Methods Section.

3.3.15 Proplatelet fragmentation *in vivo*

To address whether S1P/S1P1-signalling is also essential for PP fragmentation *in vivo*, we examined PP shedding in live mice by MP-IVM. PP shedding from MKs was a frequent event in naïve (non-transplanted) $S1P1^{+/+}$ CD41-$YFP^{ki/+}$ transgenic mice [13], but also in $S1P1^{+/+}$ CD41-$YFP^{ki/+}$ BM chimaeras (Fig. 3.39). Most MKs shed PP fragments that consist of beaded platelet-like structures (Fig. 3.39), which generate mature platelets by undergoing consecutive fragmentation steps [13, 24]. More than 60% of the $S1P1^{+/+}$ MKs carrying intravascular PP processes showed fragmentation within 1 hour (Fig. 3.40). In $S1P1^{-/-}$ lenti-GPIbα-EGFP chimaeras we barely observed intravascular PP processes due to the aberrant interstitial PP formation (Fig. 3.39-40). However, 70–100% of the PP processes that had eventually made their way into BM sinusoids remained firmly attached to their MK stems; only in rare instances MKs released large PP fragments (Fig. 3.39-40). Together, these data indicate that S1P1 is critical for both, directional PP formation and for proper intravascular PP fragmentation. There is no defect in platelet shedding in $S1P2^{-/-}$ or $S1P4^{-/-}$ mice (Fig. 3.40). Consistent with a defect in PP fragmentation and platelet shedding, the mean volume of circulating platelets was significantly increased in $S1P1^{-/-}$ compared to $S1P1^{+/+}$ chimaeras (Table. 3.2). Defective PP shedding is also likely to

explain the increase in size of S1P1$^{-/-}$ MKs (Fig. 3.19). Interestingly, the frequency of intravascular PP shedding was only moderately reduced in CD41-YFP$^{ki/+}$S1P1$^{+/-}$ mice (Fig. 3.40), suggesting that a single S1P1 allele is sufficient to maintain intravascular PP shedding and that the mild thrombocytopenia observed in S1P1$^{+/-}$ mice is mostly due to a minor defect in navigating PP processes into BM sinusoids (Fig. 3.32).

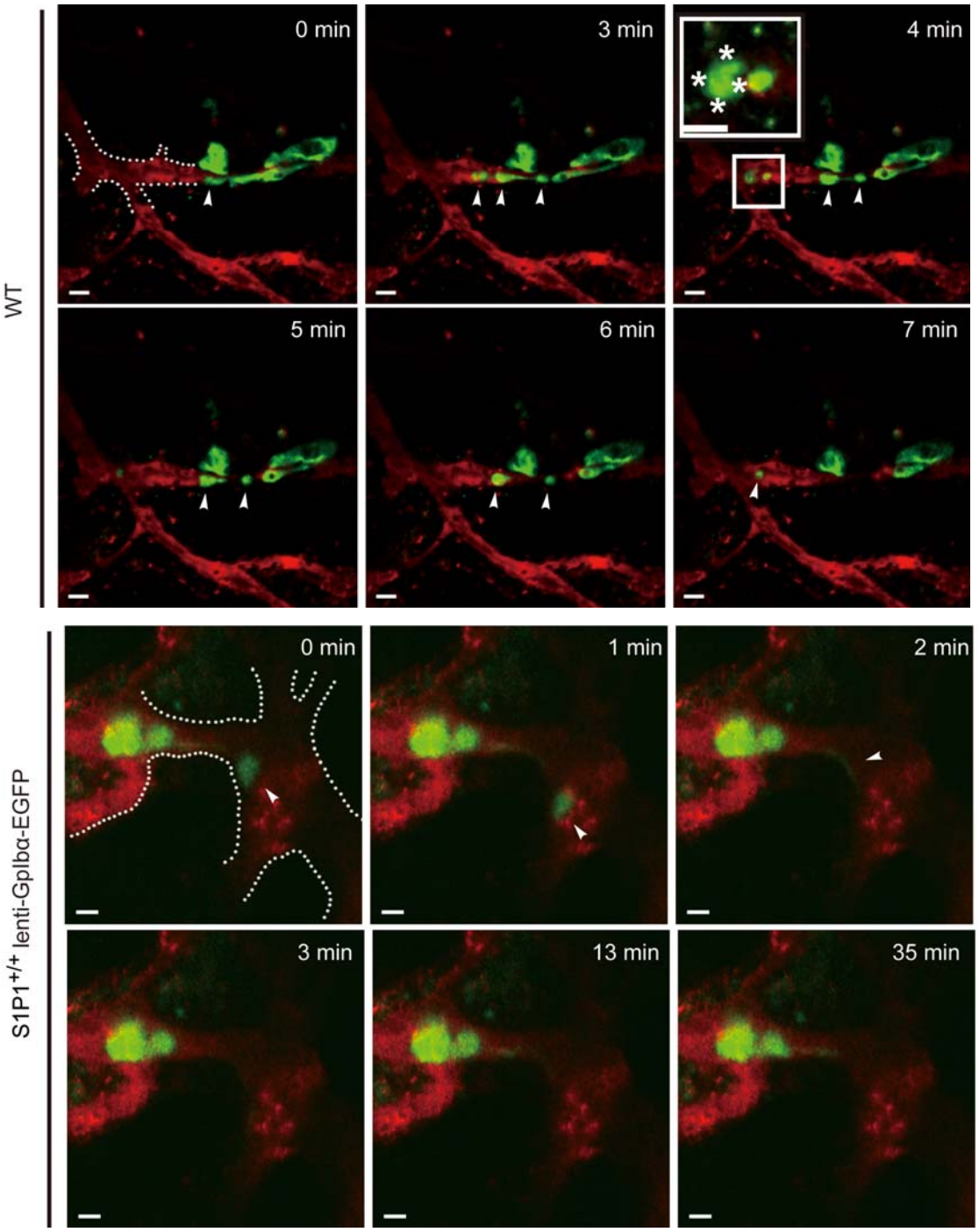

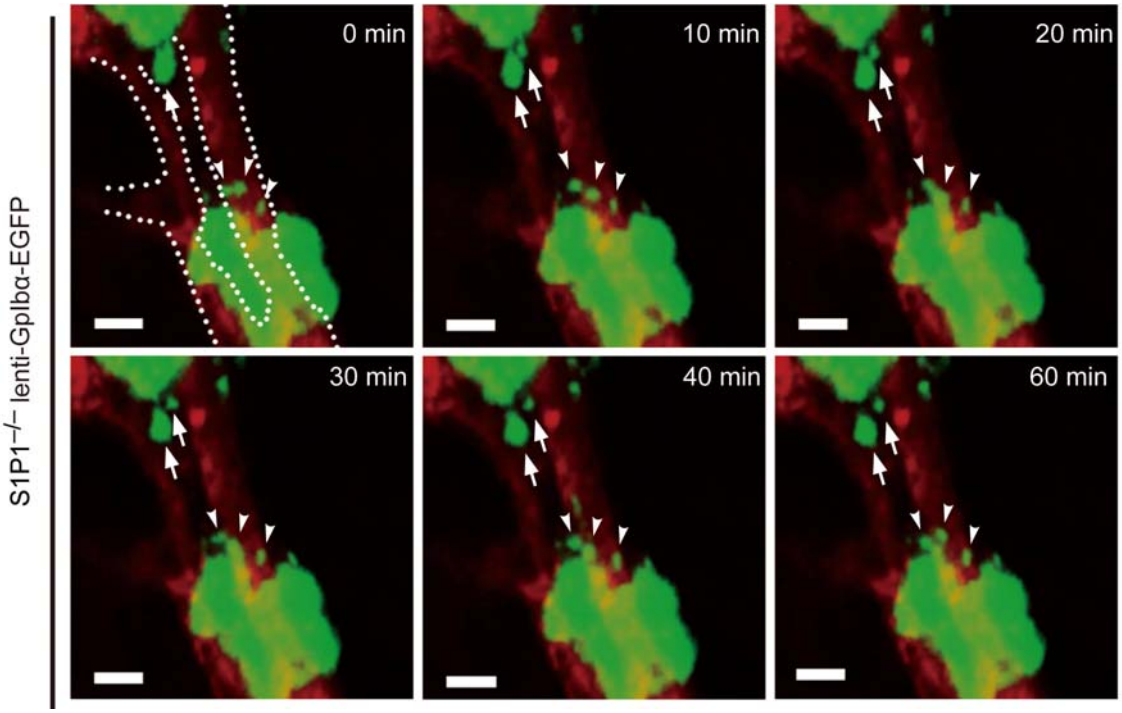

Fig. 3.39. Role of S1P1 for PP shedding *in vivo* visualized by MP-IVM. WT MKs frequently shed PPs as shown in the upper and the lower middle rows. The inset shows a magnification of a shed PP particle. Asterisks show embedded platelet-like particles. Loss or inhibition of S1P1 abolishes PP shedding (upper middle and lower rows). Arrowheads indicate intrasinusoidal PPs, arrows show extrasinusoidal PPs in S1P1 null chimaeras. The dashed line highlights the sinusoids. Green, MKs and PP; Red, Sinusoids; All scale bar, 20 μm; Time in minutes.

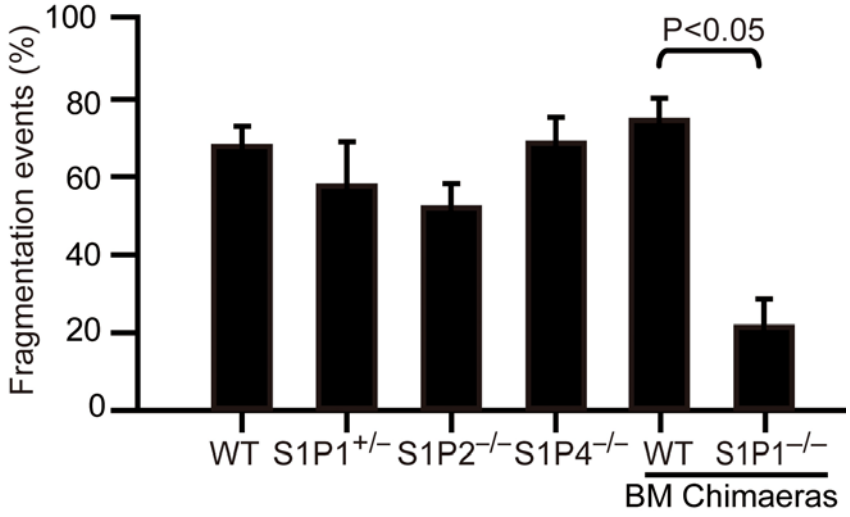

Fig. 3.40. S1P1 controls PP fragmentation *in vivo*. Percentage of PP fragmentation events observed by MP-IVM over 1 hour in the indicated groups.

3.3.16 Pharmacological inhibition of S1P1 *in vivo*

To examine, whether S1P1 regulates the dynamic process of PP shedding independently from its effects on PP invasion into BM sinusoids, we next tested the consequences of short-term pharmacological inhibition of S1P1. We treated naïve (non-transplanted) $S1P1^{+/+}$ CD41-$YFP^{ki/+}$ mice with a single dose of the selective S1P1 antagonist W146 and visualized PP shedding immediately thereafter. In contrast to protracted inhibition or genetic ablation of S1P1 (Fig. 3.31-32), this did not affect the overall number of MKs with intravascular PP protrusions. However, less than 20% of MKs with established intravascular protrusions managed to release PP fragments into the blood stream within 6 h after administration of W146, the vast majority of the intra-sinusoidal processes remained attached to their MK stems (Fig. 3.41-42). W146 maintains an adequate *in vivo* receptor blockade for only 5-6 hours [25] and shedding reoccurred 6 h after a single dose of W146, suggesting that S1P1 inhibition does not affect the viability of MKs (Fig. 3.42). In rare instances, where shedding occurred in the presence of the S1P1 inhibitor W146, the time required until an intravascular fragment dissociated from its MKs stem was significantly prolonged (Fig. 3.43). The failure to properly shed PPs resulted in the formation of abnormal, thick intravascular PP processes (Fig. 3.44). In line with this observation, the few PP fragments that were released despite the presence of W146 were significantly bigger compared to those in vehicle-treated control mice (Fig. 3.45), reminiscent of the large platelets observed in S1P1 null chimaeras (Table. 3.2).

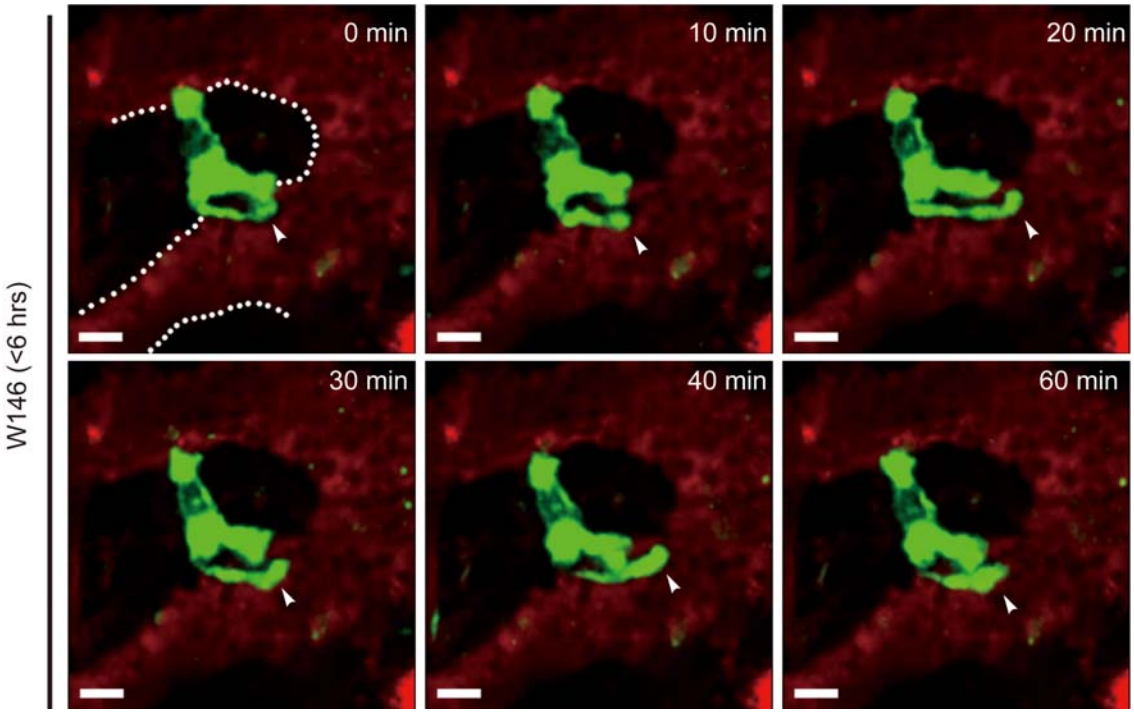

Fig. 3.41 Inhibition of S1P1 blocks PP shedding *in vivo* visualized by MP-IVM. Arrowheads indicate intrasinusoidal PPs. The dashed line highlights the sinusoids. Green, MKs and PP; Red, Sinusoids; All scale bar, 20 μm; Time in minutes.

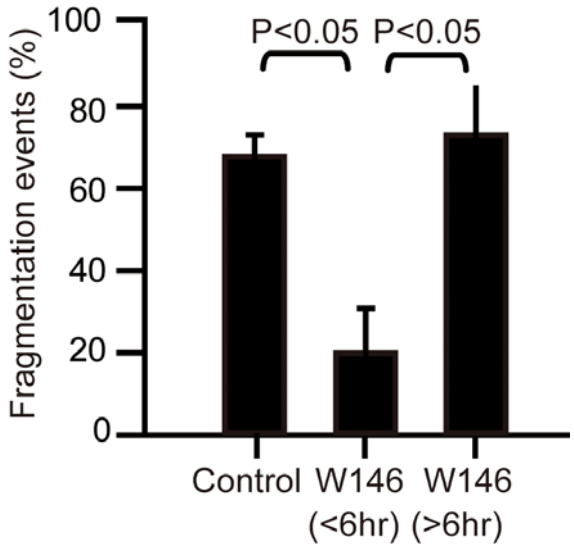

Fig. 3.42 Inhibition of S1P1 reduced the frequency of PP fragmentation *in vivo*. Percentage of PP fragmentation events observed by MP-IVM over 1 hour in the indicated groups. W146 inhibits PP fragmentation within 6 hours, while PP fragmentation recovers to the normal level 6 hours after W146 treatment.

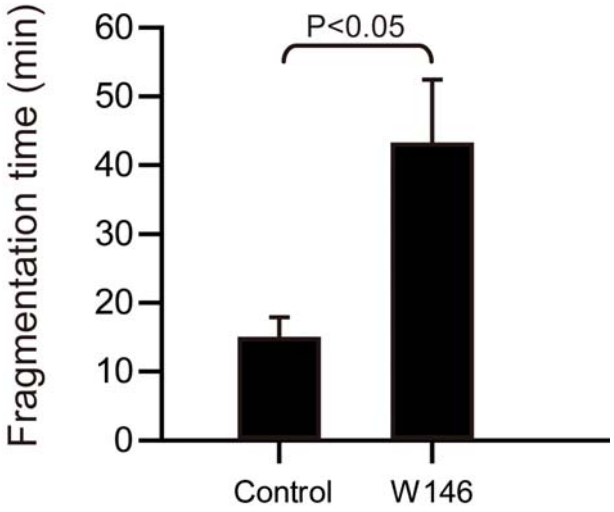

Fig. 3.43. Inhibition of S1P1 retards PP fragmentation. The time point of fragmentation detected by MP-IVM in mice treated with or without W146 (<6 hrs). (n=3 mice per group).

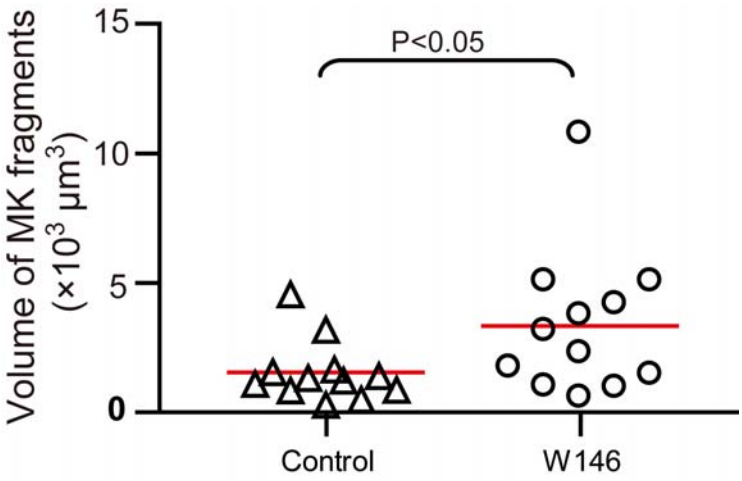

Fig. 3.44. Inhibition of S1P1 increases the size of PP fragments. Volume of PP fragments at the tips of PP from mice with or without administration of W146 (within 6 hours). (n=3 mice per group).

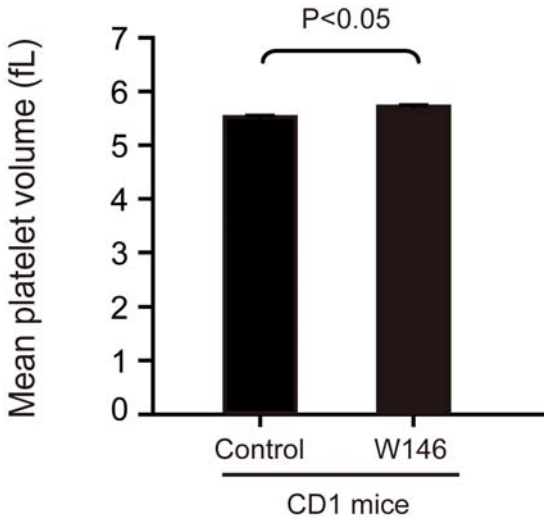

Fig. 3.45 Inhibition of S1P1 increases the size of platelets. Mean platelet volume of CD1 mice treated with or without W146

3.3.17 Molecular mechanism

S1P-S1P1 signalling can trigger Rac1, which is known to induce the formation of membrane extension [26]. We therefore tested if S1P could activate Rac1 via S1P1 in megakaryocytes and might thereby affect PP formation. We found that S1P enhances Rac1 activity in megakaryocytic cell lines (Fig. 3.46). Blockage of Rac1 completely inhibited PP formation in MKs *in vitro* (Fig. 3.47). One recent report revealed that actin filament turn over is regulated by ADF/confilin and contributes to PP formation [27]. This supports that Rac1 and its control of actin dynamics is one of the possible mechanisms how S1P1 regulates PP formation. Hence, Rac1 signalling pathway is related to the function of S1P1 on PP formation.

The myosin light chain 2 (MLC2)/non-muscle myosine II pathway is considered to be involved in the forces allowing PP to separate from their MK stem [5]. Correspondingly, patients with an autosomal dominant inherited defect in the MYH9 gene encoding myosin II reveal macrothrombocytopenia [28, 29]. Here, we found that S1P increases phosphorylation of MLC2 in MKs, as detected by Western blotting and immunofluorescence (Fig. 3.48-49). To further clarify the related signalling pathway, we

used pertussis toxin (PTX) and NSC23766 to inhibit G_i and Rac1 activity respectively. All the above mentioned inhibitors blocked S1P-induced fragmentation of PPs (Fig. 3.50). As S1P activates Rac1 in MKs via S1P1 (Fig. 3.46), this findings suggest that S1P induced-PP fragmentation is dependent on S1P1/G_i/Rac1/ p-MLC signalling.

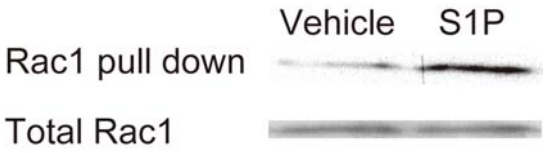

Fig. 3.46. S1P induces Rac1 activation in megakaryocytic cell lines. L8057 cells were incubated with 10 μM S1P or vehicle for 2 min. The activity of Rac1 was quantified by pull down assay. The total Rac1 amounts are shown as loading controls.

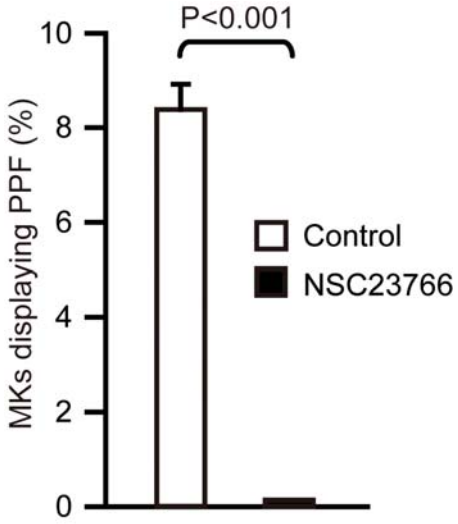

Fig. 3.47. Proplatelet formation depends on Rac1 activity. Number of MKs displaying PPF in the presence or absence of the Rac1 inhibitor, NSC23766 50 μM

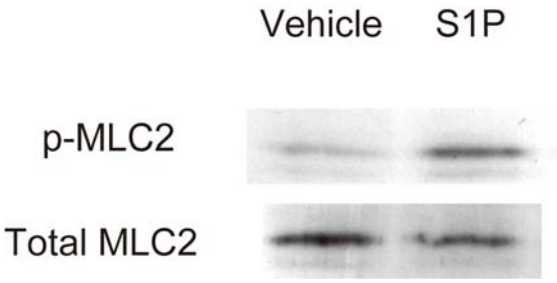

Fig. 3.48. S1P enhances phosphorylation of MLC2 in MKs. Increased MLC2 phosphorylation in MKs stimulated with 10 μM S1P. The level of p-MLC2 was studied by Western Blotting. Total MLC2 served as loading control.

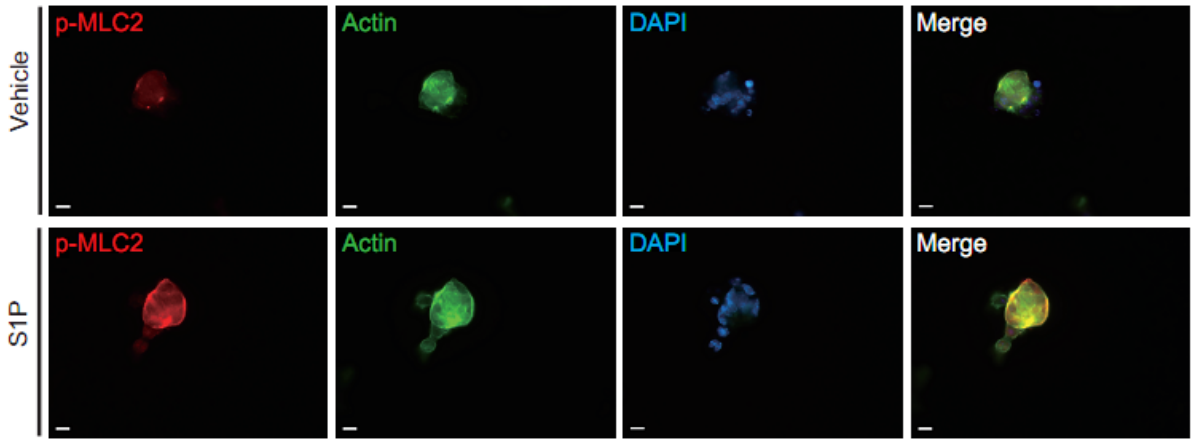

Fig. 3.49. S1P increases phosphorylation of MLC2 in MKs. Increased MLC2 phosphorylation in MKs stimulated with 10 μM S1P. The level of p-MLC2 was studied by immunostaining. Immunofluorescence analysis of p-MLC2 in MKs treated with vehicle (upper) or 10μM S1P (lower). p-MLC2, red; DAPI, blue; Actin, green. Scale bars for all images are 10 μm.

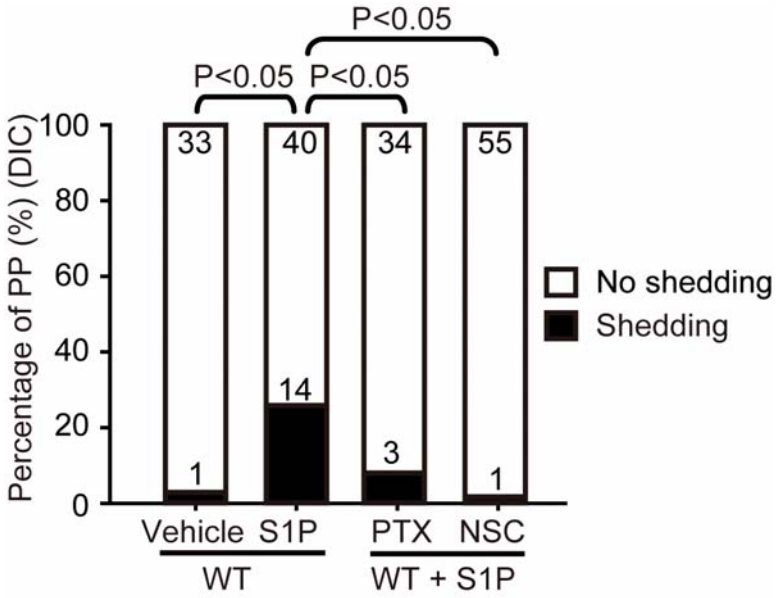

Fig. 3.50 S1P-induced PP fragmentation is dependent on Gi and Rac1. The number of PPs with or without fragmentation observed by DIC microscopy *in vitro* over 1 hour in the indicated groups

3.3.18 *In vivo* effects of S1P analogues

Recently, modulation of S1P receptor signalling by FTY720 (Fingolimod) has emerged as a promising immunosuppressive strategy and is currently being used in patients with multiple sclerosis [30]. After administration, FTY720 is metabolised to phosphorylated FTY720 (FTY720P), an agonist for four of the five S1P receptors including S1P1. FTY720 limits effector lymphocyte egress from lymph nodes [31], contributing to its immunosuppressive actions. However, FTY720 has not been examined for its potential effects on megakaryo- and thrombopoiesis. Here, we show that treatment of mice with a single-dose of FTY720 leads to a prompt increase in circulating platelets (Fig. 3.51). To further explain why FTY720 increases peripheral platelet counts, we examined the same megakaryocytes before and after a single dose of FTY720 treatment using MP-IVM. Our observation showed that megakaryocytes carried less intrasinusoidal proplatelets formation after FTY720 treatment (Fig. 3.52-53). These results indicated that the S1P analogue FTY720 enhances proplatelets fragmentation and indeed sheds proplatelet extensions from MKs, resulting in more platelet production within a relatively short time window. This suggests that FTY720 acts as an agonist on MKs and has the potential to rapidly mobilize platelets into the blood, most likely by supporting fragmentation of intravascular PP (Fig. 3.52-53). This differs from the consequences of lymphocyte S1P1 engagement by phosphorylated FTY720 within secondary lymphoid organs, which triggers down-modulation of the receptor resulting in functional antagonism of the S1P1 pathway. However, an agonistic effect of FTY720 similar to the one observed here for MK has recently been reported to promote the recirculation of BM osteoclast precursor monocytes from the bone surface [16], indicating that FTY720 predominantly exerts agonist effects in cells of the myeloid lineage. In addition, S1P1 receptors activated by FTY720P retain signalling activity for hours even in spite of a quantitative internalisation [32]. Moreover, SEW2871, an agonist against S1P1, also causes more circulating platelets, suggesting that S1P-S1P1 signalling indeed enhances thrombopoiesis and might present a possible clinical strategy to treat patients with thrombocytopenia (Fig. 3.54)

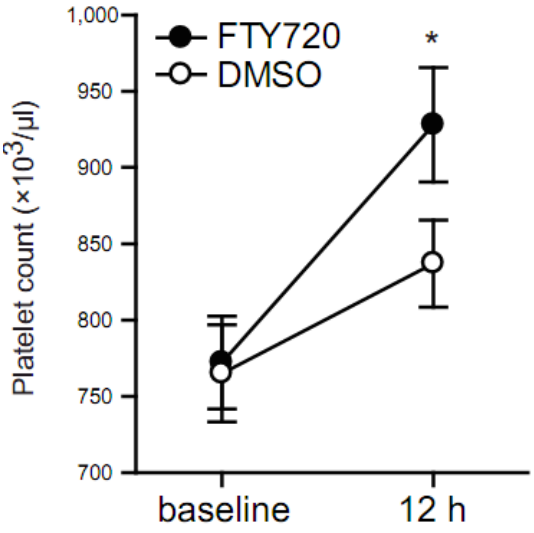

Fig. 3.51. FTY720 increases platelet counts in blood. Mice were treated with a single dose of FTY720 (3mg/kg i.p., filled circles) or DMSO (vehicle, open circles). Platelet counts were measured prior to and 12h after drug administration. Asterisk indicates P<0.05 vs. baseline.

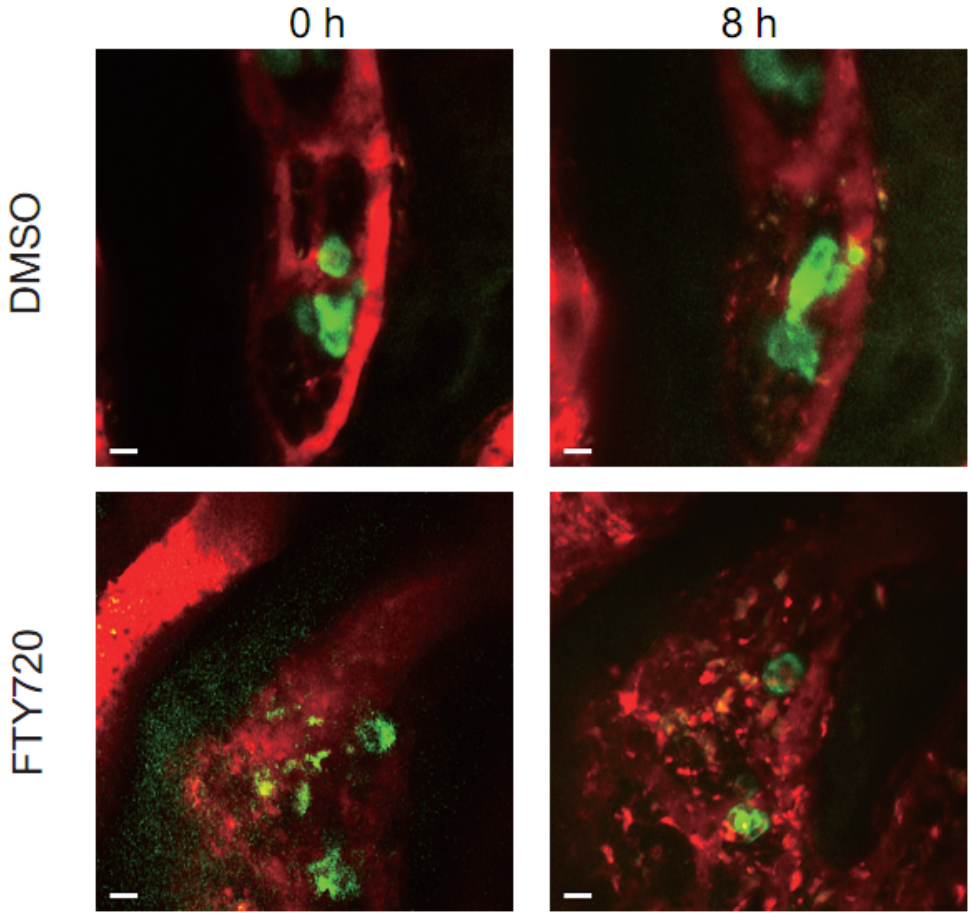

Fig. 3.52. *In vivo* imaging of MKs in mice treated with FTY720. Representative MP-IVM

images of MKs with YFP+ PPs from CD41-YFP$^{ki/+}$ mice prior to and 8 hours after a single injection of FTY720 (3mg/kg i.p.) or DMSO. Green, MKs and PP; Red, sinusoids; Scale bars, 20 μm.

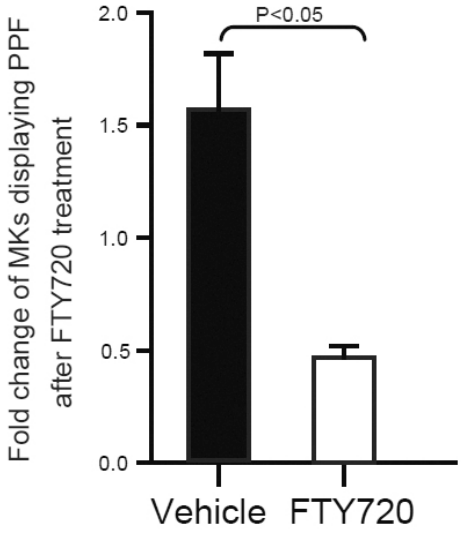

Fig. 3.53. The reduction in MKs displaying PPs in mice treated with FTY720. Fold change of MKs displaying PPF 8 hours after a single injection of FTY720 (3mg/kg i.p.) or DMSO compared to before treatment

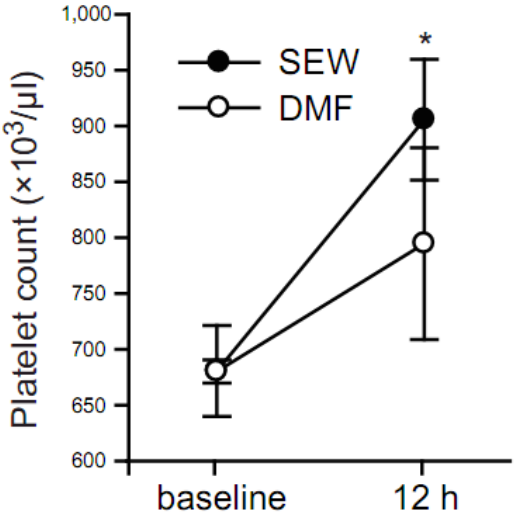

Fig. 3.54. SEW2871 increases platelet counts in blood. Mice were treated with a single dose of SEW2871 (20mg/kg i.p, filled circles) or dimethyl formamide (DMF, vehicle, open circles). Platelet counts were assessed prior to and 12h after drug administration. Asterisk, P<0.05 vs. baseline. All error bars indicate s.e.m.

3.4 Discussion

By intravital visualization of MKs, we further confirmed the proplatelet model *in vivo* and provided a detailed description of the physiology of platelet biogenesis. Immature MKs are derived from HSC that migrate to the bone marrow sinusoids, and during the same period differentiate into mature MKs with increasing cellular mass. The mature MKs will then extend pseudopodia and form proplatelets, which are navigated by biological signals into BM sinusoids. One recent study revealed that the egress of HSCs from BM also depends on a S1P gradient [33]. Our study showed that a similar mechanism acts in MKs to guide PP into sinusoids. The strategic mechanism to guide PPs into the blood physiologically may avoid the undesired platelet production inside the BM interstitium, where platelets are possibly activated by subendothelial matrix and cause *in situ* activation and aggregation. In the blood stream, the proplatelets grow at a speed of 9.76 μm/min, which is much faster than cultured MKs, which elongate at 0.85 μm/min [34]. However, the speed of PPF elaboration in sinusoids is similar to speed of microtubule assembly (10 μm/min) but slower than the red blood cell velocity in BM sinusoids (255.1-731.6 μm/sec) [6]. This observation suggested that the speed of proplatelets elaboration might be enhanced by the blood stream. The maximal growth speed of proplatelets is possibly limited by the speed of microtubule assembly, which is predicted to support the elongation of PPF in *in vitro* studies [35]. Once MKs successfully have extended their PPs into the blood, they manage to efficiently release a huge amount of platelets (about 1000 platelets/MKs) and homogenize PPs into 2-3 μm sized particles [36]. It is generally assumed that blood shear stress contributes to the fragmentation of PP [13]. However, our study revealed loss of S1P-S1P1 signalling resulted in inefficiency to release PPs even under physiological shear stress both *in vitro* and *in vivo*. This observation suggests that only extracellular force exerted by the blood shear stress was not sufficient for PP shedding.

Our research revealed that the process of platelets biogenesis is controlled through the S1P-S1P1 axis. The effect of S1P on thrombopoiesis has two separated consequences:

First, S1P initiates pseudopodia formation and enhances PP formation. The sharp transendothelial S1P gradient then polarizes their processes and directs the PP formation into BM sinusoids via S1P1. Second, higher homogenous micromolar concentrations of S1P in blood then cause the fragmentation of PP via S1P1 signalling. These distinct effects adapt to each other under physiological conditions, on one hand, since there is a sharp S1P gradient between tissue and blood, inducing diretional PP formation into the blood. Within the blood, PP will encounter micromolar concentrations of S1P, which enables fragmentation of PP. The intracellular cytoskeleton regulated by signalling pathway is also necessary for efficient PP shedding. Our study uncovers that micromolar concentrations of S1P within the blood trigger intracellular cytoskeleton rearrangements via S1P1/G_i/Rac1/p-MLC signaling, significantly enhancing PP shedding. It is known that phosphorylation of MLC enhances actin/myosin motor activation and contributes to cell contractility, cytokinesis, locomotion and maintenance of a balance between the actomyosin and microtubule cytoskeleton [5]. We propose that actin/myosin might provide intracellular forces, which are combined with the outside shear stress helps to fragmentate PP and homogenously distribute granules/organelles into mature platelets. If there is a dysfunction in actin/myosin activation, the fragmentation of PP will be affected. The defect in fragmentation possibly results in megathrombocytopenia. This could provide one possible reason for the megathrombocytopenia obtained in the MYH9-related disorder, which causes a defect in myosin-A complex [4]. Our hypothesis provides a new viewpoint to explain the clinic disease.

These data bear important implications for the study of thrombopoiesis. First, they provide a new understanding of the physiology of thrombopoiesis. Second, they indicate that the misdirection of PPF is a possible reason for thrombocytopenia, and a defect in fragmentation is a novel potent mechanism leading to megathrombocytopenia. Strategies to establish or mimic S1P gradient may provide a new approach to increase the efficiency of platelet production and could lead to the development of a new therapy to treat thrombocytopenia

3.5 References

1. Kono, M., et al., *The sphingosine-1-phosphate receptors S1P1, S1P2, and S1P3 function coordinately during embryonic angiogenesis.* J Biol Chem, 2004. **279**(28): p. 29367-73.
2. Lecine, P., et al., *Mice lacking transcription factor NF-E2 provide in vivo validation of the proplatelet model of thrombocytopoiesis and show a platelet production defect that is intrinsic to megakaryocytes.* Blood, 1998. **92**(5): p. 1608-16.
3. Pang, L., et al., *Maturation stage-specific regulation of megakaryopoiesis by pointed-domain Ets proteins.* Blood, 2006. **108**(7): p. 2198-206.
4. Chen, Z., et al., *The May-Hegglin anomaly gene MYH9 is a negative regulator of platelet biogenesis modulated by the Rho-ROCK pathway.* Blood, 2007. **110**(1): p. 171-9.
5. Chang, Y., et al., *Proplatelet formation is regulated by the Rho/ROCK pathway.* Blood, 2007. **109**(10): p. 4229-36.
6. Mazo, I.B., et al., *Hematopoietic progenitor cell rolling in bone marrow microvessels: parallel contributions by endothelial selectins and vascular cell adhesion molecule 1.* J Exp Med, 1998. **188**(3): p. 465-74.
7. Brzeska, H., et al., *Rac-induced increase of phosphorylation of myosin regulatory light chain in HeLa cells.* Cell Motil Cytoskeleton, 2004. **58**(3): p. 186-99.
8. Birukov, K.G., et al., *Shear stress-mediated cytoskeletal remodeling and cortactin translocation in pulmonary endothelial cells.* Am J Respir Cell Mol Biol, 2002. **26**(4): p. 453-64.
9. Zhang, H., et al., *A GIT1/PIX/Rac/PAK signaling module regulates spine morphogenesis and synapse formation through MLC.* J Neurosci, 2005. **25**(13): p. 3379-88.
10. Golfier, S., et al., *Shaping of terminal megakaryocyte differentiation and proplatelet development by sphingosine-1-phosphate receptor S1P4.* FASEB J. **24**(12): p. 4701-10.
11. Liu, Y., et al., *Edg-1, the G protein-coupled receptor for sphingosine-1-phosphate, is essential for vascular maturation.* J Clin Invest, 2000. **106**(8): p. 951-61.
12. Allende, M.L., T. Yamashita, and R.L. Proia, *G-protein-coupled receptor S1P1 acts within endothelial cells to regulate vascular maturation.* Blood, 2003. **102**(10): p. 3665-7.
13. Junt, T., et al., *Dynamic visualization of thrombopoiesis within bone marrow.* Science, 2007. **317**(5845): p. 1767-70.
14. Zhang, J., et al., *CD41-YFP mice allow in vivo labeling of megakaryocytic cells and reveal a subset of platelets hyperreactive to thrombin stimulation.* Exp Hematol, 2007. **35**(3): p. 490-499.
15. Lavenu-Bombled, C., et al., *Glycoprotein Ibalpha promoter drives megakaryocytic lineage-restricted expression after hematopoietic stem cell transduction using a self-inactivating lentiviral vector.* Stem Cells, 2007. **25**(6): p. 1571-7.

16. Ishii, M., et al., *Sphingosine-1-phosphate mobilizes osteoclast precursors and regulates bone homeostasis.* Nature, 2009. **458**(7237): p. 524-8.
17. Kaushansky, K., *The molecular mechanisms that control thrombopoiesis.* J Clin Invest, 2005. **115**(12): p. 3339-47.
18. Radley, J.M. and C.J. Haller, *The demarcation membrane system of the megakaryocyte: a misnomer?* Blood, 1982. **60**(1): p. 213-9.
19. Schulze, H., et al., *Characterization of the megakaryocyte demarcation membrane system and its role in thrombopoiesis.* Blood, 2006. **107**(10): p. 3868-75.
20. Schwab, S.R., et al., *Lymphocyte sequestration through S1P lyase inhibition and disruption of S1P gradients.* Science, 2005. **309**(5741): p. 1735-9.
21. Pappu, R., et al., *Promotion of Lymphocyte Egress into Blood and Lymph by Distinct Sources of Sphingosine-1-Phosphate.* Science, 2007. **316**: p. 295-298.
22. Caligan, T.B., et al., *A high-performance liquid chromatographic method to measure sphingosine 1-phosphate and related compounds from sphingosine kinase assays and other biological samples.* Anal Biochem, 2000. **281**(1): p. 36-44.
23. Berdyshev, E.V., et al., *Quantitative analysis of sphingoid base-1-phosphates as bisacetylated derivatives by liquid chromatography-tandem mass spectrometry.* Anal Biochem, 2005. **339**(1): p. 129-36.
24. Behnke, O. and A. Forer, *From megakaryocytes to platelets: platelet morphogenesis takes place in the bloodstream.* Eur J Haematol Suppl, 1998. **61**: p. 3-23.
25. Sanna, M.G., et al., *Enhancement of capillary leakage and restoration of lymphocyte egress by a chiral S1P1 antagonist in vivo.* Nat Chem Biol, 2006. **2**(8): p. 434-41.
26. Rosen, H., et al., *Sphingosine 1-phosphate receptor signaling.* Annu Rev Biochem, 2009. **78**: p. 743-68.
27. Bender, M., et al., *ADF/n-cofilin-dependent actin turnover determines platelet formation and sizing.* Blood. **116**(10): p. 1767-75.
28. Seri, M., et al., *Mutations in MYH9 result in the May-Hegglin anomaly, and Fechtner and Sebastian syndromes. The May-Hegglin/Fechtner Syndrome Consortium.* Nat Genet, 2000. **26**(1): p. 103-5.
29. Kelley, M.J., et al., *Mutation of MYH9, encoding non-muscle myosin heavy chain A, in May-Hegglin anomaly.* Nat Genet, 2000. **26**(1): p. 106-8.
30. Kappos, L., et al., *Oral fingolimod (FTY720) for relapsing multiple sclerosis.* N Engl J Med, 2006. **355**(11): p. 1124-40.
31. Matloubian, M., et al., *Lymphocyte egress from thymus and peripheral lymphoid organs is dependent on S1P receptor 1.* Nature, 2004. **427**(6972): p. 355-360.
32. Mullershausen, F., et al., *Persistent signaling induced by FTY720-phosphate is mediated by internalized S1P1 receptors.* Nat Chem Biol, 2009. **5**(6): p. 428-34.
33. Ratajczak, M.Z., et al., *Novel insight into stem cell mobilization-plasma sphingosine-1-phosphate is a major chemoattractant that directs the egress of hematopoietic stem progenitor cells from the bone marrow and its level in peripheral blood increases during mobilization due to activation of complement cascade/membrane attack complex.* Leukemia. **24**(5): p. 976-85.
34. Italiano, J.E., Jr., et al., *Blood platelets are assembled principally at the ends of proplatelet processes produced by differentiated megakaryocytes.* J Cell Biol, 1999.

147(6): p. 1299-312.

35. Thon, J.N., et al., *Cytoskeletal mechanics of proplatelet maturation and platelet release.* J Cell Biol. **191**(4): p. 861-74.

36. Kaushansky, K., *Historical review: megakaryopoiesis and thrombopoiesis.* Blood, 2008. **111**(3): p. 981-6.

Chapter 4: Effect of sphingosine kinases on thrombopoiesis

4.1 Introduction

The data outlined in the chapter 3 show that S1P-S1PRs signalling is essential for thrombopoiesis. Besides S1PRs, synthesis of S1P could also be involved in the control of thrombopoiesis. Sphingsoine kinases (Sphks) are the key enzymes producing S1P. However, nothing is known about the effect of sphingosine kinases on thrombopoiesis. In this chapter we investigated the function of Sphks in platelet biogenesis. Herein we show sphingosine kinase 2 (Sphk2) is the major isoenzyme in megakaryocytes. Loss of Sphk2 in MKs downregulates the expression of Src family kinases (SFKs) and reduces their activity in MKs, leading to a defect in PP fragmentation. Therefore, mice lacking hematopoietic Sphk2 expression display thrombocytopenia. Our data uncover the new function of Sphk2 in thrombopoiesis.

4.2 Materials and methods

4.2.1 Material

Dasatinib was purchased from Santa Cruz (Califomia, USA). D-erythro-Sphingosine-1-phospate (S1P) and PP2 were purchased from CALBIOCHEM (San Diego, CA, USA).

4.2.2 Mice

C57BL/6J (CD45.2), B6.SJL-PtprcPep3/BoyCrl (CD45.1) were purchased from Charles River Laboratories (Sulzfeld, Germany). Sphk1$^{-/-}$ and Sphk2$^{-/-}$ were produced and kindly provided by Danilo Guerini (Novartis Institute for BioMedical Research, Basel, Switzerland). CD41-YFP$^{ki/+}$ mice were described previously [1] and kindly provided from Thomas Graf (Center of Genomic Regulation and ICREA, Spain). To generate Sphk2$^{-/-}$ x CD41-YFP$^{ki/+}$ mice, the CD41-YFP$^{ki/+}$ mouse strain was crossed with Sphk2$^{-/-}$. All animals were bred and maintained at the animal facility of the German Heart Centre Munich. Age- and gender-matched mice were used in these studies. All experimental procedures performed on animals met the requirements of the German legislation on protection of animals and were approved by the Government of Bavaria/Germany.

4.2.3 Chimeras

To create Sphk2-deficient bone marrow chimeras, approximately 20 x 10^6 bone marrow mononuclear cells (CD45.2) isolated from Sphk2$^{-/-}$ were injected into lethally irradiated (two doses of 6.5 Gy) CD45.1 mice (B6.SJL-PtprcPep3/BoyCrl) via the tail vein. In all the chimeras more than 90% of the blood cells were donor-derived after haematopoietic reconstitution.

4.2.4 Western Blot analysis

The isolated BM cells were depleted of lineage positive cells using lineage depletion kit (MACS). The remaining lineage negative cell population was cultured in 2% FCS-supplemented DMEM medium containing 20 ng/mL murine SCF at 37°C under 5% CO2 for 2 days. Cells were then cultured for a further 3 days in the presence of 20 ng/ml SCF and 50 ng/ml TPO. After 5 days of culture, mature MKs were enriched using a 1.5% / 3% BSA gradient under gravity (1×g) for 45 minutes at room temperature. Mature bone marrow-derived MKs were starved for 2 hours prior to stimulation with 10 µM S1P or vehicle for 5 min. Whole cell extracts were prepared by incubating cells in 2× fold concentrated lysis buffer. The suspension was incubated on ice for 20 min and subsequently centrifuged at 14.000 g at 4°C for 10 min. the supernatant was used for Western blot analysis. The activity of SFKs in MKs lysate was detected using the antibody against p-Y 418-SFK (Invitrogen).

4.2.5 Additional methods

All the other methods in Chapter 4, such as RT-PCR, FACS, immunostaining, MP-IVM etc, were mentioned in Chapter 3.

4.3 Results

4.3.1 Sphingosine kinases expression profile in megakaryocytes

We first determined whether megakaryocytes express the Sphk isoforms, Sphk1 and 2. Semiquantitative RT-PCR results showed that both Sphk1 and Sphk2 are expressed in immature and mature MKs as well as in the megakaryocytic cell lines CMK, DAMI, Megk01 and Y-10 cells (Fig. 4.1-2). We next used real-time PCR to check the relative expression levels of Sphk1 and Sphk2 during megakaryocytic maturation. Our data show that both Sphk1 and Sphk2 are upregulated during megakaryocyte development (Fig. 4.3). Notably, Sphk2 is the major isoenzyme in mature megakaryocytes (Fig. 4.3). Further, Sphk2 protein was also detected in murine platelets by Western Blot (Fig. 4.4).

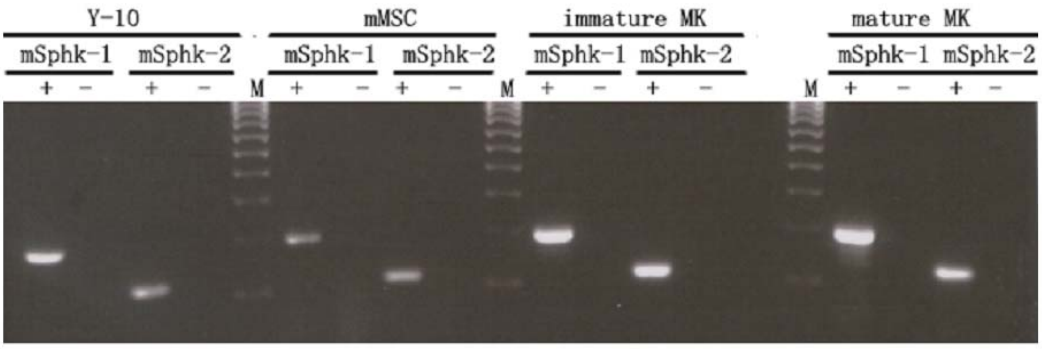

Fig. 4.1. Expression of Sphks mRNA in megakaryocytes. Y-10 is a murine megakaryocytic cell line. Both Sphk1 and Sphk2 are detected in Y-10, immature and mature megakaryocytes. Murine mesenchymal stem cells (mMSC) were used as positive controls.

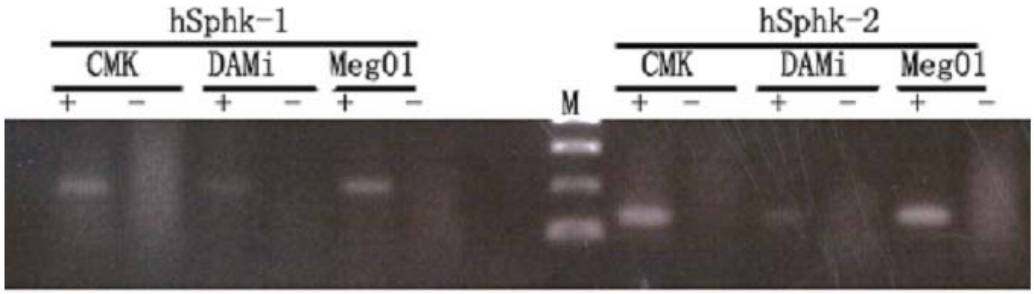

Fig. 4.2. Expression of Sphks mRNA in CMK, DAMi, and Meg01 human megakaryocytic cell lines

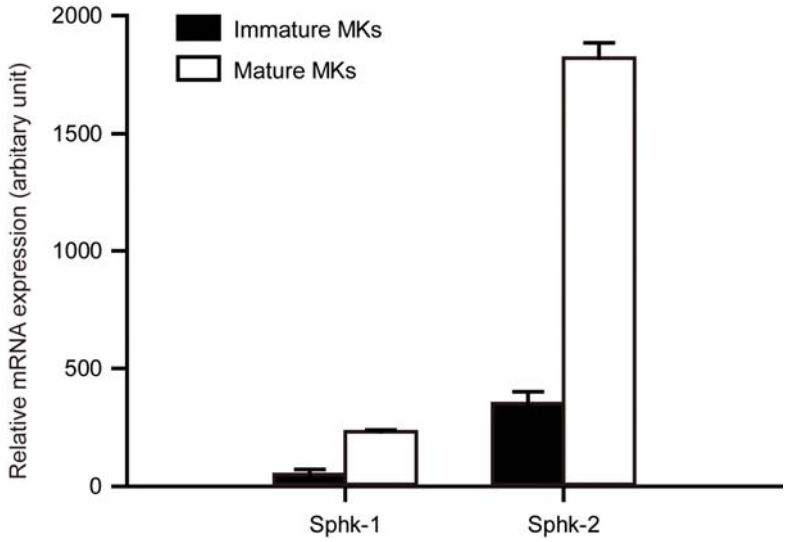

Fig. 4.3. Expression of Sphks mRNA in immature and mature MKs, Relative expression of

Sphks mRNA by fetal liver-derived mature (white) and immature megakaryocytes (black).

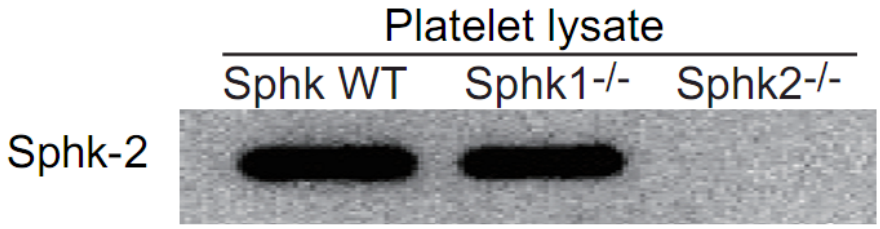

Fig. 4.4. Expression of Sphk2 protein in murine platelets.

4.3.2 Platelet counts in peripheral blood

To test whether Sphks are essential for thrombopoiesis, we measured the peripheral platelet counts in the mice, lacking Sphk1 or Sphk2. Our data shows that Sphk1$^{-/-}$ mice display normal peripheral platelet counts, whereas Sphk2^{-l-} mice have a reduction in platelets (Fig. 4.5). A similar thrombocytopenia was found in Sphk2^{-l-} mice on either Babl/c or C57Bl/6J background (Fig 4.5), suggesting that this phenotype is independent of the genetic background. To further determine whether this phenotype results from the loss of Sphk2 in the hematopoietic system, we generated BM chimaeras by transferring BM cells from either WT or Sphk2^{-l-} mice into irradiated WT recipient mice. We also found a similar reduction in peripheral platelet counts in Sphk2^{-l-} chimaeras as observed in full Sphk2 knock out mice (Fig. 4.6), indicating loss of Sphk2 in the hematopoietic system is causative for thrombocytopenia. Moreover, bigger platelets are found in full Sphk2$^{-/-}$ mice (Fig 4.5). These results demonstrate that Sphk1 is dispensable, while Sphk2 is critical for thrombopoiesis. Therefore, we focused on the function of Sphk2 in thrombopoiesis in the subsequent investigations.

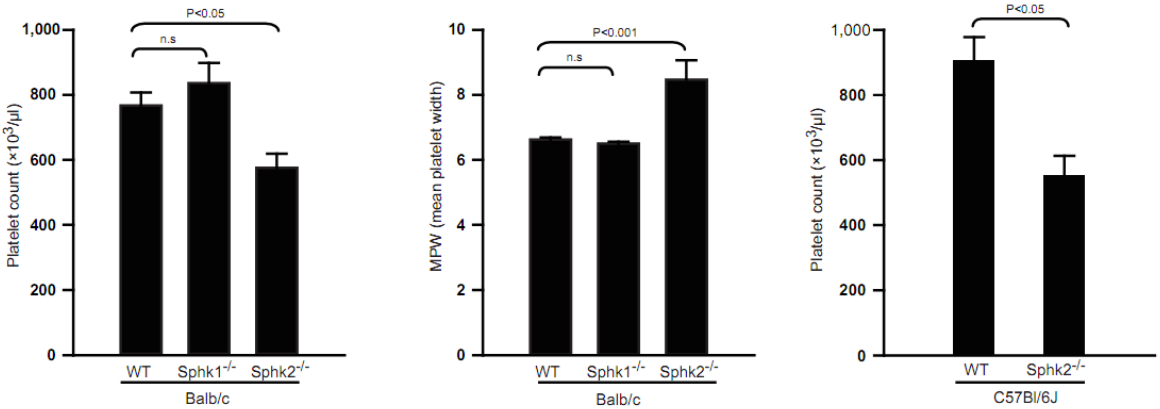

Fig. 4.5. Platelet counts and size in peripheral blood from WT, Sphk1$^{-/-}$ and Sphk2$^{-/-}$ mice.

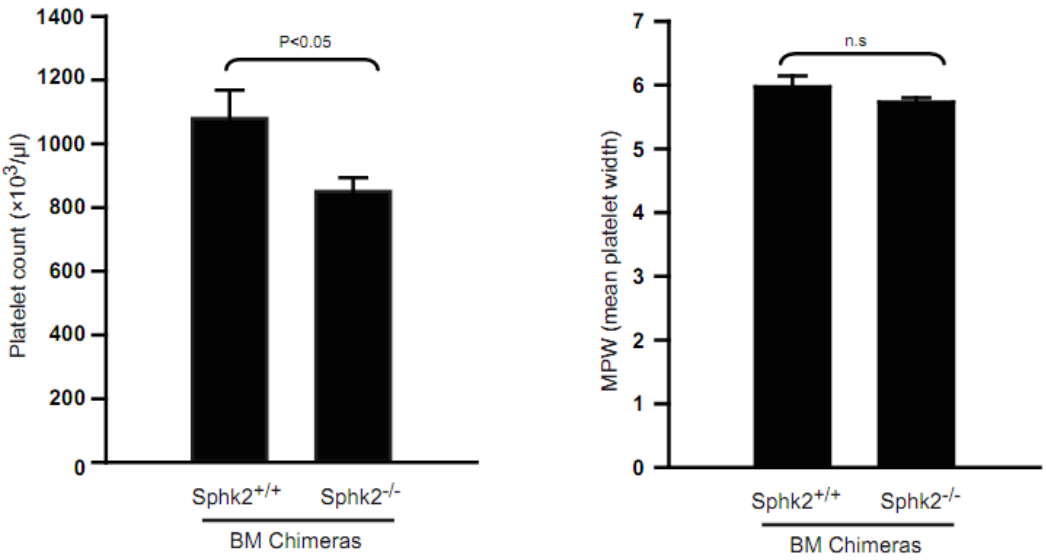

Fig. 4.6. Platelet counts and size in peripheral blood from WT or Sphk2$^{-/-}$ BM chimaeras (C57Bl/6J background).

4.3.3 Dissecting the reasons for thrombocytopenia in Sphk2$^{-/-}$ mice

To examine the reasons for the reduced platelet counts in Sphk2$^{-/-}$ mice, we next analysed the numbers of CFU-MKs between WT and Sphk2$^{-/-}$ bone marrow cells, and of bone marrow megakaryocytes, and determined serum Tpo levels as well as the platelet life span. We performed CFU-MK assays to determine the ability of BM hematopoietic stem cells (HSC) to generate MK progenitors. Our results show that Sphk2$^{-/-}$ BM cells generate similar number of CFU-MKs as WT (Fig. 4.7), suggesting that there is no defect in the generation of MK progenitors in the absence of Sphk2. As bone marrow megakaryocytes are the major source of blood platelets, we measured the number of megakaryocytes in femoral bone marrow. Histological analysis revealed no significant difference in the number of megakaryocytes between Sphk2$^{-/-}$ and WT controls (Fig. 4.8-9). Because Tpo is the principle physiological regulator of thrombopoiesis [2], we next analysed serum Tpo levels. Our data showed that the Tpo levels of Sphk2$^{-/-}$ mice were not significantly different from WT controls (Fig. 4.10), therefore excluding changes in Tpo level as a reason for the reduced platelet counts. The clearance of platelets also affects the number of peripheral platelets. To investigate platelet life span, the platelets were biotinylated by intravenous administration of N-hydroxysuccinimide-biotin, and the percentage of biotinylated platelets in peripheral blood were identified by staining with PE/cy7-conjugated streptavidin and monitored for 6 days by flow cytometry. Platelet life span and half-life were also unaffected in all those mice (Fig. 4.11), which suggested that the clearance of platelets does not explain thrombocytopenia in Sphk2$^{-/-}$ mice. Taken together, loss of Sphk2 does not cause a defect in either MK progenitors or MKs genesis or in the clearance of platelets.

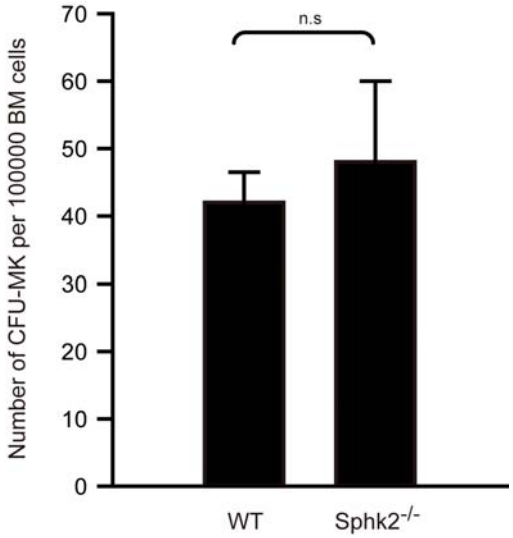

Fig. 4.7. Quantification of CFU-MKs numbers in BM cells. Error bars represent s.e.m.

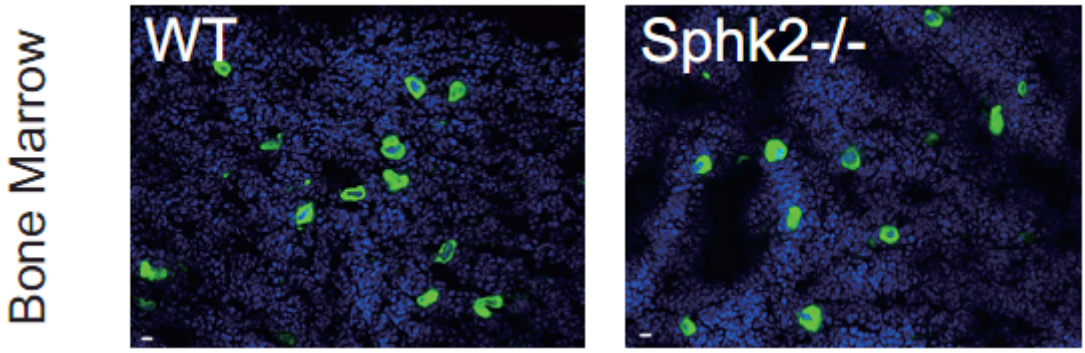

Fig. 4.8. Representative immunostaining of megakaryocytes in mouse femoral BM. Megakaryocytes were detected by the megakaryocyte-specific marker CD41 (green). DAPI (blue); Scale bar, 10 µm.

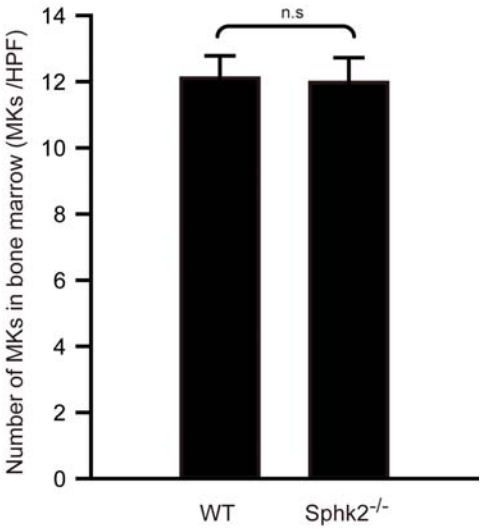

Fig. 4.9. Normal megakaryocyte counts in Sphk2$^{-/-}$ BM. Quantification of megakaryocyte numbers per 20× high-power fields in femoral BM sections.

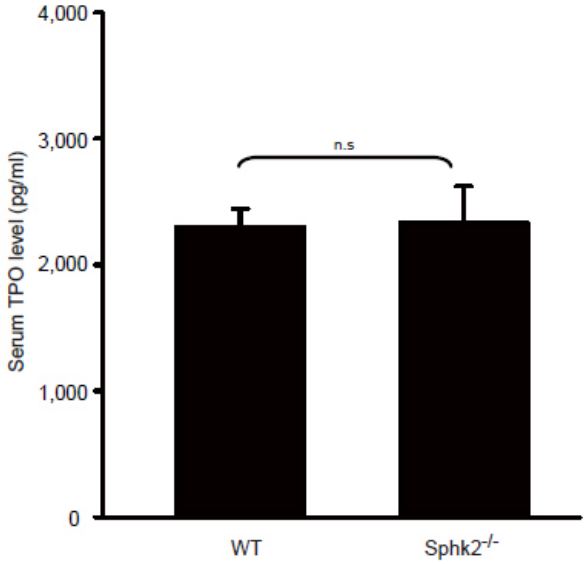

Fig. 4.10. Serum Tpo levels. Error bar, s.e,m; n=3-5 per group. t-test.

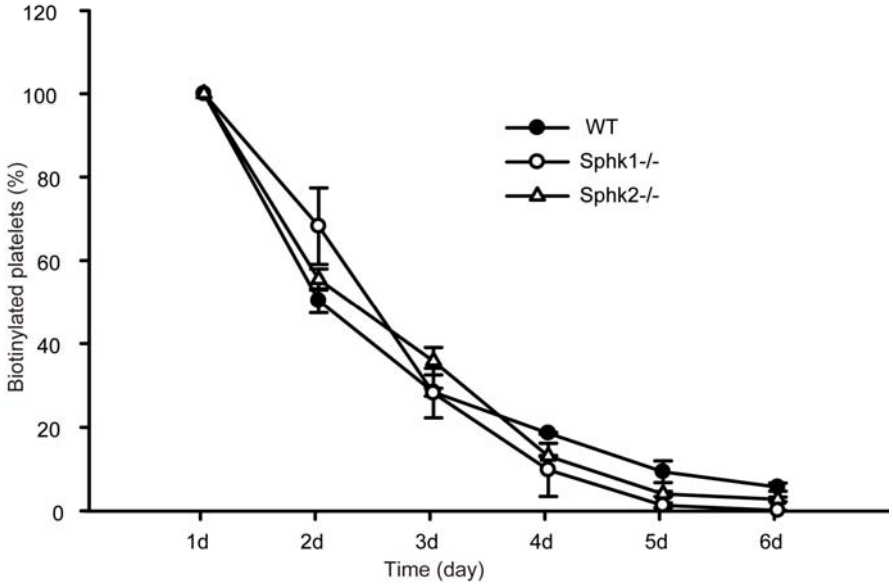

Fig. 4.11. Platelets life span of WT and Sphk mutant mice. Error bars represent s.e.m (n=3-5 per group). T-test was performed.

4.3.4 Extramedullary thrombopoiesis in Sphk2$^{-/-}$ mice

Beside the BM, the spleen also acts as source of platelets, especially under pathophysiological condition, e.g. during thrombocytopenia. Histological analysis shows that there are more MKs in Sphk2$^{-/-}$ spleens than in WT (Fig. 4.12-13). Moreover, the spleen mass of Sphk2 is much bigger than WT (Fig. 4.14-15). These results indicate that Sphk2$^{-/-}$ mice have extensive extramedullary thrombopoiesis to partially compensate for the reduction in platelets caused by loss of Sphk2.

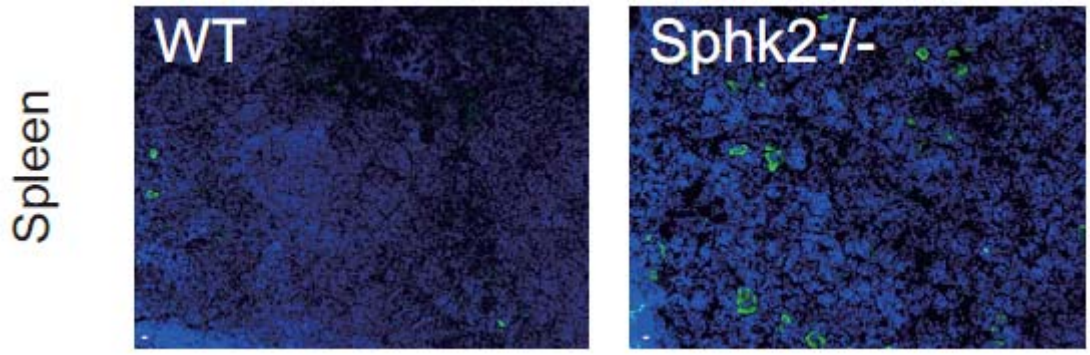

Fig. 4.12. Representative immunostaining of megakaryocytes in mouse femoral BM sections. Megakaryocytes were detected by the megakaryocyte-specific marker CD41 (green). DAPI (blue); Scale bar, 10 μm.

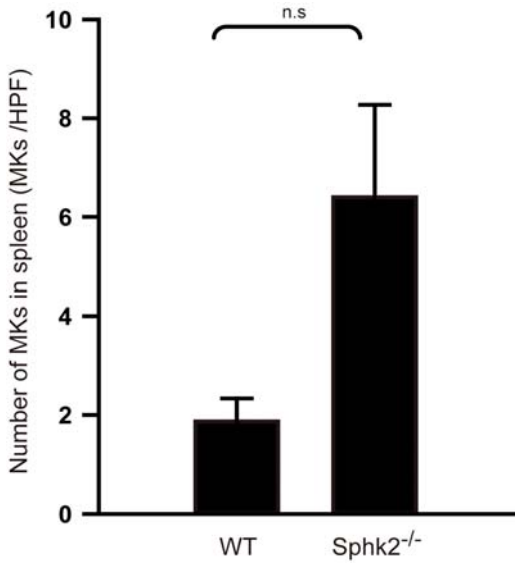

Fig. 4.13. Comparison of megakaryocytes in spleen between WT and Sphk2$^{-/-}$. Quantification of megakaryocyte numbers per 20× high-power fields in spleen.

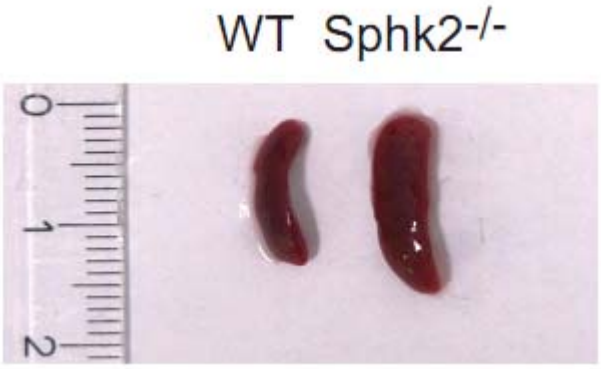

Fig. 4.14. Representative picture of extracted spleens from WT or Sphk2$^{-/-}$ mice.

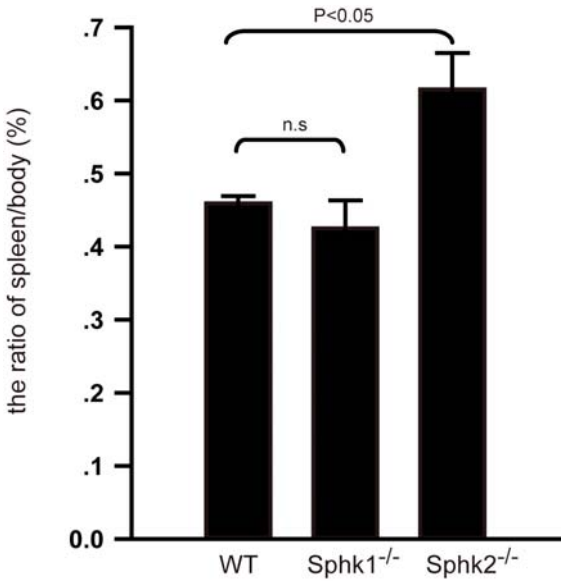

Fig. 4.15. Sphk2$^{-/-}$ mice display bigger spleen sizes. The ratio of spleen weight to the whole body weight.

4.3.5 Polyploidization of megakaryocytes

During MK maturation, MKs undergo polyploidization and increase the cell mass [3]. In order to evaluate polyploidization, we measured DNA contents in MKs by flow cytometry. The data shows that Sphk1$^{-/-}$ MKs show a higher ploidy, while Sphk2$^{-/-}$ MKs display normal polyploidization, indicating that Sphk2 does not affect the process of polyploidization in MKs.

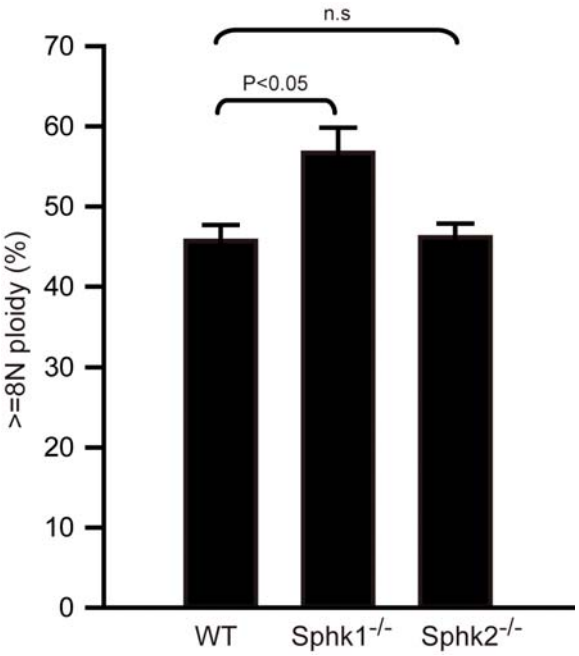

Fig. 4.16. Quantification of polyploidization of MKs in WT and Sphk mutant mice. The percentage of MKs with ploidy (>=8N) in the indicated group.

4.3.6 Proplatelet formation *in vitro* and *in vivo*

The mechanism of platelet release from megakaryocytes has been shown to follow the prevalent model of thrombopoiesis, the proplatelets model [4]. As outlined in the previous chapters, proplatelets are designated as the long cytoplasmic protrusions extended from mature megakaryocytes, which are supported by *in vitro* and *in vivo* evidence [5]. We thus examined whether Sphk2 deficiency had an effect on proplatelet formation. We analyzed proplatelet formation in fetal liver-derived MKs *in vitro*. Our results show that there is no significant difference in proplatelets formation between Sphk2$^{-/-}$ and WT (Fig. 4.17). Next, we used intravital MP-IVM to check CD41-YFP$^{ki/wt}$-Sphk2$^{-/-}$ MKs. Our results show that Sphk2$^{-/-}$ mice have a normal morphology of both MKs and proplatelets *in vivo* (Fig. 4.18). Moreover, most of Sphk2$^{-/-}$ proplatelets locate inside vessel (Fig. 4.19), similar to WT. These results suggest that there is no defect in PP formation in Sphk2$^{-/-}$ MKs both *in vitro* and *in vivo*.

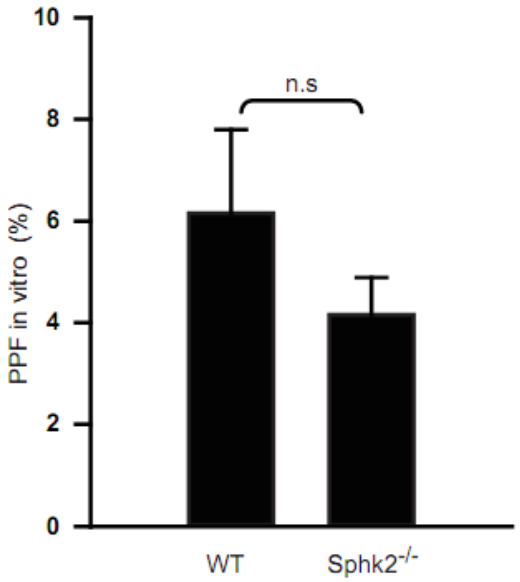

Fig. 4.17. Normal proplatelet formation in Sphk2$^{-/-}$ MKs. Number of MKs displaying PP formation (PPF).

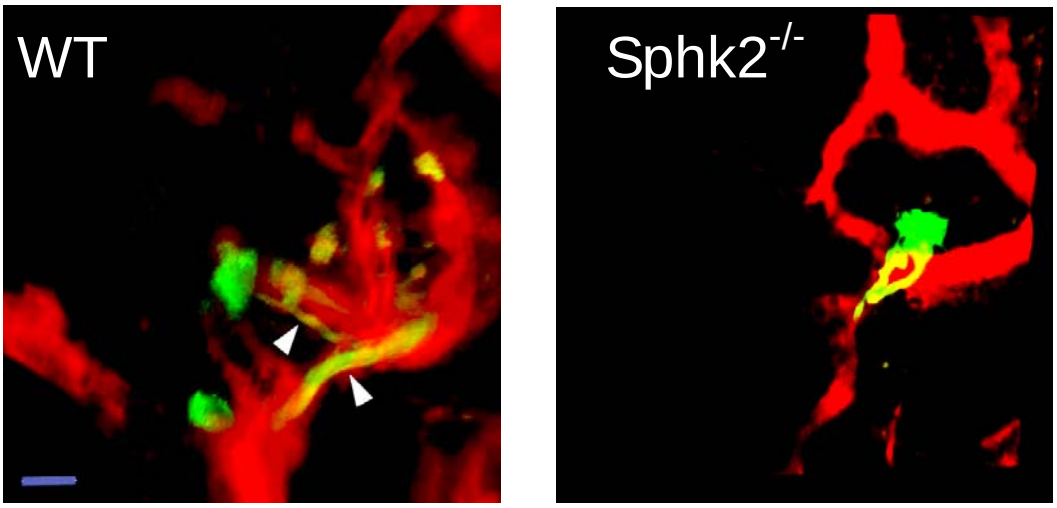

Fig. 4.18. Representative MP-IVM images of MKs with YFP^+ PPs. Green, MKs and PP; Red, sinusoids; Arrowheads, YFP^+ or $EGFP^+$ PPs; Inset, magnification for the dotted box; Arrow, connection between YFP^+ PPs.

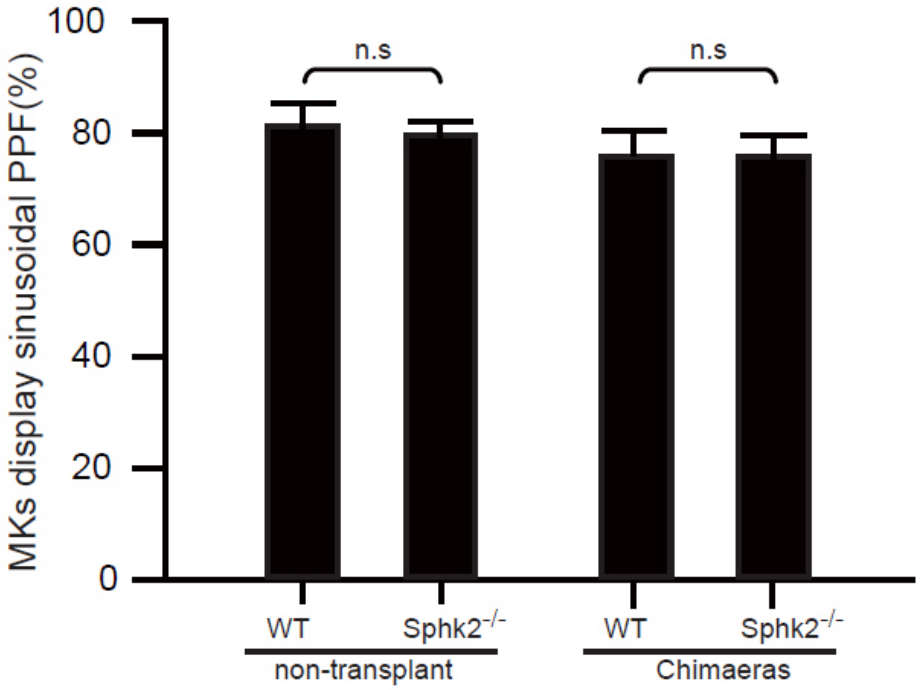

Fig. 4.19. Intrasinusoidal PP formation in WT and Sphk2 mutant mice. MKs displaying intrasinusoidal PP formation (PPF) *in vivo* presented as percentage of all MKs carrying PPs.

4.3.7 Proplatelet fragmentation *in vitro*

Platelets are supposed to be released from proplatelet stems [5]. In chapter 3, our data show that a defect in platelet shedding from MKs translates into inefficient platelet

production. To test the ability of Sphk2$^{-/-}$ MKs to release platelets from proplatelets, we used DIC microscopy to observe this process *in vitro*. As we found above (see previous chapters), S1P challenge could enhance proplatelets fragmentation and platelet release. We therefore incubated Sphk2$^{-/-}$ or WT MKs with S1P and compared PP fragmentation *in vitro*. Our results show that S1P causes immediate PP fragmentation in WT MKs, as mentioned in Chapter 3. In contrast, S1P-induced PP fragmentation is significantly reduced in Sphk2$^{-/-}$ MKs *in vitro* (Fig. 4.20-21), suggesting that the dissociation of platelets or platelet-like particles from Sphk2$^{-/-}$ MKs is not as efficient as from WT MKs, which might lead to the reduced platelet counts in peripheral blood of Sphk2$^{-/-}$ mice.

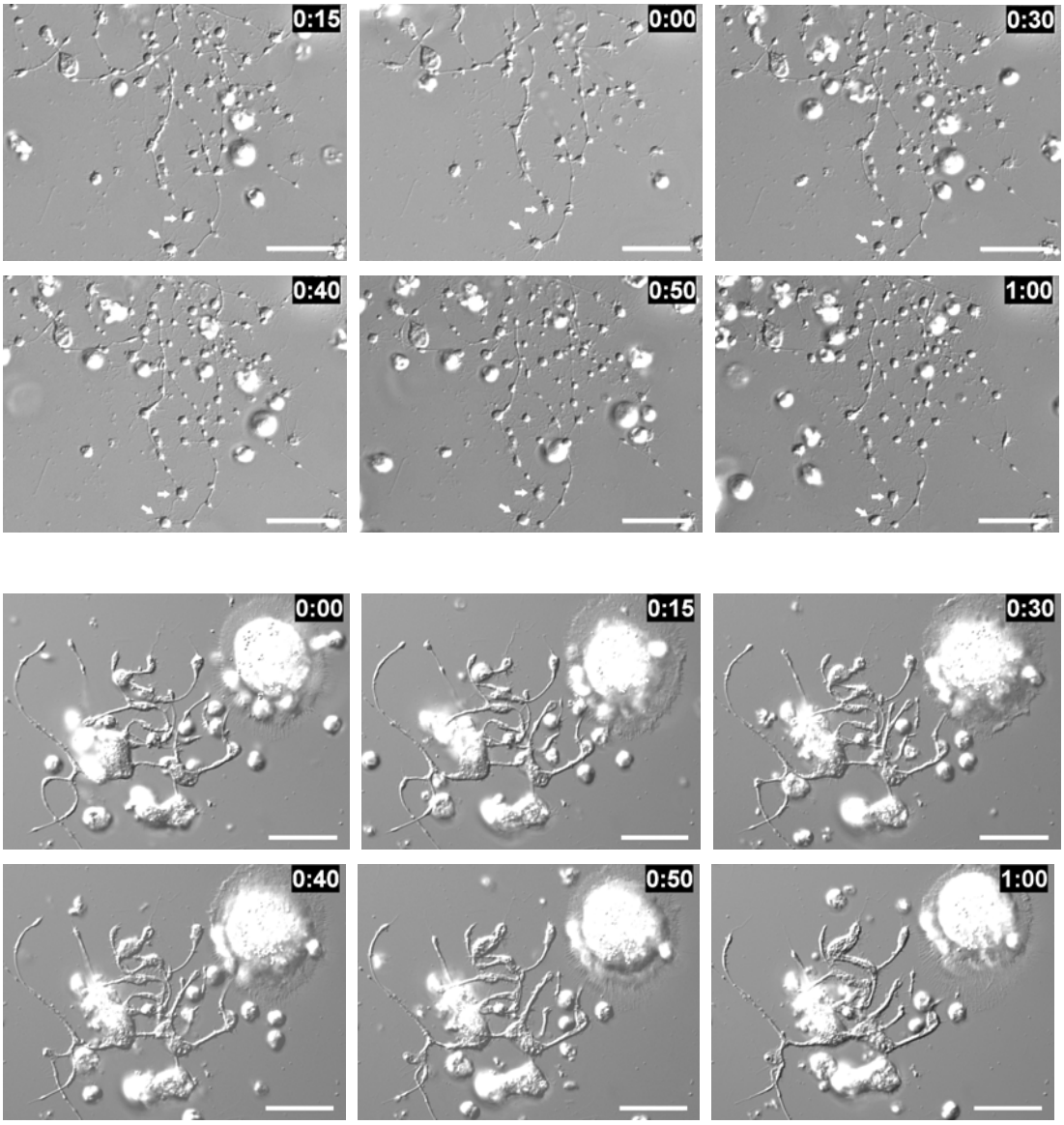

Fig. 4.20 DIC microscopic analysis of proplatelet fragmentation in the presence of S1P. DIC microscopy image sequences of PPs *in vitro*. Arrow, Platelets released from PP

stems; Scale bars, 20 μm; Time in minutes. The upper two rows indicate WT MKs, and the lower two rows indicate Sphk2$^{-/-}$ MKs

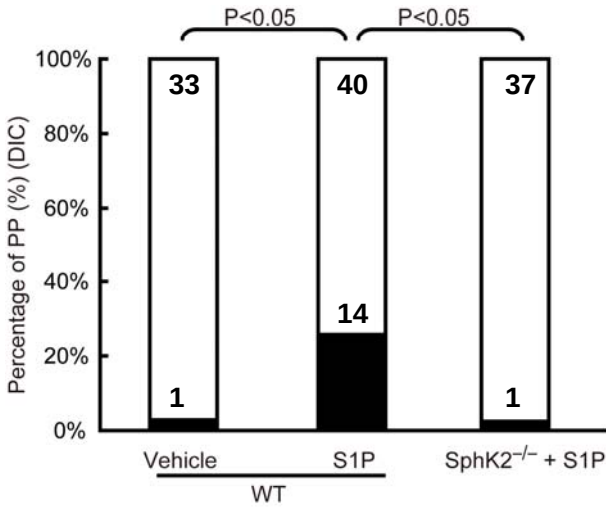

Fig. 4.21. The reduced S1P-induced PP fragmentation in Sphk2$^{-/-}$ MKs. The number of PPs with or without fragmentation observed by DIC microscopy *in vitro* over 1 hour in the indicated groups.

4.3.8 PP shedding *in vivo*

To further define the role of Sphk2 for fragmentation of PP *in vivo*, we collected the fragmentation events from MKs within 1 hour by intravital two-photon microscopy, as mentioned in Chapter 3. The frequency of fragmentation was 67.8% ±13.7% in CD41-YFP$^{ki/+}$ mice (Fig. 4.22-23). Next, we analyzed the fragmentation efficiency in Sphk2 $^{-/-}$×CD41-YFP$^{ki/+}$ mice. The complete loss of Sphk2 significantly reduced PP fragmentation (Fig. 4.22-23). Loss of Sphk2 exclusively in the hematopoietic system also results in a defect in PP fragmentation (Fig. 4.22-23). These data obtained from *in vitro* and *in vivo* experiments indicated that Sphk2 is indispensable for proper PP fragmentation. Cumulatively, a defect in fragmentation is the reason for thrombocytopenia in Sphk2$^{-/-}$ mice.

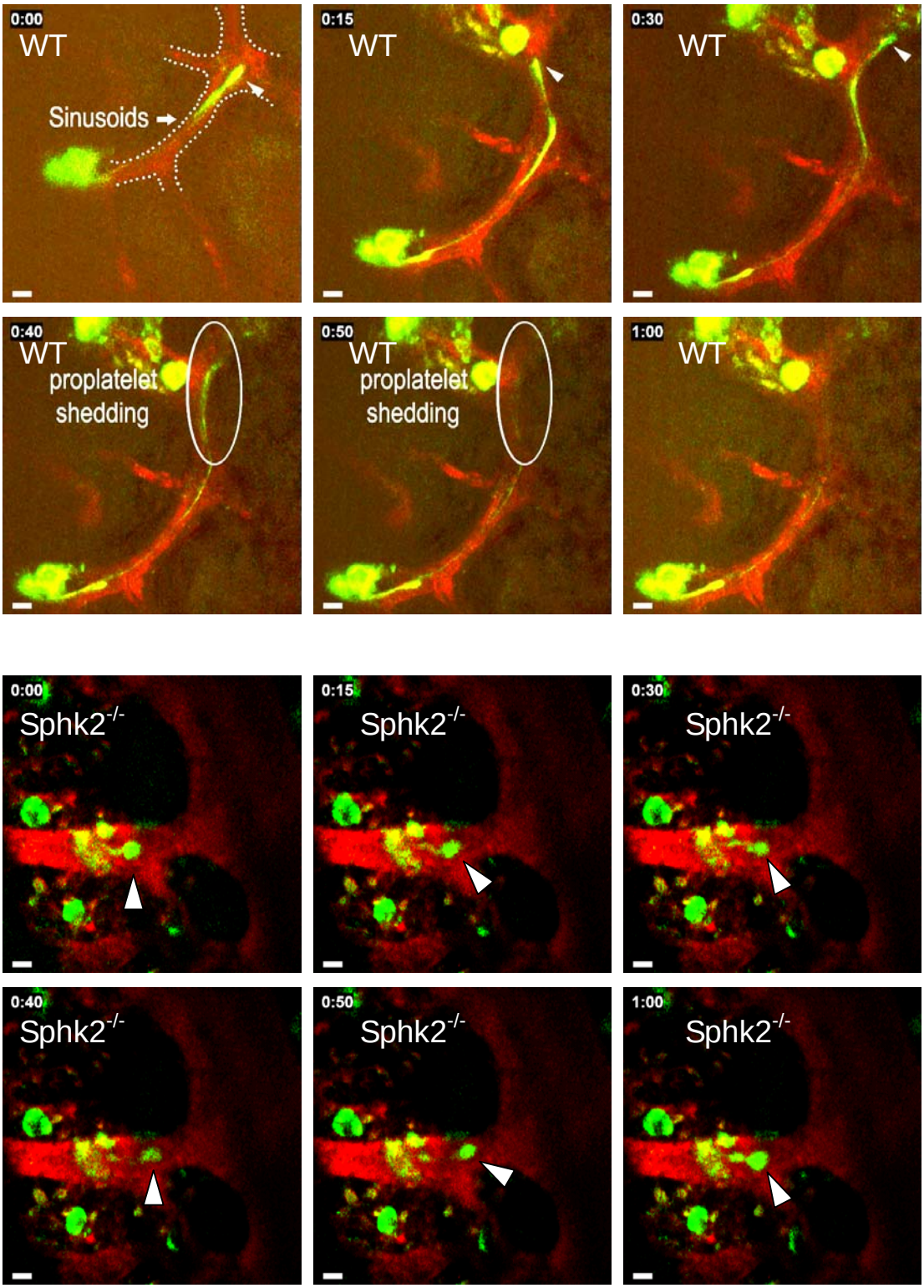
0:00
WT
Sinusoids
0:15
WT
0:30
WT
0:40
WT
proplatelet
shedding
0:50
WT
proplatelet
shedding
1:00
WT
0:00
Sphk2-/-
0:15
Sphk2-/-
0:30
Sphk2-/-
0:40
Sphk2-/-
0:50
Sphk2-/-
1:00
Sphk2-/-

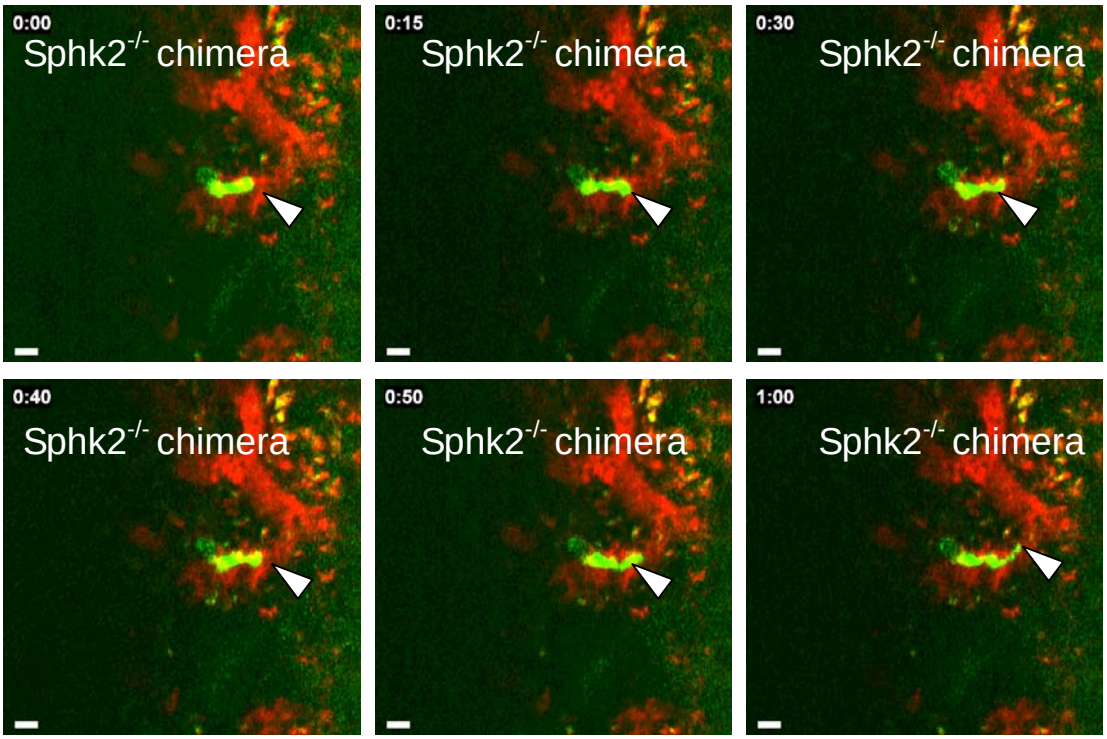

Fig. 4.22. Role of Sphk2 for PP shedding *in vivo* visualized by MP-IVM. WT MKs frequently shed PPs as shown in WT. Lack of Sphk2 in Sphk2$^{-/-}$ and Sphk2$^{-/-}$ BM chimeras abolishes PP shedding. Arrowheads indicate the tips of proplatelets. Green, MKs and PP; Red, Sinusoids; All scale bar, 20 μm; Time in minutes.

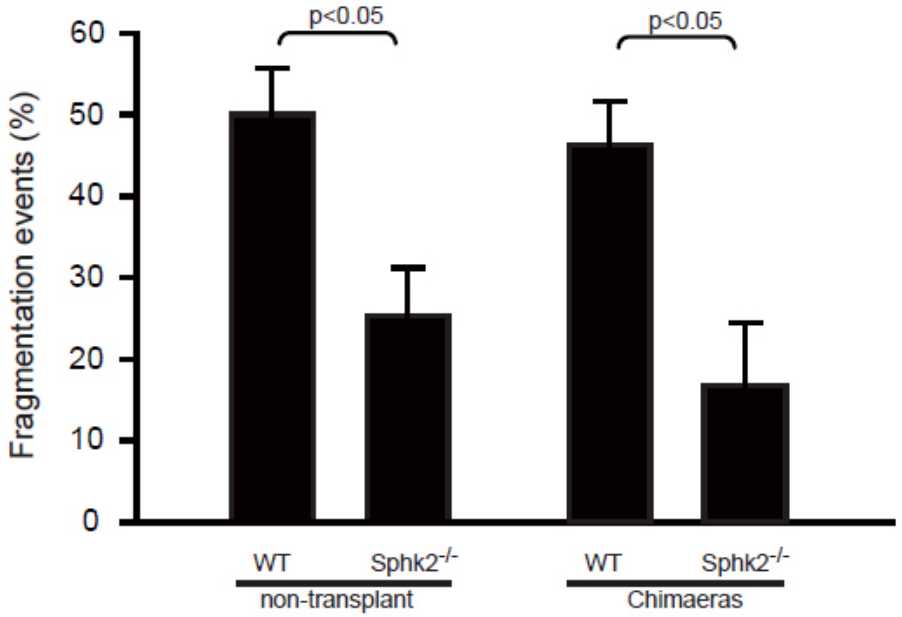

Fig. 4.23. The reduced PP fragmentation in Sphk2 mutant mice. Percentage of PP fragmentation events observed by MP-IVM over 1 hour in the indicated groups.

4.3.9 Molecular mechanism

As already mentioned in Chapter 3, S1P triggers signalling pathways that enhance PP fragmentation. Besides the dependency of S1P-induced PP fragmentation on $G_{i/o}$, Rac1 and p-MLC, our further data showed that inhibition of src family kinases (SFKs) by PP2 also blocks S1P-induced PP fragmentation (Fig. 4.24—25). We therefore next treated mice with dasatinib to inhibit the activity of SFKs *in vivo* [6]. Intravital MP-IVM data revealed that dasatinib significantly retards PP fragmentation and results in thrombocytopenia *in vivo* (Fig. 4.26-27) [6]. These results indicate that SFKs activity is necessary for S1P-induced PP fragmentation. Indeed, S1P enhanced the activity of SFKs in WT MKs (Fig. 4.28). Interestingly, S1P cannot increase the activity of SFKs in $Sphk2^{-/-}$ MKs (Fig. 4.28). Moreover, the total amount of SFKs protein expression is significantly reduced in $Sphk2^{-/-}$ MKs compared to WT MKs (Fig. 4.28). To summarize, a loss of Sphk2 in MKs results in the downregulation of SFKs expression and therefore a reduced activity of SFKs, leading to the defect in PP fragmentation.

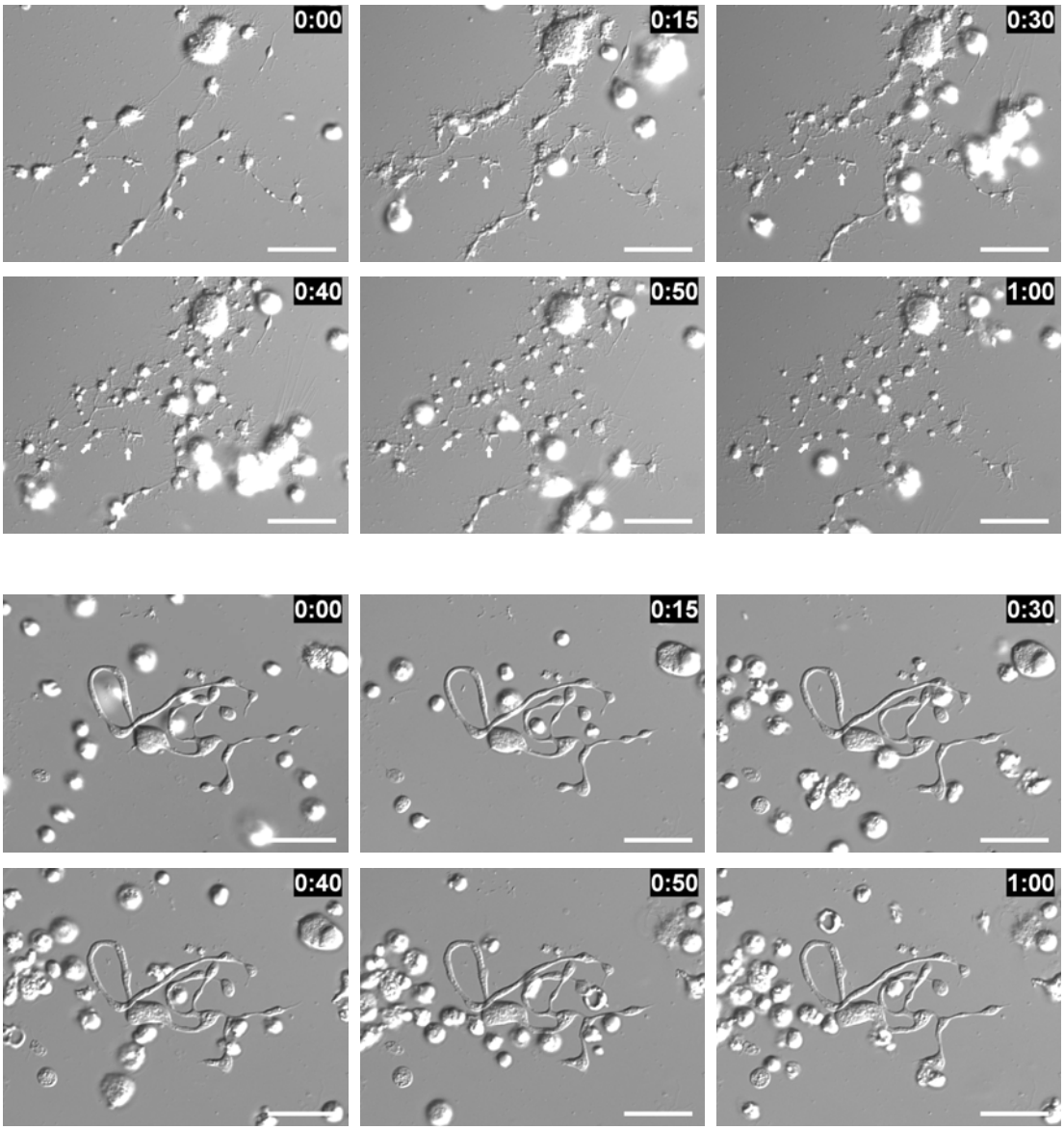

Fig. 4.24. Inhibition of SFKs activity disturbs S1P-induced PP fragmentation. DIC microscopy image sequences of PPs *in vitro*. Arrow, Platelets released from PP stems; Scale bars, 20 μm; Time in minutes. The upper two rows indicate the control group, and the lower two rows indicate PP2 group.

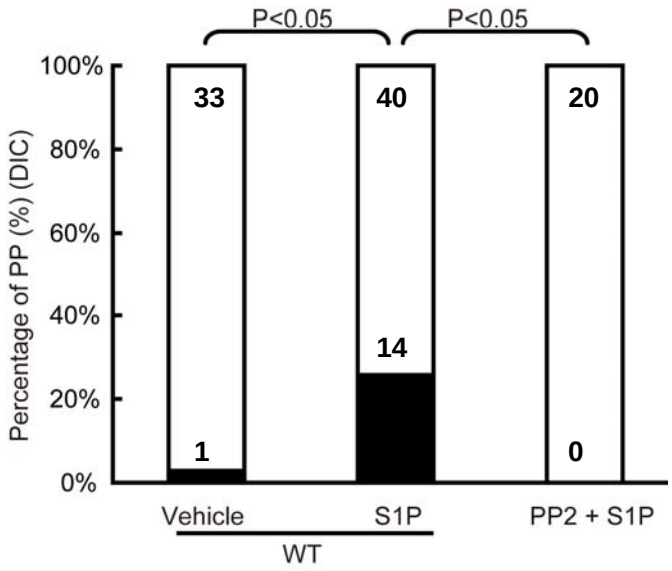

Fig. 4.25. S1P-induced PP fragmentation is dependent on SFKs activity. The number of PPs with or without fragmentation observed by DIC microscopy *in vitro* over 1 hour in the indicated groups.

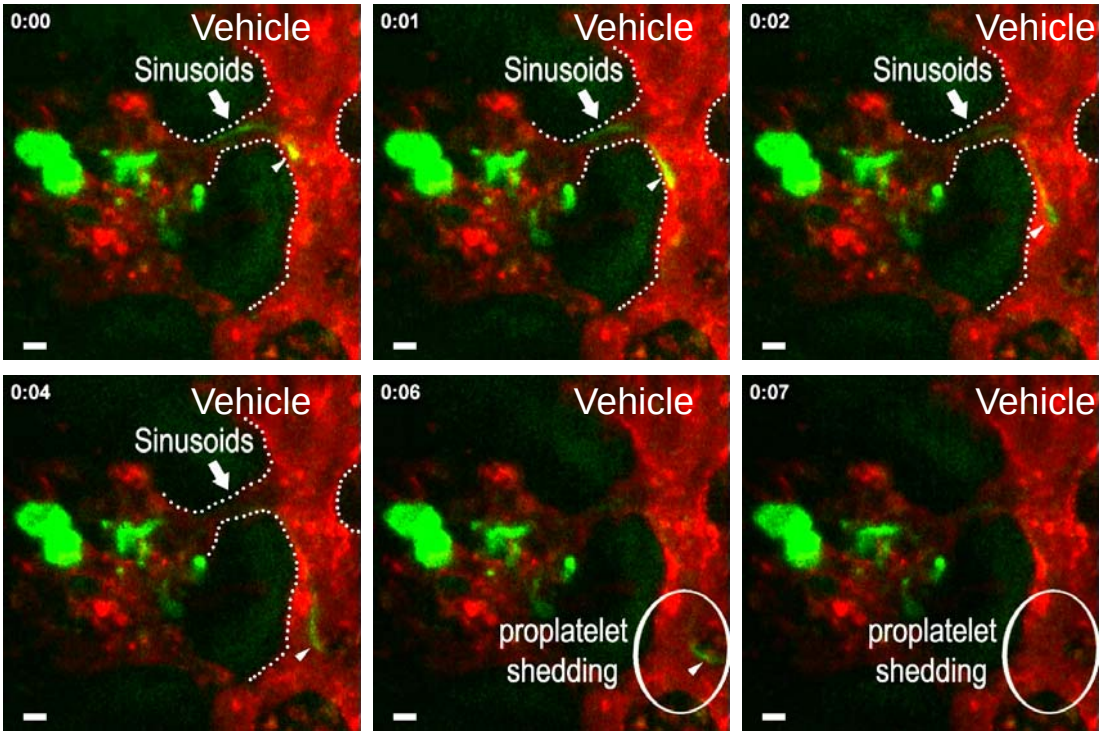

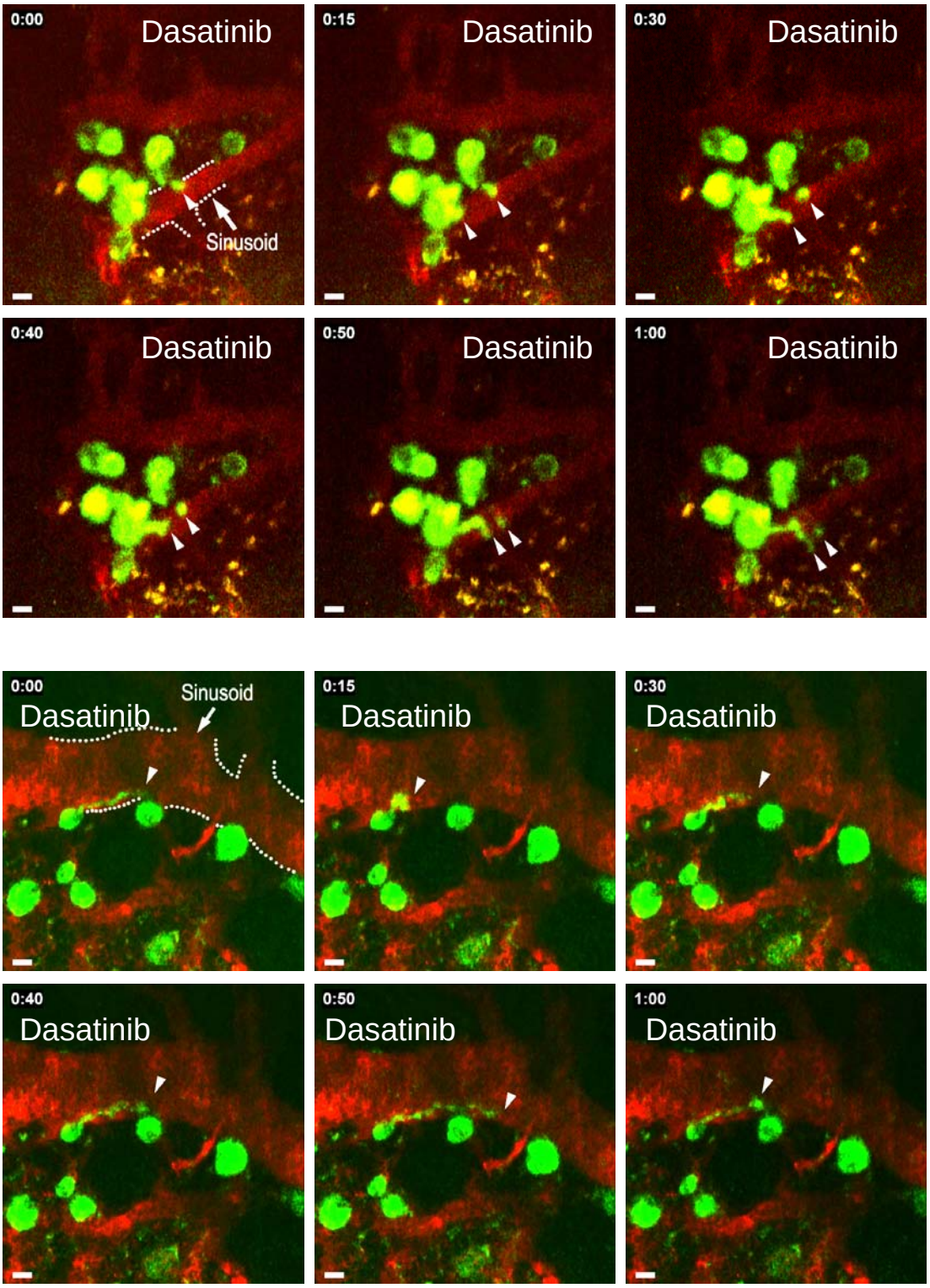

Fig. 4.26. Role of SFKs for PP shedding *in vivo* visualized by MP-IVM. Dasatinib abolishes PP shedding *in vivo*. Arrowheads indicate the tips of proplatelets. Green, MKs and PP; Red, Sinusoids; All scale bar, 20 µm; Time in minutes.

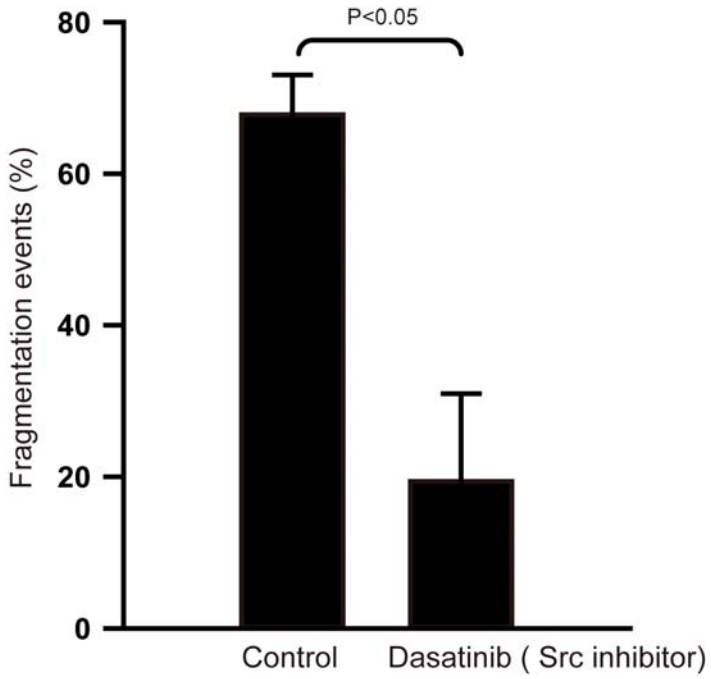

Fig. 4.27. Inhibition of SFKs activity reduces PP fragmentation *in vivo*. Percentage of PP fragmentation events observed by MP-IVM over 1 hour in the indicated groups.

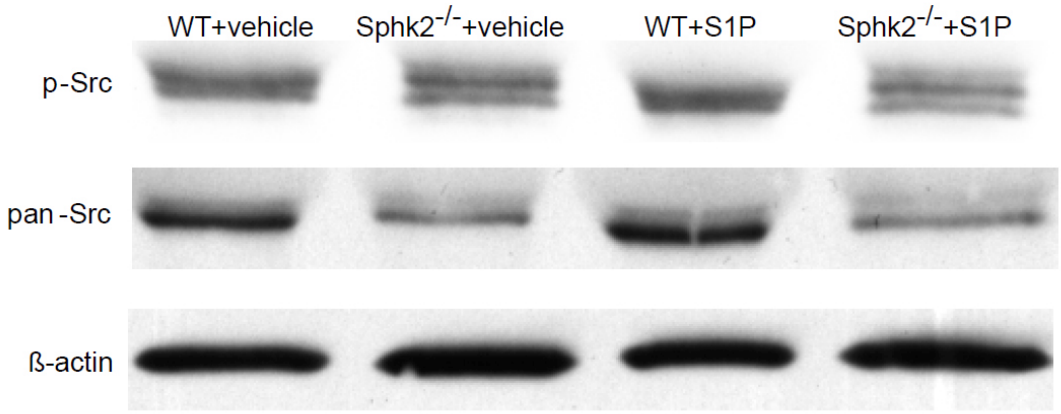

Fig. 4.28. Loss of Sphk2 reduces SFK expression and activity in MKs. Reduced expression and activity of SFKs in Sphk2$^{-/-}$ MKs. MKs were treated with or without 10 micromolar S1P for 5 min.

4.4 Discussion

Our investigations indicate that sphingosine kinases, which produce S1P, are also important to regulate thrombopoiesis. We found the major isoenzyme of sphingosine kinases in MKs was Sphk2. Correspondingly, loss of Sphk2 causes significant reduction in synthesis of S1P in MKs, while loss of Sphk1 is associated with normal S1P levels in MKs (data not shown). Hematopoietic deficiency of Sphk2 results in significant reduction in

peripheral platelets. We didn't find any abnormality in MK progenitor generation, MK maturation, proplatelet formation and life span of platelets. However, in the last step of platelet biogenesis, Sphk2$^{-/-}$ MKs have a defect in proplatelet fragmentation, leading to inefficient platelet production and thrombocytopenia.

Members of the Src family of tyrosine kinases (SFKs) are reported to regulate thrombopoiesis [6, 7]. A recent study shows that SFKs regulate MK spreading, migration and proplatelet formation. Inhibition of SFK impairs proplatelet formation and MK migration [6, 7], leading to a mild reduction in peripheral platelets. Herein we used DIC microscopy and MP-IVM to observe the behaviour of MKs treated with the SFKs inhibitor, PP2 or Dasatinib, *in vitro* and *in vivo*, respectively. Both *in vitro* and intravital observation reveals that inhibition of SFKs retards proplatelet fragmentation, although the distribution of MKs and proplatelets is normal *in vivo*. This study supports and completes the previous findings to further understand the mechanism how SFKs regulate thrombopoiesis [6]. Furthermore, SFKs expression and activation are found to be regulated by Sphk2 in our study. Our data show that loss of Sphk2 in MKs not only downregulates the gross expression levels of SFKs, but also inhibits the activation of SFKs triggered by S1P signaling, leading to a defect in SFKs-dependent PP fragmentation and inefficient platelet production. It has been shown that Sphk2 plays a role in epigenetic regulation of gene expression [8]. Hait et al reported that Sphk2 was associated in the nucleus with HDAC1 and HDAC2 in repressor complexes and Sphk2 produced nuclear S1P to inhibit HDAC1 and HDAC2 activity, leading to the epigenetic regulation of gene expression, e.g. cyclin-dependent kinase inhibitor p21 and the transcriptional regulator c-fos [8]. This scenario could possibly explain our observation that Sphk2 regulates SFKs expression during MK maturation. Besides downregulation of SFK expression, Sphk2 deficiency also impairs the activation of SFKs, which cannot be simply explained by an epigenetic regulation. There are two possible mechanisms to explain this. First, S1P generated by Sphk2 possibly enhances SFKs activation via "inside-out" transactivation of S1PRs. Our results have already shown that extracellular S1P could signal via S1PRs leading to an increased activity of SFKs. It has also been reported that Sphk2 is translocated to the cellular membrane and releases S1P to transactivate S1PRs through "inside-out" signalling [9], although Sphk1 is more often reported to play such a role [10]. Thus, loss of Sphk2 in megakaryocytes possibly causes insufficient "inside-out" signalling via S1PRs, which contributes to the enhancement of SFK activity. Second, intracellular S1P generated by Sphk2 in MKs acts as an intracellular second messenger to regulate SFKs activation. Emerging evidence from yeast to mammals suggests that S1P regulates cellular processes as a classical intracellular second messenger, which is independent on S1PRs [11-14]. It is possible that the intracellular S1P levels is an important second

messenger to regulate the activation of SFKs. Therefore, the reduced intracellular S1P in Sphk2$^{-/-}$ MKs possibly disturb the activation of SFKs. However, the exact mechanism how Sphk2 regulates the activation of SFKs still needs to be further clarified.

Together, Chapter 3 and Chapter 4 demonstrate the essential role of S1P for thrombopoiesis. On one hand, our investigations reveal that extracellular S1P controls thrombopoiesis through S1P1 to direct proplatelet formation and to enhance proplatelet dissociation from megakaryocytes into the blood stream. Loss of S1P1 in MKs leads to severe thrombocytopenia. On the other hand, this study shows that Sphk2 is the major isoenzyme of sphingosine kinases to synthesize S1P in megakaryocytes. Mice lacking hematopoietic Sphk2 display thrombocytopenia because of the defective intravascular proplatelet shedding. Our work in this thesis revealed the role of sphingosine-1 phosphate and S1P receptors in the regulation of thrombopoiesis. These findings could lead to novel therapeutic strategies for patients with thrombocytopenia

4.5 References

1. Zhang, J., et al., *CD41-YFP mice allow in vivo labeling of megakaryocytic cells and reveal a subset of platelets hyperreactive to thrombin stimulation.* Exp Hematol, 2007. **35**(3): p. 490-499.
2. Kaushansky, K., *The molecular mechanisms that control thrombopoiesis.* J Clin Invest, 2005. **115**(12): p. 3339-47.
3. Jackson, C.W., *Megakaryocyte endomitosis: a review.* Int J Cell Cloning, 1990. **8**(4): p. 224-6.
4. Italiano, J.E., Jr., S. Patel-Hett, and J.H. Hartwig, *Mechanics of proplatelet elaboration.* J Thromb Haemost, 2007. **5 Suppl 1**: p. 18-23.
5. Italiano, J.E., Jr., et al., *Blood platelets are assembled principally at the ends of proplatelet processes produced by differentiated megakaryocytes.* J Cell Biol, 1999. **147**(6): p. 1299-312.
6. Mazharian, A., et al., *Dasatinib enhances megakaryocyte differentiation but inhibits platelet formation.* Blood. **117**(19): p. 5198-206.
7. Mazharian, A., et al., *Critical role of Src-Syk-PLC{gamma}2 signaling in megakaryocyte migration and thrombopoiesis.* Blood. **116**(5): p. 793-800.
8. Hait, N.C., et al., *Regulation of histone acetylation in the nucleus by sphingosine-1-phosphate.* Science, 2009. **325**(5945): p. 1254-7.
9. Olivera, A., et al., *IgE-dependent activation of sphingosine kinases 1 and 2 and secretion of sphingosine 1-phosphate requires Fyn kinase and contributes to mast cell responses.* J Biol Chem, 2006. **281**(5): p. 2515-25.
10. Alemany, R., et al., *Regulation and functional roles of sphingosine kinases.* Naunyn Schmiedebergs Arch Pharmacol, 2007. **374**(5-6): p. 413-28.

11. Lanterman, M.M. and J.D. Saba, *Characterization of sphingosine kinase (SK) activity in Saccharomyces cerevisiae and isolation of SK-deficient mutants.* Biochem J, 1998. **332 (Pt 2)**: p. 525-31.
12. Pandey, S. and S.M. Assmann, *The Arabidopsis putative G protein-coupled receptor GCR1 interacts with the G protein alpha subunit GPA1 and regulates abscisic acid signaling.* Plant Cell, 2004. **16**(6): p. 1616-32.
13. Olivera, A., et al., *The sphingosine kinase-sphingosine-1-phosphate axis is a determinant of mast cell function and anaphylaxis.* Immunity, 2007. **26**(3): p. 287-97.
14. Meyer zu Heringdorf, D., et al., *Sphingosine kinase-mediated Ca2+ signalling by G-protein-coupled receptors.* EMBO J, 1998. **17**(10): p. 2830-7.

APPENDIX

Abbreviations

3D	3 dimension
4D	4 dimension
AC	adenylyl cyclase
ADF	actin depolymerizing factor
ATP	Adenosine triphosphate
Bcl-xL	B-cell lymphoma-extra large
BFU-MK	burst-forming unit-megakaryocyte
BM	bone marrow
BSA	bovine serum albumin
cDNA	complementary DNA
CFU	colony-forming unit
CFU-MK	colony-forming unit-megakaryocyte
CFU-MKs	megakaryocyte colony-forming unit
CLP	common lymphoid progenitor
CMP	common myeloid progenitor
CMV	CytoMegalie-Virus
CoA	Coenzym A
DC	dendritic cells
DH-Cer	dihydroceramide
DH-SM	dihydrosphingomyelin
DIC	differential interference contrast
DMEM	Dulbecco’s Modified Eagle Medium
DMF	dimethyl formamide
DMS	Demarcation membrane system
DMS	demarcation membrane system
DMSO	Dimethyl sulfoxide
EDG	endothelial differentiation gene
EGFP	enhanced green fluorescent protein
eNos	Endothelial Nitric Oxide Synthase
ER	endoplasmic reticulum
FACS	Fluorescence-activated cell sorting
FBS	fetal bovine serum
FITC	fluorescein isothiocyanate
FL	fetal liver
fl	floxed gene
Flt3	fms-like tyrosine kinase receptor-3
FSC	forward scatter
GAPDH	Glyceraldehyde 3-phosphate dehydrogenase
G-CSF	granulocyte colony-stimulating factor

GFP	green fluorescent protein
GM-CSF	granulocyte-macrophage colony-stimulating factor
GPCR	G protein-coupled receptors
Gy	gray
HCT	hematocrit
HDAC	Histone deacetylases
HGB	hemoglobin
HPP-CFU-MK	high proliferative potential-colony-forming unit-Megakaryocyte
HSC	hematopoietic stem cells
i.p	Intraperitoneal injection
IgG	Immunoglobulin G
IL- 3	Interleukin-3
IMDM	Iscove's Modified Dulbecco's Medium
Kd	Dissociation constant
Keto	3-ketosphinganine
ki	knock in
KO	knock out
LPS	lipopolysaccharide
Lym	Lymphocytes
mAb	monoclonal antibody
MAPK	Mitogen-Activated Protein Kinase
MCH	mean corpuscular hemoglobin
MCHC	mean corpuscular hemoglobin concentration
MCV	mean corpuscular volume
MEP	MK/Erythro progenitor
min	minute
MK	megakaryocyte
MKs	megakaryocytes
MLC2	myosin light chain 2
mMSC	Murine mesenchymal stem cells
MP-IVM	multi-photon intravital microscopy
MPP	multipotent progenitors
MPV	mean platelet volume
mRNA	messenger RNA
NA	numerical aperture
NF-E2	nuclear factor (erythroid-derived 2)
NGF	nerve growth factor
NK	natural killer cell
P12	pheochromcytoma 12
Palm-CoA	palmitoyl CoA
PBS	Phosphate buffered saline
PCR	polymerase chain reaction

PDGF	Platelet Derived Growth Factor
PE	phycoerythrin
PF4	platelet factor 4
PI3K	hosphoinositide 3-kinase
pIpC	polyinosinic-polycytidzlic acid
PLC	Phospholipase C
PMA	phorbol 12-myristate 13-acetate
p-MLC	phosphorylation of myosine light chain
PP	proplatelet
PPF	proplatelet formation
PPs	proplatelets
PTX	pertussis toxin
RBC	red blood cells
RT-PCR	reverse transcriptase-PCR
s.e.m	the standard error of mean
S1P	Sphingosine 1-phosphate
S1P1	S1P receptor 1
S1P2	S1P receptor 2
S1P3	S1P receptor 3
S1P4	S1P receptor 4
S1P5	S1P receptor 5
S1PRs	S1P receptors
SCF	stem cell factor
SDF	stromal cell-derived factor
Ser	serine
SFKs	Src family of kinases
SM	sphingomyelin
SPH	Sphingosine
Sphk1	Sphingosine kinase 1
Sphk2	Sphingosine kinase 2
Sphks	Sphingosine kinases
SPL	S1P lyase
SPP	S1P phosphatases
SPT	Serine palmitoyltransferase
SRE	sterol regulatory element
TH17	T helper 17 cell.
TNFα	Tumor necrosis factor α
Tpo	thrombopoietin
TRITC	Tetramethylrhodaminoisothiocyanato-dextran
WBC	white blood cells
WT	wild type
YFP	yellow fluorescent protein

List of primers

Gene	Forward	Reverse
mS1P1	5’ ACT ACA CAA CGG GAG CAA CAG 3’	5’ GAT GGA AAG CAG GAG CAG AG 3’
mS1P2	5’ CTC ACT GCT CAA TCC TGT CAT C 3’	5’ TTC ACA TTT TCC CTT CAG ACC 3’
mS1P3	5’ TTC CCG ACT GCT CTA CCA TC 3’	5’ CCA ACA GGC AAT GAA CAC AC 3’
mS1P4	5’ TGC GGG TGG CTG AGA GTG 3’	5’ TAG GAT CAG GGC GAA GAC C 3’
mS1P5	5’ CTT AGG ACG CCT GGA AAC C 3’	5’ CCC GCA CCT GAC AGT AAA TC 3’
mGADPH	5’ GAC TTC AAC AGC AAC TCC CAC 3’	5’ TCC ACC ACC CTG TTG CTG TA 3’
mCD41	5’ CAC TCC TAA TCG GTG CTG ACA 3’	5’ GCC ACC CTG GAC TCA TTC TC 3’
hS1P1	5’ TGT CAG CCT CCG TGT TCA G 3’	5’ GTT ATT GCT CCC GTT GTG G 3’
hS1P2	5’ GGA AAC GCA GGA GAC GAC 3’	5’ GAC AGA GCC AGA GAG CAA GG 3’
hS1P3	5’ TTC AAG GCT CAG TGG TTC ATC 3’	5’ GAG AGT GGC TGC TAT TGT TGC 3’
hS1P4	5’ GCT GAA GAC GGT GCT GAT G 3’	5’ CTG CTG CGG AAG GAG TAG A 3’
hS1P5	5’ GAA CTC GGT GAT GAA ATA ATG G 3’	5’ AAG GTC CTT CGG GAA CTA CTC 3’
hGAPDH	5’ GAA GGT GAA GGT CGG AGT C 3’	5’ GAA GAT GGT GAT GGG ATT TC 3’

List of Publications

Zhang L, Massberg S et al. The sphingosine 1-phosphate receptor S1P1 controls bone marrow thrombopoiesis. (under revision)

Mazharian A, Ghevaert C, **Zhang L**, Massberg S, Watson SP. Dasatinib enhances megakaryocyte differentiation but inhibits platelet formation. Blood. 2011 Mar 8.

Acknowledgments

I would like to thank my supervisor, Prof. Dr. Steffen Massberg. Without his supporting and guiding, I cannot finish my study. He is an excellent supervisor and scientist.

I am very appreciated of guidance from my thesis committee members. Without your help and suggestion, I cannot fulfil my thesis.

I'd like to thank all my colleagues in our lab. I am very grateful to all of you. Special thanks to our molecular biologist, Michael Lorenz, who gave me a lot of help and insightful suggestions.

I would like to thank my family for the love and support. In particular, I would like to thank my wife, my parents and my brother. It is impossible to finish my study without you.